Vol. 68 • No. 8

August 2025

Microwave Journal

EUROPEAN MICROWAVE WEEK
JAARBEURS UTRECHT
THE NETHERLANDS
21-26 SEPTEMBER 2025
www.eumw.eu
WAVES OF INNOVATION

SPECIAL FOCUS: mmWaves

horizon house®
Founded in 1958
mwjournal.com

CBN SERIES

Phase Stable Flex Cables

Stable Output Performance in Almost Any Bend Shape!

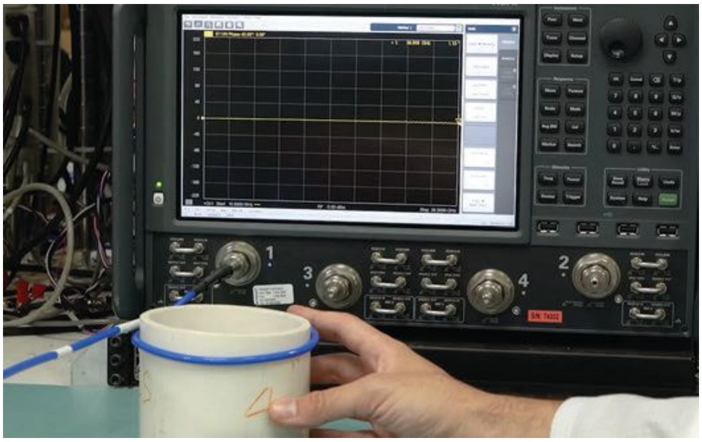

Figure 1: 1-port phase stability test with 360 ° bend around a 4-inch mandrel.

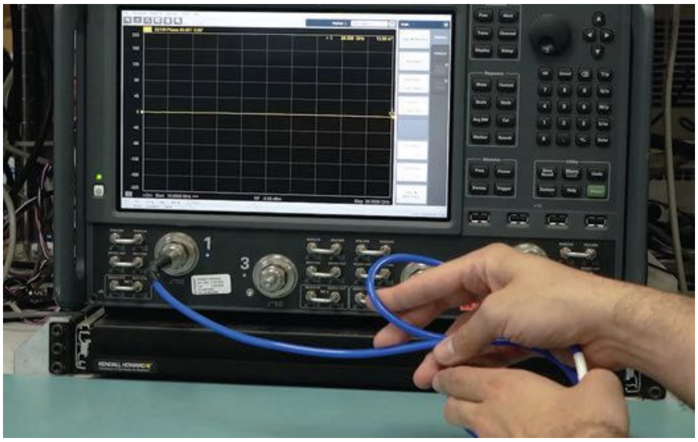

Figure 2: 2-port phase stability test with arbitrary flexure at multiple angles.

Models In Stock

MODEL #	CONNECTOR 1	CONNECTOR 2	LENGTH (FT)	FREQ. HIGH (GHz)	INSERTION LOSS
CBN-1FT-SMSM+	SMA-Male	SMA-Male	1.0	26.5	0.8
CBN-1.5FT-SMSM+	SMA-Male	SMA-Male	1.5	26.5	1.0
CBN-2FT-SMSM+	SMA-Male	SMA-Male	2.0	26.5	1.4
CBN-3FT-SMSM+	SMA-Male	SMA-Male	3.0	26.5	2.1
CBN-1.5M-SMSM+	SMA-Male	SMA-Male	3.3	26.5	3.2
CBN-3.5FT-SMSM+	SMA-Male	SMA-Male	3.5	26.5	2.3
CBN-4FT-SMSM+	SMA-Male	SMA-Male	4.0	26.5	2.5
CBN-5FT-SMSM+	SMA-Male	SMA-Male	5.0	26.5	3.5
CBN-6FT-SMSM+	SMA-Male	SMA-Male	6.0	26.5	3.8
CBN-10FT-SMSM+	SMA-Male	SMA-Male	10.0	26.5	6.3
CBN-15FT-SMSM+	SMA-Male	SMA-Male	15.0	26.5	9.4

Develop the Future

Integrated, miniaturized RF+Digital solutions for rapid development and deployment of high-precision systems

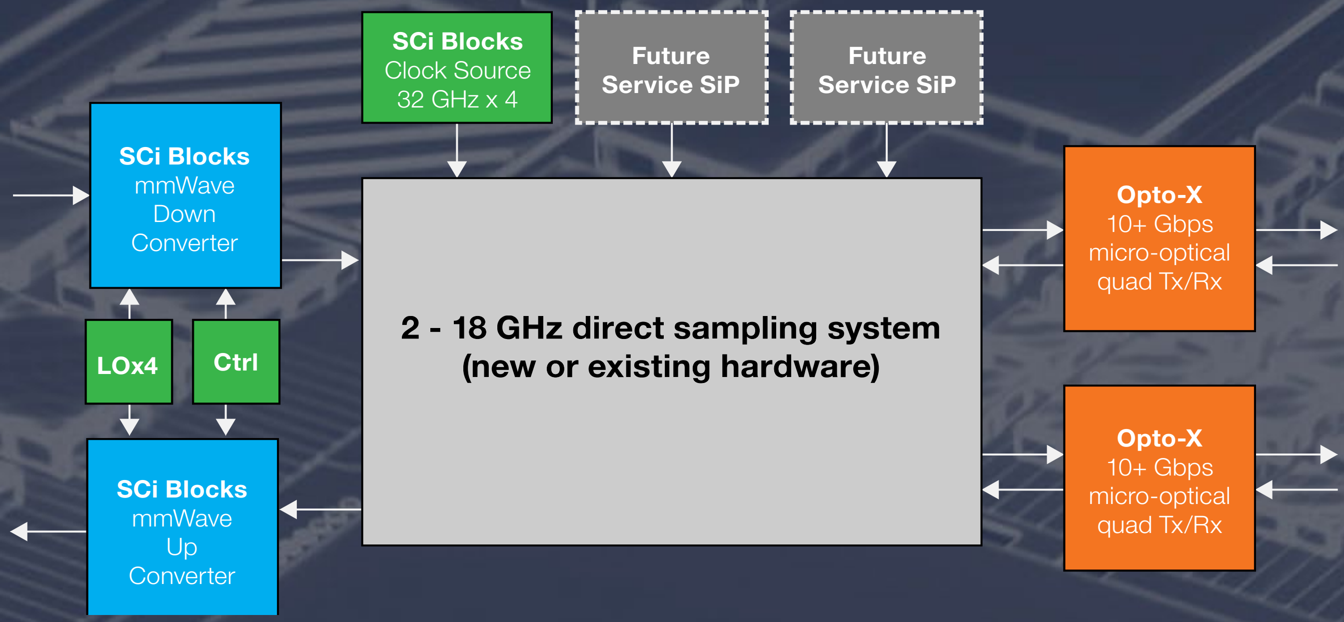

Use our SiP platform to upgrade to 40 GHz or add a custom RF personality to your front end

- Highly integrated RF, digital, power
- Software-instrumented for tuning & control
- Single or multi-channel
- Surface-mount for rapid production
- Cost-effective and volume-ready
- Standard and custom solutions available

Get high speed optical transmission for extreme environments

- Multi-mode optical wavelength (850nm).
- Quad channel Tx/Rx from 20Mbps to >10Gbps.
- -50°C to +125°C
- Pluggable optical connector interface
- BGA solder ball contacts or LGA with interposer
- Hermetic enclosure

To learn more or to connect with our team at European Microwave Week or visit **spectrumcontrol.com/sci-blocks**

SPECTRUM CONTROL™


RF-LAMBDA
THE LEADER OF RF BROADBAND SOLUTIONS
BROADBAND SSPA / EMC BENCHTOP
SOLID STATE POWER AMPLIFIER
0.1-22GHZ
ULTRA BROADBAND SSPA
RFLUPA01M22GA
4W 0.1-22GHZ
RFLUPA0218GB
20W 1-19GHZ
6-18GHZ 800W
CW REMC06G18GG
18-40GHZ 200W
CW REMC18G40GQ
0. 1-6GHZ VHZ,
UHF, L, S, C BAND
RFLUPA02G06GC
100W 2-6GHZ
RFLUPA0706GD
30W 0.7-6GHZ
MADE IN
USA
6-18GHZ C, X, KU BAND
RFLUPA08G11GA
50W 8-11GHZ
RFLUPA0618GD
60W 6-18GHZ
RFLUPA06G12GB
25W 6-12GHZ
18-50GHZ K, KA, V BAND
RFLUPA18G47GC
2W 18-47GHZ
RFLUPA27G34GB
15W 27-34GHZ
RFLUPA47G53GA2
10W 47-53GHZ
RFLUPA27G34GB
30W 18-40GHZ
BENCHTOP RF MICROWAVE SYSTEM POWER AMPLIFIER
REMC02G06GE
600W 2-6GHZ
REMC18G40GC2
40W 18-40GHZ
RAMP30G65GG
8W 30-65GHZ
RAMP06G18GA
10W 6-18GHZ
RAMP00M65GA
DC-65GHZ
www.rflambda.com
sales@rflambda.com
1-888-976-8880
1-972-767-5998
San Diego, CA, US
Carrollton, TX, US
Ottawa, ONT, Canada
Frankfurt, Germany

Microwave Journal

CONTENTS

August 2025
Vol. 68 • No. 8
EuMW Show Issue +
mmWave Technology Special Focus
mwjournal.com

Cover Feature

Technical Feature

2025 SHOW COVERAGE

For complete coverage of the EuMW 2025 conference, event news, exhibitor product information and special reports from the editors of *Microwave Journal*, visit our online show daily at mwjournal.com/eumw2025.

73 SPECIAL FOCUS mmWave Technology

ACCESS NOW!
digital.microwavejournal.com

eXclusive Digital Content ›››

68 YEARS OF PUBLISHING EXCELLENCE

Unlocking mmWave Technology

New Components | ***New*** Possibilities

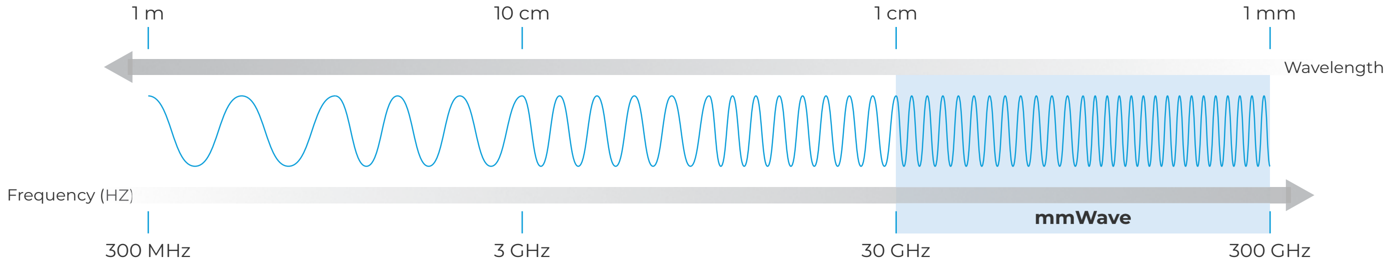

UBC Series

- Flat Frequency Performance up to 110 GHz +
- Ultra Low Insertion Loss
- Case Sizes as low as 01005 Available
- Now Available in Working Voltages up to 100V

Download the datasheet

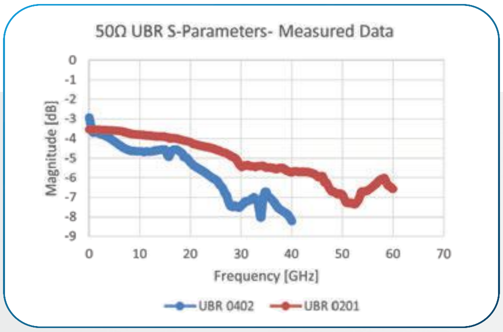

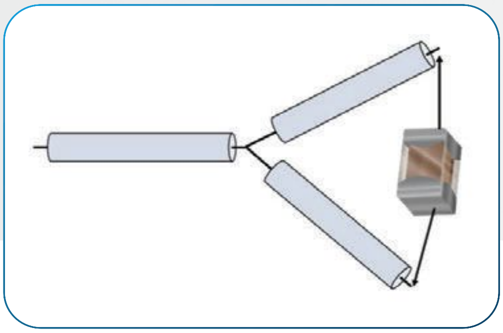

- Now Available in 0201 Case Size
- Made in the US
- Broadband Performance up to 40 GHz
- Glass-Sandwich Technology and Laser Trimming to Reduce Parasitic Noise

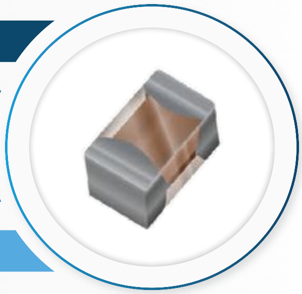

UBR Series

Download the datasheet

Learn more at www.kyocera-avx.com

KYOCERA AVX

Microwave Journal

CONTENTS

mwjournal.com

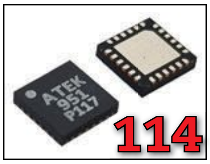

Tech Brief

Departments

SUBSCRIBE & RENEW NOW

Microwave Journal (USPS 396-250) (ISSN 0192-6225) is published monthly by Horizon House Publications Inc., 685 Canton St., Norwood, MA 02062. Periodicals postage paid at Norwood, MA 02062 and additional mailing offices.

POSTMASTER: Send address corrections to Microwave Journal, PO Box 1028, Lowell, MA 01853 or e-mail mwj@e-circ.net.com. Subscription information: (978) 671-0446. This journal is issued without charge upon written request to qualified persons working in the RF & microwave industry. Other subscriptions are: domestic, $130.00 per year, two-year subscriptions, $200.00; foreign, $225.00 per year, two-year subscriptions, $400.00; back issues (if available) and single copies, $20.00 domestic and $30.00 foreign. Claims for missing issues must be filed within 90 days of date of issue for complimentary replacement.

STAFF

Group Director: Carl Sheffres
Associate Publisher: Michael Hallman
Media Director: Patrick Hindle
Brand & Content Director: Jennifer DiMarco
Technical Editor: Del Pierson
Associate Technical Editor: Cliff Drubin
Editorial & Media Specialist: Kelley Roche
Associate Editor: Kaitlyn Joyner
Multimedia Staff Editor: Barbara Walsh
Electronic Marketing Manager: Chris Stanfa
Senior Digital Content Specialist: Lauren Tully
Digital Content Specialist: Vincent Carrabino
Director of Production & Distribution: Edward Kiessling
Art Director: Janice Levenson
Graphic Designer: Ann Pierce

EUROPE

Office Manager: Nina Plesu

CORPORATE STAFF

CEO: William M. Bazzy
President: Ivar Bazzy
Vice President: Jared Bazzy

EXECUTIVE EDITORIAL OFFICE

685 Canton Street, Norwood, MA 02062
Tel: (781) 769-9750
FAX: (781) 769-5037
e-mail: mwj@mwjournal.com

EUROPEAN EDITORIAL OFFICE

16 Sussex Street, London SW1V 4RW, England
Tel: Editorial: +44 207 596 8730 Sales: +44 207 596 8740
FAX: +44 207 596 8749

SUBSCRIPTION SERVICES

Send subscription inquiries and address changes to:
Tel: (978) 671-0446
e-mail: mwj@e-circ.net

www.mwjournal.com

Printed in the USA

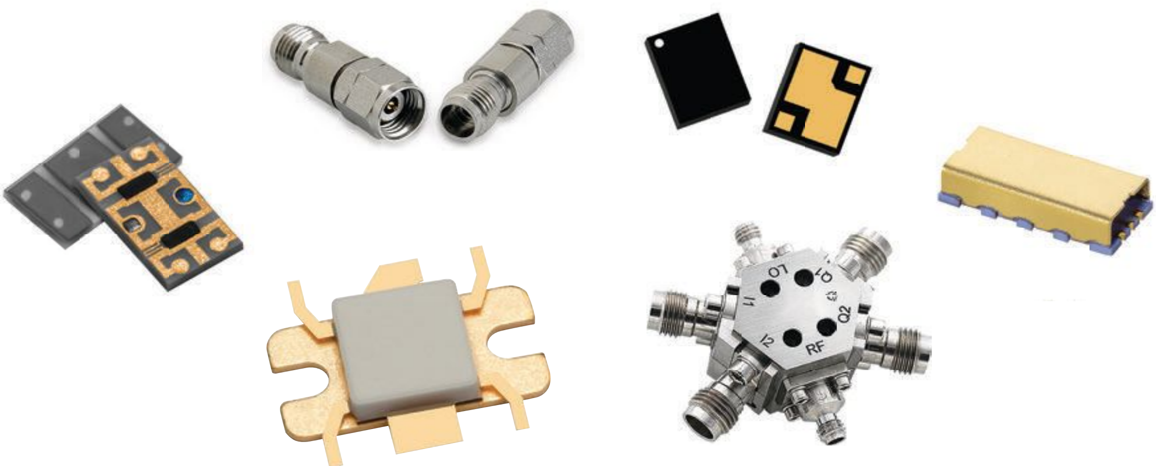

Microwave Journal ONLINE .COM

E LEARNING CENTER

Access webinars on-demand from the archived webinars and events page at www.mwjournal.com/events

WHITE PAPERS

Coilcraft — Key Parameters for Selecting RF Inductors

ALTAIR — Large Platform Co-site Interference Mitigation

ANALOG DEVICES (AHEAD OF WHAT'S POSSIBLE™) — How to Maintain Maximum Dynamic Range in Wideband High IP2 Receivers

Maury Microwave — Next-Gen EMC Testing: Selecting Amplifiers for 5G, EVs, and Beyond

AI in RF – 9/9

This half day event will cover the various ways AI is being used in the development and production of RF and microwave products.

12 to 4 pm ET, with 30-min sessions followed by a 60-min panel session.

Sponsored by: MILLER MMIC

Philip Pratt, Vice President of Marketing at **Jariet Technologies**, discusses his transition from engineering to marketing, Jariet's 10-year anniversary and his vision for Jariet's future.

Executive Interview

Join Us Online

Follow us @Pathindle @MWJEditor

Join us at the RF and Microwave Community

Become a fan at facebook.com/microwavejournal

Microwave Journal podcasts include the RF/microwave update series, Frequency Matters, plus interviews with industry experts and executives.

Catch *Frequency Matters,* the industry update from *Microwave Journal,* microwavejournal.com/FrequencyMatters

Visit us @ mwjournal.com

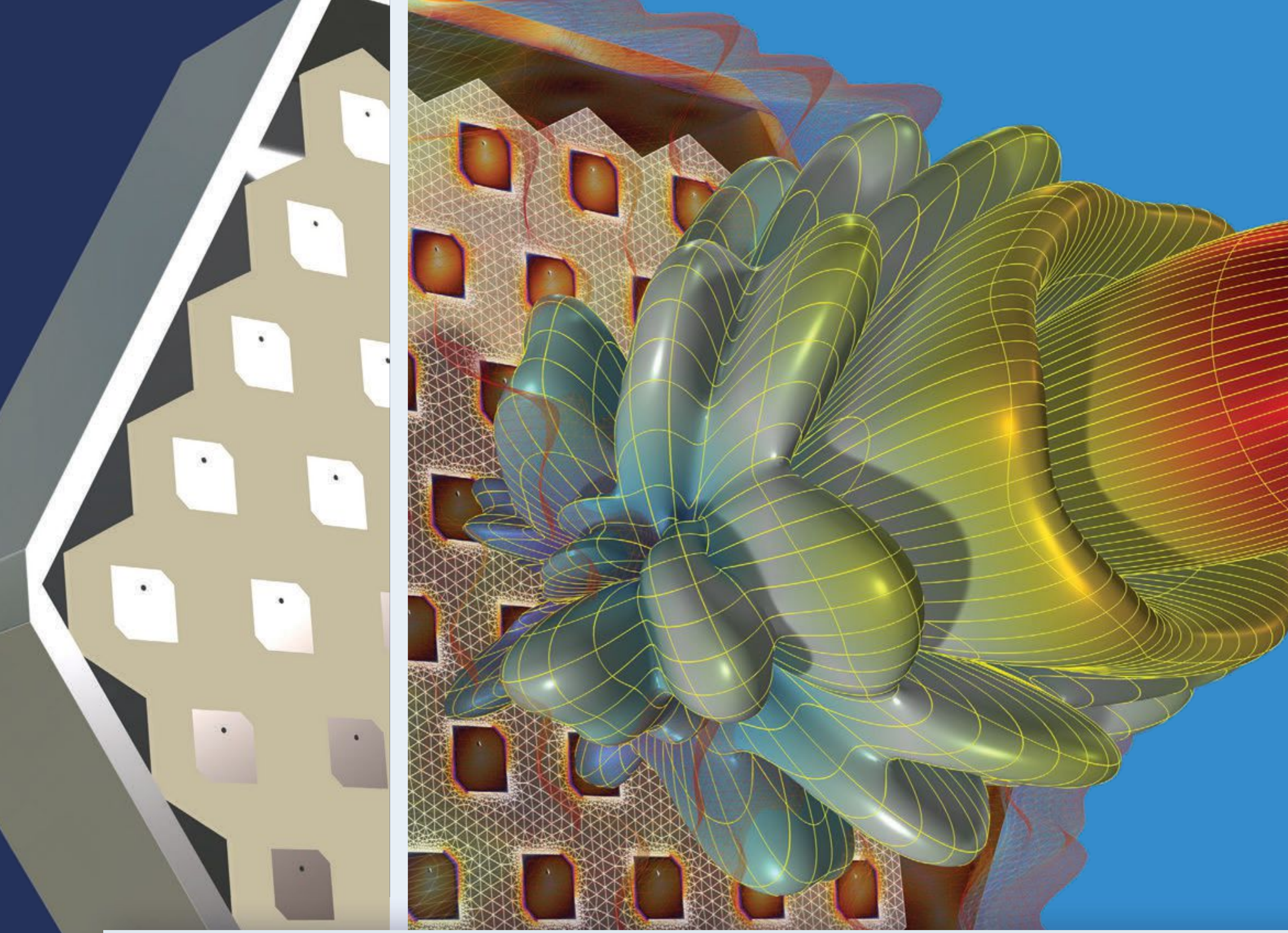

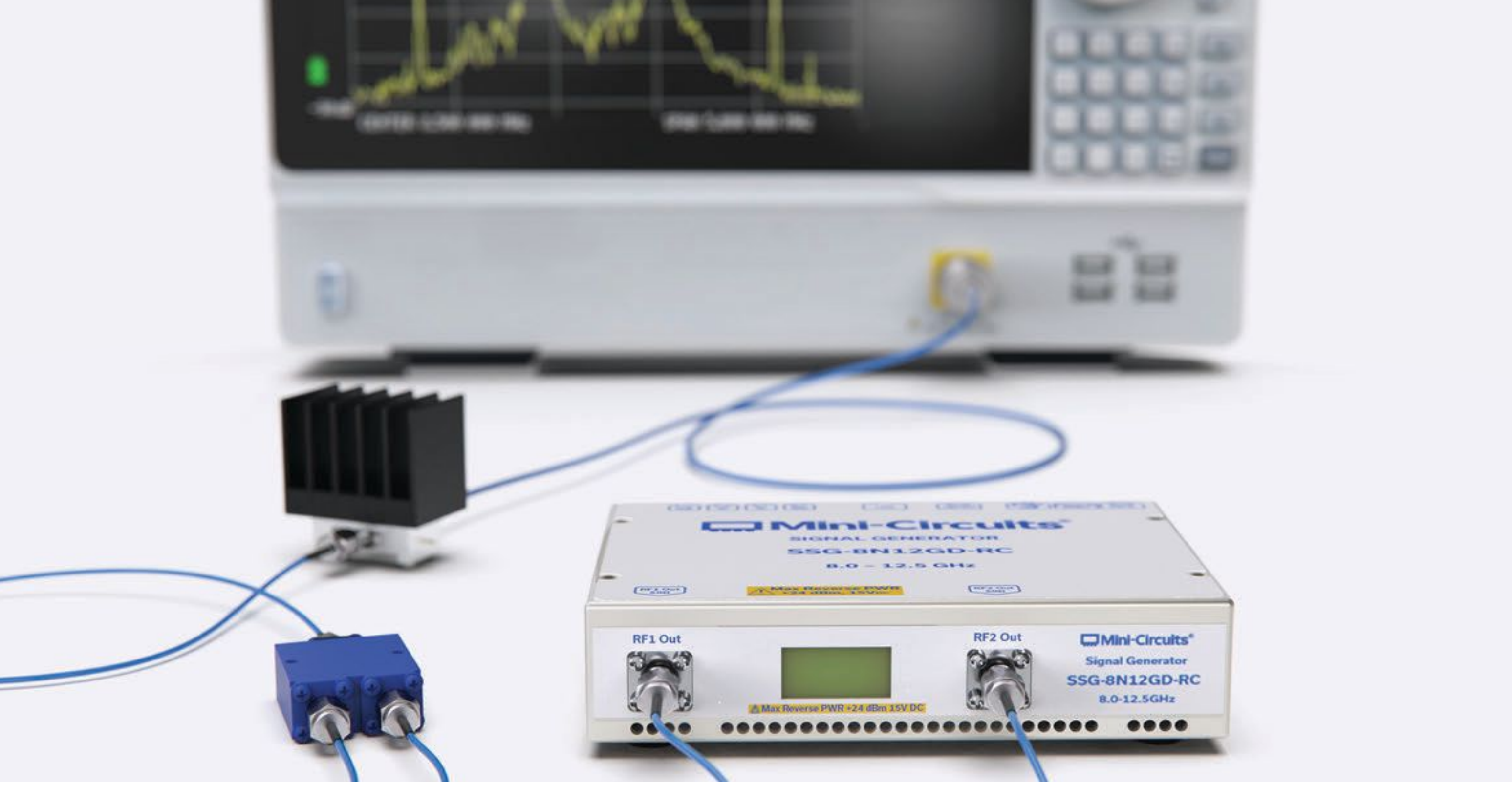

SSG SERIES

Signal Generators

Single-Channel & Dual Channel

LEARN MORE

Highlights

- Wide output power range
- Dual outputs with 360° independent phase control
- Pulsed, CW, AM, FM, and chirp modulations
- USB, Ethernet & PoE control interfaces
- Daisy chain port for multi-module control
- Compact housing, 3.6 x 5.1 x 1.2″

Model Number	Frequency	Output Power	# Channels	Release Status
SSG-8N12G-RC	8 to 12.5 GHz	-55 to 23 dBm	1	Production
SSG-8N12GD-RC	8 to 12.5 GHz	-55 to 23 dBm	2	Production
SSG-5N9G-RC	5 to 9 GHz	-55 to 23 dBm	1	Production
SSG-5N9GD-RC	5 to 9 GHz	-55 to 23 dBm	2	Production
SSG-9G-RC	0.01 to 9 GHz	-50 to 15 dBm	1	Q2, 2025
SSG-9GD-RC	0.01 to 9 GHz	-50 to 15 dBm	2	Q2, 2025
SSG-R7N6G-RC	0.7 to 6 GHz	-55 to 23 dBm	1	Q2, 2025
SSG-R7N6GD-RC	0.7 to 6 GHz	-55 to 23 dBm	2	Q3, 2025
SSG-1R5G-RC	0.02 to 1.5 GHz	-55 to 23 dBm	1	Q3, 2025
SSG-1R5GD-RC	0.02 to 1.5 GHz	-55 to 23 dBm	2	Q3, 2025

Mini-Circuits®

MARK YOUR CALENDAR

STAY CONNECTED TO COMING EVENTS

AUGUST

18-22
IEEE EMC + SIPI
Raleigh, N.C.
https://emc2025.org

27-30
IEEE RFID-TA
Valence, France
https://2025.ieee-rfid-ta.org

SEPTEMBER

3-4
C-UAS & Integrated Protection Summit
Huntsville, Ala.
https://cuas.dsigroup.org

21-26
EuMW 2025
Utrecht, The Netherlands
www.eumw.eu

OCTOBER

8-10
Comsol Conference 2025
Boston, Mass.
www.comsol.com/conference

12-15
BCICTS
Scottsdale, Ariz.
https://bcicts.org

NOVEMBER

2-7
AMTA
Tucson, Ariz.
https://2025.amta.org

3-6
Global MilSatCom
London, U.K.
www.smgconferences.com/defence/uk/conference/global-milsatcom

18-20
Space Tech Expo EU
Bremen, Germany
www.spacetechexpo-europe.com

DECEMBER

6–10
IEDM 2025
San Francisco, Calif.
www.ieee-iedm.org

Register online at signalintegrityjournal.com

ONLINE PANEL SERIES

9/12
Challenges Bring a 112 G and 224 G System to Market

Call for Papers Deadlines

10/1 IEEE IMFW 2026

9/14 IEEE WCNC 2026

FOR DETAILS VISIT MWJOURNAL.COM/EVENTS

Has Amplifier Performance or

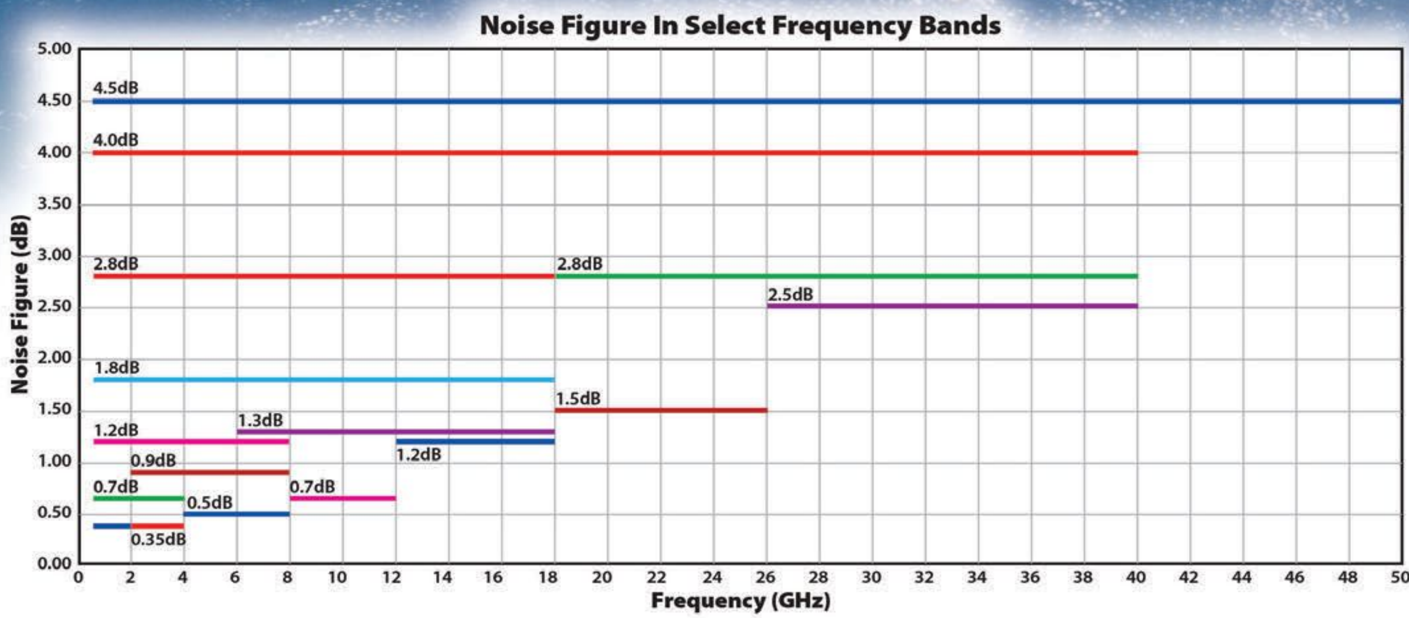


Delivery Stalled Your Program?
Features:
5 kHz to 50 GHz
Noise Figures:
from 0.35 dB @ 23°C
from 10 K @ Cryogenic
P1 dB >+30 dBm
Up to 75 dB Gain
Input Power Limiter
Excellent Group Delay
Gain & Phase Matching
Temperature Compensation
Waveguide Connectors
Weather-Proof Enclosures
B&Z is the preferred source for
high performance amplifiers.
B&Z TECHNOLOGIES
INNOVATING TO EXCEL
www.bnztech.com

The Netherlands and Belgium: Crossroads of the European Microwave Industry

Helen Duncan
MWE Media Ltd.

Belgium has frequently been called "the crossroads of Europe," and its neighbor, the Netherlands, can rightly share in that description too. The region is collectively known as Benelux, incorporating the tiny Grand Duchy of Luxembourg (population 660,000) as well as the Netherlands and Belgium, with populations of 17.8 million and 11.7 million, respectively. The Benelux region is bordered by France to the south and by Germany to the east, with the U.K. just a short hop across the English Channel (or a short train ride via the Channel Tunnel).

It was fitting that the Netherlands was chosen as the location for the very first European Microwave Week (EuMW), which took place in Amsterdam in 1998. At the center of Europe, it was a choice that recognized the notable concentration of EU research and development (R&D) capability in the region.

Utrecht was originally intended to be the venue for EuMW 2020, but the COVID-19 pandemic intervened, forcing the cancellation of the physical conference and exhibition, which was replaced by a virtual event online. 2025 will therefore be the first time since its inception that EuMW has taken place in Utrecht — a picturesque city that can easily be reached in around 30 minutes by train, direct from Amsterdam Schiphol airport.

Benelux can truly be called the birthplace of today's EU, since the 1958 Treaty of the Benelux Economic Union — which made Benelux the world's first free international labor market — later provided the blueprint for the foundation of the European Economic Community, forerunner of the EU. The region still plays a key role in the government of the EU, being home to the Community Research and Development Information Service (CORDIS), which coordinates and disseminates the results from Horizon 2020 and other projects funded by the EU's framework programs for research and innovation.

SEMICONDUCTOR EXCELLENCE

Astonishingly, for a country that makes up only 4 percent of the total EU population, the Netherlands can boast the largest semiconductor industry in Europe — even larger than Germany's. This is due to the world-leading position of ASML Holding NV, the Veldhoven-based manufacturer of photolithography equipment. ASML produces the only equipment capable of fabricating chip geometries below 7 nm.

In the manufacture of the chips themselves, however, it is the legacy of the former Philips Semiconductor in Eindhoven that dominates. Philips was once a leader in the consumer and professional electronics sectors, but now specializes in healthcare technology. There are many surviving RF and microwave spinoffs from Philips, like NXP (which later absorbed Freescale Semiconductor) and Ampleon, as well as startups founded by its alumni. This means there is a concentration of semiconductor expertise around Eindhoven


The only
QPL Certified
MECHANICAL
SWITCH
House!
Quick Turn
RF FILTER
Prototypes
are in our DNA!
Huge Library
of PASSIVES
with Best in Show
HIGH POWER
COUPLER
offering!
RUGGED & RELIABLE
AGILE & ADAPTIVE
HIGH POWER & VARIETY
RLC
RF MECHANICAL SWITCHES,
RF FILTERS & RF PASSIVES
AS9100 CERTIFIED, MADE IN USA
High Performance Precision Microwave Components
Serving the world-wide aerospace & defense community since 1959
Robust Catalog Portfolio - no hassle, quick turn, custom solutions our specialty
RLC Electronics | 83 Radio Circle, Mt. Kisco, NY 10549 | 914-241-1334 | sales@rlcelectronics.com | www.rlcelectronics.com

Fig. 1 Map of the Benelux region.

and the other former Philips facility in Nijmegen. The ecosystem around these campuses continues to foster new startups.

While NXP's flagship design and manufacturing operations are located at the Eindhoven High Tech Campus (HTCE), most of its RF work takes place in Nijmegen, where the ICN8 8-in. SiGe wafer fab is located, along with further R&D facilities. The fab produces a range of RF ICs for applications such as near field communication (NFC), secure identification, smart antennas for 5G and various industrial and IoT applications. However, NXP is increasingly focusing its efforts on automotive applications, as evidenced by its acquisition earlier this year of TTTech Auto. RF products for automotive currently include the Trimension Ultra-Wideband (UWB) IC family for smart access, KW45/47 wireless MCUs for Bluetooth Low Energy and the NCx332x automotive NFC frontend.

There have been reports that NXP plans to cease production at ICN8 over the next few years, as well as at three 8-in. fabs in the U.S., in favor of transitioning to 12-in. (300 mm) production at its new joint venture in Singapore, VSMC, where it is partnered with Vanguard International Semiconductor. NXP is also a partner in the European Semiconductor Manufacturing Company (ESMC) in Dresden, along with TSMC, Bosch and Infineon. 300 mm production is planned to start at both VSMC and ESMC in 2027. Nevertheless, there is speculation that the Nijmegen fab could be sold to another semiconductor company rather than be closed.

RF power specialist Ampleon was founded in Nijmegen in 2015 and offers a range of discrete transistors, MMICs, pallets and modules in LDMOS, as well as GaN technology for applications such as mobile broadband infrastructure, radar and air-traffic control, RF cooking, heating and plasma lighting and other industrial applications.

New in May this year was the CLF24H4LS300P and CLP24H4S30P high-efficiency GaN-on-SiC-based 2.4 GHz RF power amplifier (PA) lineup, designed for ISM applications and shown in ***Figure 2***. With up to 350 W CW output, the pair provides a compact, rugged, solid-state alternative to traditional magnetron-based systems.

The CLF24H4LS300P final stage and CLP24H4S30P driver amplifier cover the full 2.4 to 2.5 GHz ISM band. The dual-stage architecture achieves more than 66 percent drain efficiency, which not only helps reduce power consumption but also simplifies thermal management. It is suited to applications such as

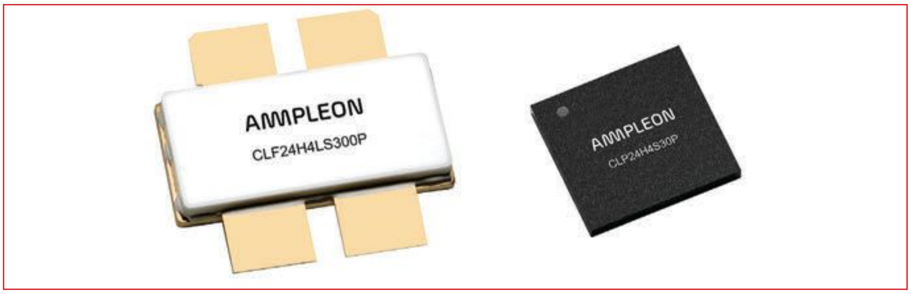

Fig. 2 The Ampleon CLF24H4LS300P power amplifier and CLP24H4S30P driver amplifier.

industrial heating, medical therapies, plasma generation, microwave chemistry, MW-PECVD processes and solid-state cooking, including combi oven systems.

Featuring an internally matched 50 Ohm input and output, onboard analog temperature sensor, surface-mount circulator and directional coupler, real-time monitoring and system-level protection are enabled. The compact 105 × 33 mm footprint makes it easy to integrate into space-constrained environments, and the amplifier lineup performs under mismatch conditions up to 20:1 VSWR at 50 V.

TECH CAMPUS

Smaller RF and microwave companies and startups with connections to the Noviotech Campus in Nijmegen, where both NXP and Ampleon are based, include:

- pinkRF, which specializes in solid-state RF energy systems for applications in the industrial, medical and scientific sectors. Its flagship products are solid-state RF signal generators and power generators, including a four-channel 2.45 GHz RF power generator, MPG4×250S, in which the channels can be used either as independent 250 W generators in coherent or incoherent operation, or with an optional external combiner as a single-channel, 1000 W generator.
- Leijenar Electronics became a full-time business at the Novitech Campus in 2021 but then relocated to Venray in 2024 to acquire more space for further expansion. The company provides RF and microwave design services from the initial concept to a working product, for applications that include RF energy, satcom, CATV, satellite transponders, antennas and IoT. It has the equipment and expertise to test and characterize devices up to 20 GHz and in the field of RF power, it has an automated setup that can measure up to 2 kW and above in CW mode, with a frequency range of up to 3 GHz.

EINDHOVEN

Altum RF in Eindhoven designs

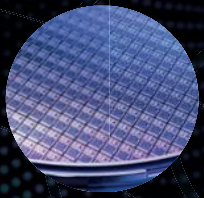

and manufactures high performance RF to mmWave components for systems with demanding performance requirements, including telecoms, satcom, radar and test and measurement.

At this year's IMS, Altum RF introduced a new family of bare die E-Band PAs and low noise amplifiers to support mmWave telecom and satcom applications, with the PAs featuring high output power and gain levels for longer-range links. ARF1018 is a 71 to 76 GHz PA offering 1.8 W (32.5 dBm) saturated output power and 27 dB gain, with a power-added efficiency (PAE) of 18 percent and 39 dBm output IP3. The ARF1019 high-band PA at 81 to 86 GHz has 1.6 W (32 dBm) Psat, 15 percent PAE and an OIP3 level of 38 dBm. Both E-Band PAs integrate an on-chip power detector.

A companion LNA, ARF1206, operates across the full 71 to 86 GHz band with a noise figure of 2.5 dB to 3.5 dB, a gain of 20 dB and a typical input and output return loss of 10 dB. It consumes 45 mA of current from a 4 V supply, and has a footprint of 1.3 × 1.35 mm.

ANTENNAS

In January of this year, Altum RF announced a milestone in its partnership with The Antenna Company, a startup also based at Eindhoven's HTCE. The A-3 Project is supported by the Metropoolregio Eindhoven (Metropolitan Region Eindhoven), a collaboration between 21 municipalities in the Eindhoven area — also known as the Brainport Region — set up to foster the local economy and business relationships, particularly in the technology ecosystem that has built up with NXP and ASML at its center.

The A-3 Project has focused on antenna-amplifier co-design to improve efficiency and interface characteristics at frequencies around 6 GHz and above, and on the development of new antenna arrays using LTCC technology to improve heat management. The initiative has so far yielded two antenna prototypes, one for 5.8 GHz Wi-Fi and another for mmWave 5G at 28 GHz.

The Antenna Company's other products include both standard and customized solutions for 4G/5G, NB-IoT, LoRa, Bluetooth, UWB, GPS/GNSS, Wi-Fi and mmWave, at frequency ranges from 410 MHz to 39 GHz.

Antennex develops advanced over-the-air (OTA) test systems tailored for integrated antennas and complex RF front-ends. Headquartered in Eindhoven, the company works with leading aerospace, telecom and automotive customers to streamline performance character-

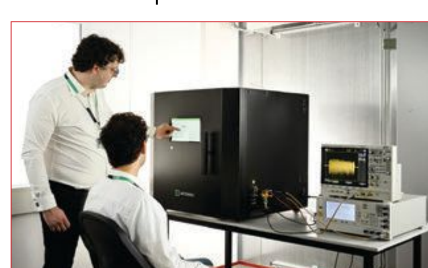

▲ Fig. 3 The Antennex over-the-air measurement system for antennas.


WWW.RFECHO.COM

ization in integrated environments. Introduced at IMS2025, a new radar testing feature, shown in ***Figure 3***, allows engineers to measure chirp rate, chirp linearity and radiated power spectral density accurately OTA on high frequency radar systems, independent of the direction of radiation of the radar. The system can rapidly acquire radiated signal measurements, allowing tests over several GHz of bandwidth in a few seconds.

Testing the radiated power or chirp linearity and rate of a radar is traditionally very difficult due to the variation in direction of radiation over frequency. The Antennex measurement platform solves this issue, making the tests easier and faster, and can help avoid weeks to months of debugging. The Antennex system comes with instrument integration libraries that automatically control instruments from well-known vendors without the need to write SCPI commands for instrument compatibility.

Anouk Hubrechsen, CEO of Antennex (who is also the Women in Microwave Engineering Chair for EuMW this year), commented, "There is a trend for devices to become significantly more integrated, with the antenna as an integral part. This means that many tests can only be done OTA. Wireless tests are traditionally slow and inaccurate, and Antennex has set out to solve that with a disruptive new technology."

Staal Instruments is also based in Eindhoven. Its maxSHIFT60 wireless radar level sensor at 60 GHz is designed to offer reliable level monitoring for tanks, containers and sewers. With a 10 m range, 4G connectivity and battery power, it provides accurate data and integrates with the cloud for monitoring and alerts.

RESEARCH AND DEVELOPMENT

An organization always at the forefront of R&D in the Netherlands RF and microwave community is TNO, an independent research organization based in The Hague, which has played a pivotal role in EuMW over many years. Frank van den Bogaart, the president of the European Microwave Association, was a principal advisor at TNO until last year and was also a member of the steering committee of the Dutch Radar Centre of Expertise (D-RACE), a strategic cooperation between TNO and Thales Nederland. A special session at EuRAD 2025 will explore the past, present and future of the Dutch ecosystem for defense radar. It will feature speaker Frank van Vliet, who is a principal scientist at TNO and a member of the EuMA Board of Directors.

TNO has a broad mission to connect people and knowledge, creating innovations that enhance the competitive strength of industry and the well-being of society in a sustainable manner. It focuses on driving change and improvement across several areas, including defense, safety, security, energy, healthy living, smart manufacturing, ICT and transportation applications where microwave technology plays

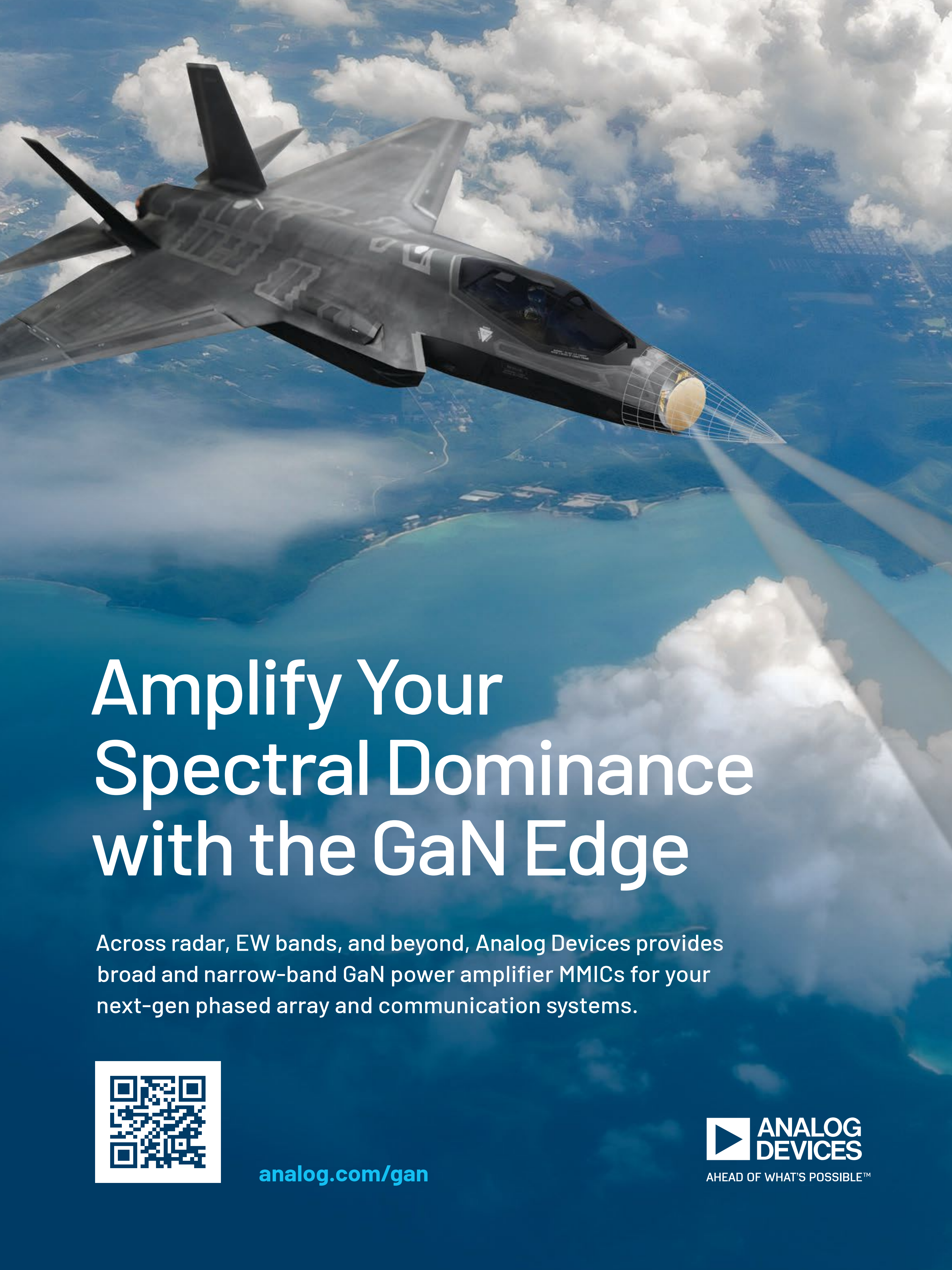
Amplify Your Spectral Dominance with the GaN Edge
Across radar, EW bands, and beyond, Analog Devices provides broad and narrow-band GaN power amplifier MMICs for your next-gen phased array and communication systems.
analog.com/gan
ANALOG DEVICES
AHEAD OF WHAT'S POSSIBLE™

a significant role.

Recent technical publications by TNO researchers include a paper at last year's European Microwave Conference on the topic of CVD diamond heat spreaders to improve the performance of a 400 W AlGaN/GaN S-Band PA MMIC, by M. van Heijningen et al. Another paper, presented at an international metamaterials conference, featured the design of cloaking and transparent metasurfaces using split-ring resonators.

EUROPEAN SPACE AGENCY

The European Space Research and Technology Centre (ESTEC) in Noordwijk is both the largest site of the European Space Agency (ESA) and its main technology hub for R&D. ESA and ESTEC both celebrated their 50th anniversary this year with a series of events.

Earlier this year, ESA's Radio Frequency Equipment and Technology section tested a new patented antenna beamforming technique that used geometrical symmetry to direct the beams in the desired directions, thus reducing the number of components required and consequently, the size, mass and power consumption.

Figure 4 shows the advanced beamforming technique under test in the recently extended anechoic chamber at the Hybrid European Radio Frequency and Antenna Test Zone (HERTZ) at ESTEC.

SIMULATION

Dutch software vendor COMSOL provides multiphysics simulation software that can be used for modeling designs, devices and processes in all fields of engineering, including electromagnetics and is particularly applicable for modeling antennas and their radiation patterns. New to COMSOL Multiphysics version 6.3 is a chatbot window functionality that connects the user directly to OpenAI GPT models, allowing them to generate or debug COMSOL API code to automate workflows, add custom functionality to apps and integrate with external tools. For example, it is capable of helping convert repetitive tasks into loops or locate logic errors in a method. It can also be used to query for general modeling advice.

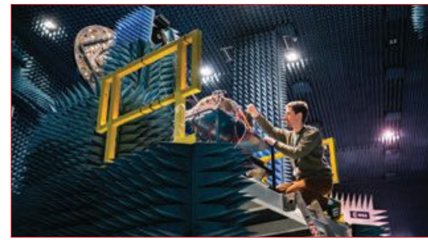

Fig. 4 **A new beamforming technique being tested in ESA's HERTZ chamber.** ***Source:*** **ESA-SJM Photography.**

ANECHOIC CHAMBERS AND MATERIALS

Given the prominence of antenna design in the Benelux region, it is not surprising that there is a proliferation of suppliers of test chambers, absorber materials and test equipment in Belgium and the Netherlands.

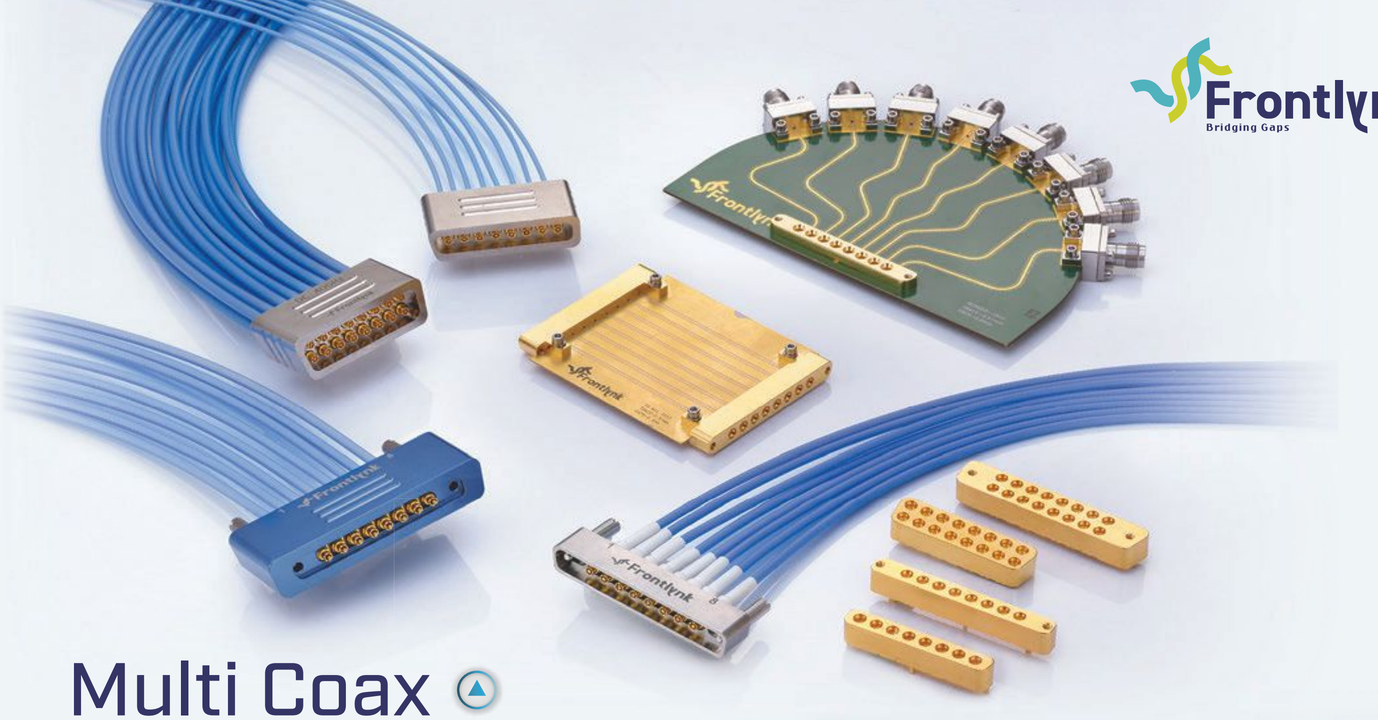

Holland Shielding Systems in Dordrecht makes a range of EMC and EMI shielding materials, Faraday cages and test enclosures (including those for military bunkers and TEMPEST rooms) and absorbers. They specialize in short delivery times, with the ability to design and manufacture custom-made products in two to three days.

Comtest is a family-owned business in Zoeterwoude, the Netherlands, owned by the de Groot family. The company, which celebrated its 40th anniversary in July this year, builds anechoic chambers, EMC test chambers and antenna test ranges for a wide range of industrial and research applications.

Dutch Microwave Absorber Solutions (DMAS), also in Zoeterwoude, is an independent supplier of high performance expanded polystyrene microwave absorbers suitable for anechoic and semi-anechoic chambers for both EMC and broadband microwave testing.

E&C Anechoic Chambers develops and manufactures microwave absorbing materials and anechoic chambers in Westerlo, Belgium. Originally a division of Emerson & Cuming, it is now part of German anechoic chamber company Albatross Projects.

CHIP DESIGN IN BELGIUM

Imec in Leuven, Belgium, is a center of excellence in the European electronics industry, not only in microwave and RF but in all branches of electronics. It claims to be the world's largest independent research and innovation center for nanoelectronics and digital technology, with a global ecosystem that includes startups, industrial partners and over 200 universities.

The specialist research and innovation organization has offices and labs across Belgium and the Netherlands, with others in the U.S. and across Asia Pacific, as well as a recently opened office in Cambridge, U.K. The Leuven facility includes both 200 and 300 mm semiconductor pilot lines with extensive cleanrooms and labs, enabling innovation spanning R&D, prototyping and manufacturing.

In June this year, Imec announced a new RF transistor process aimed at integrating GaN technology into next-generation mobile devices, particularly those targeting the 6G FR3 band between 7 and 24 GHz. The GaN-on-Si metal-oxide-semiconductor high-electron-mobility transistor (MOSHEMT) offers exceptional efficiency and output power for an enhancement-mode (E-mode) device operating at low supply voltage. At the same time, they demonstrated a record-low contact resistance of 0.024 Ohm·mm, which will further boost output power in future designs.

The shift to higher frequencies required to meet the data rate demands of 6G systems means that existing GaAs HBTs will struggle to achieve the required performance, as their efficiency and gain degrade sig-

RF-LAMBDA

MADE IN USA

THE LEADER OF RF BROADBAND SOLUTIONS

EMC Broadband RF Power Amplifier

High Power Solid State

HUNDREDS IN STOCK

FAST SHIPPING

FREQUENCY UP TO 90GHZ

POWER UP TO 2KW CW

BENCHTOP AND RACKMOUNT

REMC06G18GG 6-18GHZ 400W

- AUTOMATIC BUILT IN SELF CALIBRATION AND BIAS ADJUSTMENT.
- OVER TEMPERATURE, CURRENT, INPUT POWER PROTECTION.
- VSWR MEASUREMENT AND OPEN CIRCUIT PROTECTION.
- USER FRIENDLY CONTROL INTERFACE.
- REMOTE ETHERNET CONTROL AND FIRMWARE UPDATE.
- HIGH POWER EFFICIENCY AND LIGHTWEIGHT.

RAMP42G47GA 42-47GHZ 8W

REMC02G06GE 2-6GHZ 500W

RAMP18G40GB-U 18-40G 20W

RAMP05M80GC 0.5-80GHZ

REMC18G40GQ 18-40GHZ 200W CW

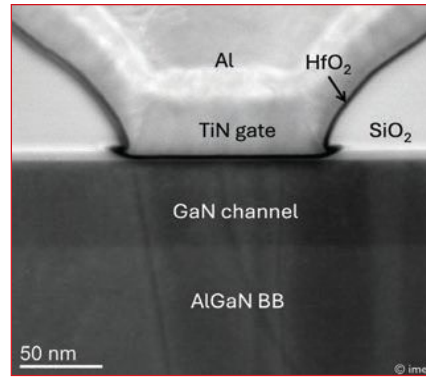

Fig. 5 **Cross-sectional TEM image of Imec's MOSHEMT transistor.**

nificantly above 10 to 15 GHz. GaN has been recognized as a promising alternative due to its higher power density and breakdown voltage. Although GaN-on-SiC transistors have shown good performance in higher frequency base station applications, the cost of the SiC process is a barrier for the mobile market. Building high-efficiency GaN-on-Si transistors has previously been challenging due to the lattice and thermal mismatch between the two materials, which can compromise material quality and device reliability, a challenge that is even greater for E-mode designs that typically require thinning the transistor barrier and channel under the gate.

The GaN-on-Si E-mode MOSHEMT developed by Imec reaches 27.8 dBm output power — equivalent to 1 W/mm — and 66 percent PAE at 13 GHz when operating at 5 V. This result was obtained from a single device with an eight-finger gate layout, providing the gate width needed for high output power without requiring the combined power of multiple transistors. ***Figure 5*** shows a cross-sectional TEM image of the gate structure in Imec's GaN-on-Si MOSHEMT transistor for 6G mobile applications.

In another recent development, Photonics Research Group and IDlab, which are both Imec research groups at Ghent University, published in *Nature Communications* a demonstration of a fully-integrated single-chip microwave photonics system, combining optical and microwave signal processing on a single silicon chip. The chip integrates high speed modulators, optical filters, photodetectors and trans-


HIGH FREQUENCY Components
PPI
Passive Plus
RF & Microwave Components
HIGH QUALITY
RF/MICROWAVE PASSIVE COMPONENTS FOR HIGH FREQUENCY APPLICATIONS
Broadband Capacitors
5 case sizes, 10nF & 100nF
up to 67 GHz
Broadband Resistors
1209 & 2010 sizes
up to 67 GHz
Broadband Conical Inductors
Flying Leads & SMT
up to 110 GHz
Reach out for Availability
www.passiveplus.com
+ (631) 425-0938
sales@passiveplus.com

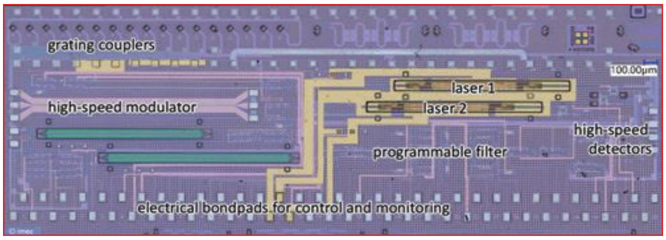

Fig. 6 Microscope image of Imec/University of Ghent microwave photonic chip.

fer-printed lasers, making it a compact, self-contained and programmable solution for high frequency signal processing. By replacing larger, power-hungry components, the new chip will enable faster wireless networks, low-cost microwave sensing and scalable deployment in applications like 6G, as well as satcom and radar systems. ***Figure 6*** shows a microscope image of the microwave photonic chip, integrating high speed modulators and detectors, a programmable optical filter bank and two transfer-printed lasers.

Tusk IC is a specialist mmWave IC design house based in Antwerp, Belgium. It was founded in January 2018 and focuses on designs for satcom beamforming and similar applications in CMOS, RFSOI and SiGe process nodes. Other work has included designs from 60 to 600 GHz in bulk CMOS.

Tusk IC's current NEBULA project aims to develop cost-effective, modular Ka-Band RF beamforming solutions for the LEO/MEO/GEO ground segment of Ka-Band satellite communication links. This product is currently under development with the ESA under the ARTES program.

Also under development is a customizable multi-channel Ka-Band beamformer IC for satcom and 5G infrastructure, supporting both receive (17.3 to 21.2 GHz) and transmit (27.5 to 31 GHz) for phased arrays and active electronically steered antenna. Although targeted at LEO, MEO and GEO satellite applications, the transmitter is also suitable for use in 5G infrastructure.

CONCLUSION

The Benelux region holds a pivotal position in R&D in Europe, providing a home not only for the EU's principal R&D administrative organization but also three world-class research hubs: TNO, Imec and ESTEC. The strength of both countries, but particularly the Netherlands, in both silicon and compound semiconductor technology is primarily due to the legacy of Philips Semiconductors, which continues to inspire a new generation of younger companies and startups. Expertise in antenna technology, as well as the test facilities required for this, has also flowed from the presence there of ESTEC and its leading position in developing satellite communications technology. ■

Advertorial

ROHDE&SCHWARZ

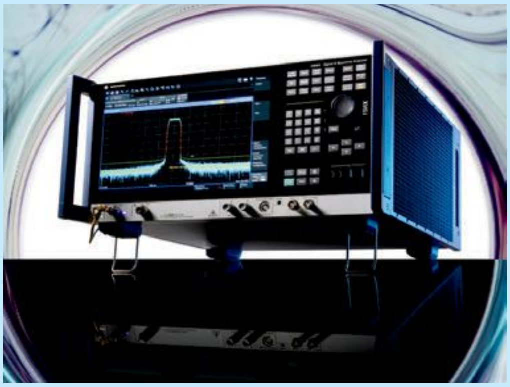

FSWX Signal and Spectrum Analyzer:
Measure the Impossible

Revolutionizing Signal and Spectrum Analysis: The FSWX with its Cross-Correlation Technology

Rohde & Schwarz has introduced the FSWX signal and spectrum analyzer, a game-changing instrument that redefines how engineers approach RF system testing. With its innovative architecture, which integrates multiple input ports and advanced cross-correlation technology, the FSWX is designed to overcome the limitations of traditional analyzers and meet the demands of increasingly complex RF systems.

CROSS-CORRELATION: ELIMINATING NOISE FOR UNPARALLELED PRECISION

One of the most transformative features of the FSWX is its built-in cross-correlation technology, which addresses a critical challenge in spectrum analysis: the instrument's own noise floor. Traditional analyzers often struggle to detect weak signals or small spurs near the thermal noise level due to noise introduced by the measurement system itself. The FSWX resolves this issue by employing cross-correlation to suppress its internal noise.

This capability dramatically improves the dynamic range, allowing engineers to uncover signals that were previously masked or to measure performance beyond the limitations of the signal analyzer's own signal-to-noise ratio. For example, for error vector magnitude (EVM) measurements cross-correlation extends the range of accurate measurements even for low-power signals. It also enhances mid-to-high power accuracy by mitigating the impact of the analyzer's phase noise. This results in more precise and reliable data, critical for applications such as radar, satellite communication, amplifier characterization or signal source analysis.

SIMPLIFYING COMPLEX SETUPS WITH MULTI-PORT ANALYSIS

Beyond its noise suppression capabilities, the multi-port input architecture of the FSWX opens up new possibilities for simultaneous multi-channel analysis. Engineers can now measure phase, amplitude and timing variations across multiple signal paths in systems like phased array antennas, or they can analyze multi-standard communication scenarios.

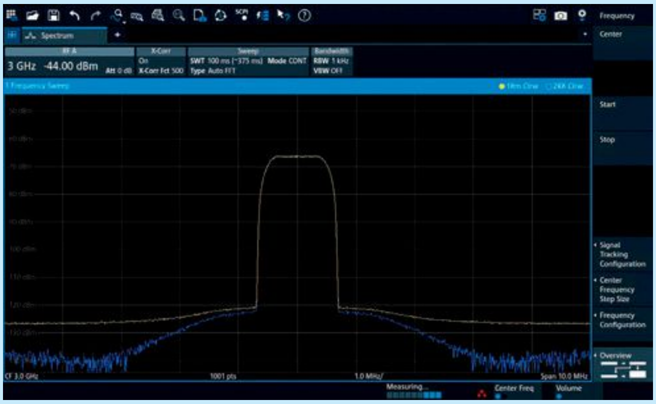

Cross-correlation eliminates the analyzer's inherent noise, providing unobstructed view of the signal

For active two-port device characterization, the two paths simplify testing while improving accuracy by enabling real-time comparisons between input and output signals.

For example, in amplifier testing, the FSWX, with its ability to simultaneously capture input and output signals, provides insights into nonlinearities, spectral regrowth, and AM-AM conversion. Similarly, in electronic warfare scenarios, the analyzer's advanced pulse analysis capabilities allow for precise characterization of radar signals or DRFMs.

MEASURE THE IMPOSSIBLE

The FSWX signal and spectrum analyzer from Rohde & Schwarz represents a paradigm shift in RF testing, combining cutting-edge cross-correlation technology with a multi-port design to address the challenges of modern RF systems. By suppressing noise and simplifying complex setups, the FSWX empowers engineers to achieve measurement precision and reliability that were previously out of reach. Whether working with faint signals, multi-channel scenarios or complex wideband setups, the FSWX is poised to transform how engineers measure the impossible.

www.rohde-schwarz.com/measure-the-impossible

EUROPEAN MICROWAVE WEEK
JAARBEURS UTRECHT
THE NETHERLANDS
21-26 SEPTEMBER 2025
www.eumw.eu
WAVES OF INNOVATION

VISIT ROHDE & SCHWARZ AT EUMW 2025 IN UTRECHT AT BOOTH A026 TO EXPERIENCE THE FSWX FOR YOURSELF.

RF Amplifiers and Sub-Assemblies for Every Application

Delivery from Stock to 2 Weeks ARO from the catalog or built to your specifications!

- Competitive Pricing & Fast Delivery
- Military Reliability & Qualification
- Various Options: Temperature Compensation, Input Limiter Protection, Detectors/TTL & More
- Unconditionally Stable (100% tested)

ISO 9001:2000 and AS9100B CERTIFIED

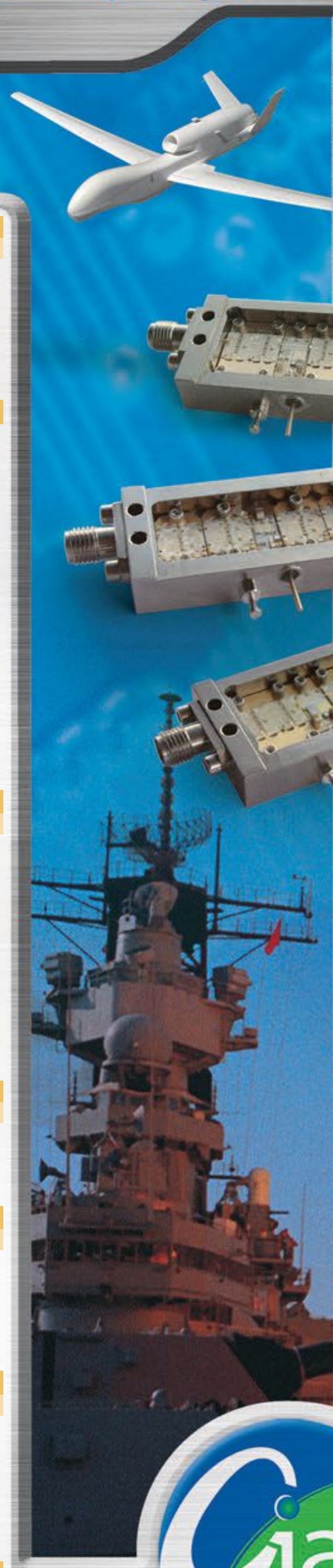

OCTAVE BAND LOW NOISE AMPLIFIERS

Model No.	Freq (GHz)	Gain (dB) MIN	Noise Figure (dB)	Power-out @ P1-dB	3rd Order ICP	VSWR
CA01-2110	0.5-1.0	28	1.0 MAX, 0.7 TYP	+10 MIN	+20 dBm	2.0:1
CA12-2110	1.0-2.0	30	1.0 MAX, 0.7 TYP	+10 MIN	+20 dBm	2.0:1
CA24-2111	2.0-4.0	29	1.1 MAX, 0.95 TYP	+10 MIN	+20 dBm	2.0:1
CA48-2111	4.0-8.0	29	1.3 MAX, 1.0 TYP	+10 MIN	+20 dBm	2.0:1
CA812-3111	8.0-12.0	27	1.6 MAX, 1.4 TYP	+10 MIN	+20 dBm	2.0:1
CA1218-4111	12.0-18.0	25	1.9 MAX, 1.7 TYP	+10 MIN	+20 dBm	2.0:1
CA1826-2110	18.0-26.5	32	3.0 MAX, 2.5 TYP	+10 MIN	+20 dBm	2.0:1

NARROW BAND LOW NOISE AND MEDIUM POWER AMPLIFIERS

Model No.	Freq (GHz)	Gain (dB) MIN	Noise Figure (dB)	Power-out @ P1-dB	3rd Order ICP	VSWR
CA01-2111	0.4 - 0.5	28	0.6 MAX, 0.4 TYP	+10 MIN	+20 dBm	2.0:1
CA01-2113	0.8 - 1.0	28	0.6 MAX, 0.4 TYP	+10 MIN	+20 dBm	2.0:1
CA12-3117	1.2 - 1.6	25	0.6 MAX, 0.4 TYP	+10 MIN	+20 dBm	2.0:1
CA23-3111	2.2 - 2.4	30	0.6 MAX, 0.45 TYP	+10 MIN	+20 dBm	2.0:1
CA23-3116	2.7 - 2.9	29	0.7 MAX, 0.5 TYP	+10 MIN	+20 dBm	2.0:1
CA34-2110	3.7 - 4.2	28	1.0 MAX, 0.5 TYP	+10 MIN	+20 dBm	2.0:1
CA56-3110	5.4 - 5.9	40	1.0 MAX, 0.5 TYP	+10 MIN	+20 dBm	2.0:1
CA78-4110	7.25 - 7.75	32	1.2 MAX, 1.0 TYP	+10 MIN	+20 dBm	2.0:1
CA910-3110	9.0 - 10.6	25	1.4 MAX, 1.2 TYP	+10 MIN	+20 dBm	2.0:1
CA1315-3110	13.75 - 15.4	25	1.6 MAX, 1.4 TYP	+10 MIN	+20 dBm	2.0:1
CA12-3114	1.35 - 1.85	30	4.0 MAX, 3.0 TYP	+33 MIN	+41 dBm	2.0:1
CA34-6116	3.1 - 3.5	40	4.5 MAX, 3.5 TYP	+35 MIN	+43 dBm	2.0:1
CA56-5114	5.9 - 6.4	30	5.0 MAX, 4.0 TYP	+30 MIN	+40 dBm	2.0:1
CA812-6115	8.0 - 12.0	30	4.5 MAX, 3.5 TYP	+30 MIN	+40 dBm	2.0:1
CA812-6116	8.0 - 12.0	30	5.0 MAX, 4.0 TYP	+33 MIN	+41 dBm	2.0:1
CA1213-7110	12.2 - 13.25	28	6.0 MAX, 5.5 TYP	+33 MIN	+42 dBm	2.0:1
CA1415-7110	14.0 - 15.0	30	5.0 MAX, 4.0 TYP	+30 MIN	+40 dBm	2.0:1
CA1722-4110	17.0 - 22.0	25	3.5 MAX, 2.8 TYP	+21 MIN	+31 dBm	2.0:1

ULTRA-BROADBAND & MULTI-OCTAVE BAND AMPLIFIERS

Model No.	Freq (GHz)	Gain (dB) MIN	Noise Figure (dB)	Power-out @ P1-dB	3rd Order ICP	VSWR
CA0102-3111	0.1-2.0	28	1.6 Max, 1.2 TYP	+10 MIN	+20 dBm	2.0:1
CA0106-3111	0.1-6.0	28	1.9 Max, 1.5 TYP	+10 MIN	+20 dBm	2.0:1
CA0108-3110	0.1-8.0	26	2.2 Max, 1.8 TYP	+10 MIN	+20 dBm	2.0:1
CA0108-4112	0.1-8.0	32	3.0 MAX, 1.8 TYP	+22 MIN	+32 dBm	2.0:1
CA02-3112	0.5-2.0	36	4.5 MAX, 2.5 TYP	+30 MIN	+40 dBm	2.0:1
CA26-3110	2.0-6.0	26	2.0 MAX, 1.5 TYP	+10 MIN	+20 dBm	2.0:1
CA26-4114	2.0-6.0	22	5.0 MAX, 3.5 TYP	+30 MIN	+40 dBm	2.0:1
CA618-4112	6.0-18.0	25	5.0 MAX, 3.5 TYP	+23 MIN	+33 dBm	2.0:1
CA618-6114	6.0-18.0	35	5.0 MAX, 3.5 TYP	+30 MIN	+40 dBm	2.0:1
CA218-4116	2.0-18.0	30	3.5 MAX, 2.8 TYP	+10 MIN	+20 dBm	2.0:1
CA218-4110	2.0-18.0	30	5.0 MAX, 3.5 TYP	+20 MIN	+30 dBm	2.0:1
CA218-4112	2.0-18.0	29	5.0 MAX, 3.5 TYP	+24 MIN	+34 dBm	2.0:1

LIMITING AMPLIFIERS

Model No.	Freq (GHz)	Input Dynamic Range	Output Power Range Psat	Power Flatness dB	VSWR
CLA24-4001	2.0 - 4.0	-28 to +10 dBm	+7 to +11 dBm	+/- 1.5 MAX	2.0:1
CLA26-8001	2.0 - 6.0	-50 to +20 dBm	+14 to +18 dBm	+/- 1.5 MAX	2.0:1
CLA712-5001	7.0 - 12.4	-21 to +10 dBm	+14 to +19 dBm	+/- 1.5 MAX	2.0:1
CLA618-1201	6.0 - 18.0	-50 to +20 dBm	+14 to +19 dBm	+/- 1.5 MAX	2.0:1

AMPLIFIERS WITH INTEGRATED GAIN ATTENUATION

Model No.	Freq (GHz)	Gain (dB) MIN	Noise Figure (dB)	Power-out @ P1-dB	Gain Attenuation Range	VSWR
CA001-2511A	0.025-0.150	21	5.0 MAX, 3.5 TYP	+12 MIN	30 dB MIN	2.0:1
CA05-3110A	0.5-5.5	23	2.5 MAX, 1.5 TYP	+18 MIN	20 dB MIN	2.0:1
CA56-3110A	5.85-6.425	28	2.5 MAX, 1.5 TYP	+16 MIN	22 dB MIN	1.8:1
CA612-4110A	6.0-12.0	24	2.5 MAX, 1.5 TYP	+12 MIN	15 dB MIN	1.9:1
CA1315-4110A	13.75-15.4	25	2.2 MAX, 1.6 TYP	+16 MIN	20 dB MIN	1.8:1
CA1518-4110A	15.0-18.0	30	3.0 MAX, 2.0 TYP	+18 MIN	20 dB MIN	1.85:1

LOW FREQUENCY AMPLIFIERS

Model No.	Freq (GHz)	Gain (dB) MIN	Noise Figure dB	Power-out @ P1-dB	3rd Order ICP	VSWR
CA001-2110	0.01-0.10	18	4.0 MAX, 2.2 TYP	+10 MIN	+20 dBm	2.0:1
CA001-2211	0.04-0.15	24	3.5 MAX, 2.2 TYP	+13 MIN	+23 dBm	2.0:1
CA001-2215	0.04-0.15	23	4.0 MAX, 2.2 TYP	+23 MIN	+33 dBm	2.0:1
CA001-3113	0.01-1.0	28	4.0 MAX, 2.8 TYP	+17 MIN	+27 dBm	2.0:1
CA002-3114	0.01-2.0	27	4.0 MAX, 2.8 TYP	+20 MIN	+30 dBm	2.0:1
CA003-3116	0.01-3.0	18	4.0 MAX, 2.8 TYP	+25 MIN	+35 dBm	2.0:1
CA004-3112	0.01-4.0	32	4.0 MAX, 2.8 TYP	+15 MIN	+25 dBm	2.0:1

CIAO Wireless can easily modify any of its standard models to meet your "exact" requirements at the Catalog Pricing.

Visit our web site at www.ciaowireless.com for our complete product offering.

Ciao wireless

Ciao Wireless, Inc. 4000 Via Pescador, Camarillo, CA 93012

Tel (805) 389-3224 Fax (805) 389-3629 sales@ciaowireless.com

An American Shield: LM and MDA Demo Critical Radar Capability, Strengthening Homeland Defense

Lockheed Martin and the Missile Defense Agency (MDA) have successfully executed Flight Test Other-26a (FTX-26a). During FTX-26a, the Lockheed Martin-built Long Range Discrimination Radar (LRDR) successfully detected, tracked and discriminated a live ballistic missile threat in a complex environment, demonstrating its ability to provide critical data to homeland defense systems.

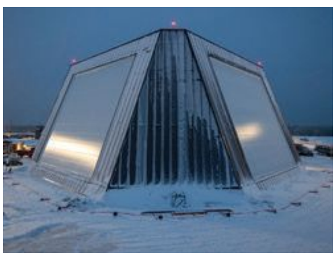

LRDR (Source: Lockheed Martin)

"Deterrence begins with detection, and the successful FTX-26a demonstration underscored LRDR's ability to detect and track threats at extended ranges, while accurately distinguishing between targets and non-targets," said Rick Cordaro, vice president of Lockheed Martin's Radar and Sensor Systems. "This technical advancement will significantly bolster our nation's deterrence capabilities, providing a game-changing asset for homeland defense. With its open architecture, LRDR will facilitate the seamless integration of emerging technologies and software, enabling warfighters to receive timely, actionable information for decision-making and drives rapid response."

FTX-26a took place over the North Pacific and demonstrated LRDR's capabilities against an air-launched threat — representative target with countermeasures. Under the command of Command and Control Battle Management and Communications (C2BMC), LRDR successfully tracked the target and forwarded data to C2BMC which then successfully shared the flight test data to support a simulated Ground-Based Midcourse Defense (GMD) engagement.

The mission achieved the following firsts:

- LRDR demonstrated the detection, tracking and discrimination of threats in a complex environment.
- C2BMC provided LRDR flight test data to support a simulated GMD engagement.

Revolutionary Drone Capabilities for Warfighters

Five cutting-edge unmanned aerial systems (UAS) began flight testing in June to highlight the versatility of vertical takeoff and landing for UAS weighing less than 330 pounds.

The vertical takeoff and landing (VTOL) aircraft for the demonstration, known as EVADE — Early VTOL Aircraft Demonstration — boast significantly enhanced range, endurance and control compared to existing VTOL UAS of similar size. The primary objective for EVADE is to demonstrate rapid deployment of advanced UAS capabilities to the warfighter.

"With EVADE, our focus is on speed of development, not on first flight perfection," said DARPA Program Manager Phillip Smith, who is a major in the U.S. Marine Corps Reserves and was previously deployed as an AV-8B Harrier pilot. "The faster we can get these demonstration aircraft airborne, the quicker we can identify and resolve any issues and ultimately, deliver game-changing capabilities to our warfighters in the field."

The EVADE initiative accelerates DARPA's AdvaNced airCraft Infrastructure-Less Launch And RecoverY (ANCILLARY) program Phase 2 plan, which the agency initially projected to conduct flight testing in late 2026. By prioritizing the integration of autonomy and payloads, EVADE aims to rapidly demonstrate the critical value of this UAS size class. Furthermore, by postponing specific requirements related to maximum physical dimensions and autonomous takeoff/landing in high sea states, the program has dramatically shortened the timeline to first flight.

To further accelerate production timelines and maximize resource efficiency, all EVADE platforms leverage the Sikorsky MATRIX flight autonomy algorithms developed in DARPA's Aircrew Labor In-Cockpit Automation System (ALIAS) program. The autonomy software manages flight control and navigation needs for entire missions — from takeoff to landing — and minimizes the need for user interaction during long transit flights. Having standardized autonomy software across all five performers and designs also simplifies user engagement.

EVADE (Source: DARPA)

Complementing this, the Naval Surface Warfare Center Dahlgren Division's payload management software Battle Management System (BMS) is used across all platforms, interfacing directly with the Tactical Assault Kit available to every warfighter. The integrated suite of tools allows ANCILLARY aircraft to immediately share relevant information with individual troops at the point of need. It also effectively eliminates the need for dedicated ground control stations, thereby reducing programmatic and operational costs.

"EVADE is designed to democratize air power across the military, empowering the smallest operational units to directly receive and control an air asset when needed," Smith said. "We're testing five potential mission sets and payloads to showcase the breadth of capabilities EVADE can provide: logistics, communications relay, weapons delivery, synthetic aperture radar and ISR/RSTA (intelligence, surveillance, reconnaissance and

For More Information Visit mwjournal.com for more defense news.

target acquisition)."

The five ANCILLARY designs vary in their capabilities, but all have a minimum of 12 hours of endurance at 100 nautical miles with a 60-pound payload. "I think of these aircraft as 'flying trucks,'" Smith said. "They have a high load fraction for their size and VTOL configurations and can be readily adapted to support a wide range of missions by carrying the necessary payload."

The five performers in EVADE — AeroVironment, Griffon Aerospace, Karem Aircraft, Method Aeronautics and Sikorsky — show some of the ways these aircraft can be optimized for different strengths, including VTOL control, airspeed, storage capacity, cruise altitude, time on station, powertrain configurations and control methodologies.

"With ANCILLARY, we aim to cultivate a thriving supplier ecosystem for these drones, or similar-sized systems, that can fundamentally transform the capabilities and situational awareness available to every warfighter," Smith said. "We're invested in the success of each UAS we're testing. The U.S. military requires a diverse portfolio of performers capable of maximizing design tradeoffs to achieve success across an array of mission sets."

To help accelerate transition to the field, the ANCILLARY team has worked on the certification process concurrently with aircraft design and testing, while also ensuring the performers and their supply chains are ready for rapid, on-demand aircraft production.

"We're taking a full 360 look at what it takes — considering performance, cost, usability, interoperability, certification, manufacturing, etc. — to ensure we rapidly deliver a game-changing capability," Smith said. "We've got five outstanding American companies we expect to be ready to accept and deliver orders at scale within the upcoming budget year."

The under-330-pound (150 kilograms) maximum gross takeoff weight threshold for ANCILLARY aircraft is a pivotal factor. To date, the Department of Defense (DOD) has required any drone over 55 pounds (25 kilograms) be owned by an aviation unit and operated by a fully licensed pilot, creating significant barriers to widespread fielding. On a case-by-case basis, aircraft up to 330 pounds are now permitted to be purchased and operated by a non-aviation unit. DOD policies around drones of this size are evolving and the department is considering a policy change to allow UAS operators to fly all drones of this size without requiring special permissions.

"ANCILLARY fills a critical gap, bringing operational capabilities comparable to much larger — Group 4 and 5 — drones to smaller units, such as Army, Marine Corps, special operations units or a ship's company," Smith said. "These drones can be deployed without additional infrastructure or equipment, even in austere environments — offering a game-changing toolset for warfighters."


Reactel, Inc.
Reacting First to All Your Filter Needs.
Filter Solutions For Mission Critical Applications
High Performance, Rugged Packaging, Small Size and Weight
Great things can come in small packages. Reactel filters are ideally suited for the demanding environments that unmanned vehicles encounter.
Many manufacturers rely on Reactel to provide units which are:
High performance - Lightweight - Low profile
Contact a Reactel engineer with your filter or multiplexer requirements. We can create a unit which will be the perfect fit for your applications.
REACTEL, INC.
RF & Microwave Filters - Multiplexers - Multifunction Assemblies
REACTEL, INC.
REACTEL, INC.
REACTEL, INC.
8031 Cessna Avenue • Gaithersburg, Maryland 20879 • (301) 519-3660 • reactel@reactel.com • reactel.com
Intertek
RoHS
RoHS Compliant 2002/95/EC
in
MADE IN MD
Since 1979

UP TO 110 GHz

High-Frequency Solutions

Amplifiers & Modules for mmWave Applications

WAVEGUIDE AMPLIFIERS

- Bandwidths from 40 to 110 GHz
- Low noise, high gain & medium power options
- WR10, WR12, WR15 & WR15 interfaces
- Ideal for TRP & TIS over-the-air testing

CONNECTORIZED AMPLIFIERS

- Bandwidths from 50 kHz to 95 GHz
- 2.92, 2.4, 1.85 & 1.0mm connector options
- Gain up to 45 dB
- NF as low as 1.7 dB
- Power up to 1W

VARIABLE GAIN AMPLIFIERS

- Bandwidths from 18 to 54 GHz
- Gain up to 50 dB
- Calibrated 17 dB attenuation with analog or TTL control
- PSAT up to +1W
- Interactive GUI with telemetry

Mini-Circuits®

Cliff Drubin, Associate Technical Editor

Increased Demand for Bandwidth-Intensive Services Drives Mobile Data Traffic to Surge

The worldwide mobile connectivity market is undergoing a significant transformation, with mobile data traffic increasing rapidly while subscriber growth slows. According to ABI Research, mobile data traffic is expected to increase by a 23 percent compound annual growth rate (CAGR) from 2025 to 2030, reaching over 5,241 exabytes (EB) by the decade's end. This surge in data usage is primarily driven by the rising demand for bandwidth-intensive services like high-definition video streaming, immersive gaming and always-on mobile apps, all of which require greater network capacity and lower latency. In contrast, mobile subscriptions are projected to grow at a much slower pace, increasing by just 0.17 percent annually and reaching 5.659 billion subscribers globally by 2030.

While subscriber growth remains steady, the real transformation lies in the increasing amount of data individual users are consuming. The slower pace of subscriber growth in many regions can be attributed to market saturation, especially in mature markets where most potential customers already have mobile subscriptions. "In contrast, subscriber numbers are growing in many emerging markets, driven by population growth and greater access to mobile services. However, economic challenges, infrastructure limitations and the affordability of smartphones continue to hinder faster adoption in these regions. The real growth lies in how much more data individual users are consuming," said Samuel Bowling, research analyst at ABI Research.

Mobile data traffic increasing rapidly while subscriber growth slows

As users engage in data-heavy activities, networks must evolve to meet these higher demands. The rollout of 5G networks plays a central role in this shift. 5G's advanced capabilities, such as faster speeds, ultra-low latency and better support for applications like augmented reality and IoT are significantly increasing mobile data traffic. Between 2025 and 2030, 5G is expected to account for a 2,200 EB rise in global data traffic as more users transition to 5G networks. To accommodate this surge in demand, operators must enhance their infrastructure to deliver the performance required by next-generation technologies.

Although 4G networks will see a decline in subscribers — expected to drop to around 1.4 billion by 2030 — their data consumption will continue to grow, at a rate of 16 percent annually. This highlights that while newer 5G networks will take the lead, 4G will still support significant data usage across the globe.

Regionally, India is expected to be a major contributor to global data consumption, driven by a growing population, expanding 5G deployment and some of the most affordable data plans. By 2030, India's mobile data traffic is projected to reach approximately 1,275 EB. At the same time, older technologies like 2G and 3G are rapidly fading, with subscriptions expected to decline sharply, especially as countries like Sweden and Israel plan to shut down their legacy networks by 2026.

These findings are from ABI Research's Network Technology and Market Tracker market data report. This report is part of the company's 5G, 6G, and Open RAN research service.

Growing Monetization Appeal of 5G FWA

Fixed Wireless Access (FWA) continues to grow in appeal to communications service providers (CSPs) around the world, with the ability to offer speed-based tariff plans enhanced by 5G capabilities proving particularly attractive, the June 2025 Ericsson Mobility Report (EMR) shows.

While about 80 percent of the global CSPs sampled by Ericsson currently offer FWA services, the most rapid area of growth continues to be among CSPs offering 5G-enabled speed-based tariff plans.

With 5G FWA, service providers can offer a range of subscriber packages with different data speeds and entertainment options, like cable or fiber offerings, increasing monetization opportunities for CSPs compared to earlier generations of FWA.

The EMR shows that more than half (51 percent) of global CSPs with FWA offerings now include speed-based options — up from 40 percent in the same period in June 2024 — driven by high adoption in North America, and growth in Europe and the Middle East.

FWA is projected to account for more than 35 percent of new fixed broadband connections, with an expected increase to 350 million by the end of 2030. 5G FWA plays a crucial role in expanding broadband access, especially in areas where traditional wired infrastructure may be less feasible.

On 5G subscriptions, the June 2025 EMR forecasts subscriptions to top 2.9 billion globally by the end of 2025, about one-third of all mobile subscriptions. The 5G subscription forecast for the end of 2030 remains at 6.3 billion.

Mobile network data traffic increased by 19 percent from the first quarter of 2024 to the corresponding period in 2025. Despite a declining growth rate, net added traffic will continue to increase year-on-year, with the June 2025 EMR forecasting that mobile data traffic will more than double through the forecast period through the end of 2030.

In Europe, 5G mid-band coverage topped 50 percent population coverage by the end of 2024. While the figure puts the region in line with the global average,

For More Information Visit mwjournal.com for more commercial market news.

it lags far behind frontrunner countries such as North America, where 5G mid-band deployment has topped 90 percent population coverage and India, where 5G mid-band population coverage reached 95 percent by the end of 2024.

Through commentary, insights and customer/partner case stories, the June 2025 EMR highlights the ability of 5G Standalone and 5G Advanced to create monetization opportunities for CSPs globally, based on value delivery rather than data volume.

The report highlights how CSPs are pursuing new commercial opportunities by offering differentiated connectivity services to consumers, enterprises and public authorities.

NGMN Calls for Harmonized 6G Standards to Drive Seamless Mobile Evolution

As the telecommunication standards body 3GPP prepares for setting the scope for Release 20, the Next Generation Mobile Networks Alliance (NGMN) has released a publication advocating the critical need for harmonized global standards for 6G.

"6G Key Messages — An Operator View" says that standards should build upon the features and capabilities introduced with 5G and create value through new services that are essential to support continuous innovation, delivering real benefits to users and operators while addressing evolving societal needs and fostering a sustainable ecosystem.

> 6G should be viewed as a seamless evolution...

The publication consolidates key messages from previous NGMN deliverables around 6G and puts them into an operator perspective, reiterating the renowned NGMN's 6G Position Statement published in 2023. Industry leaders stress that the transition to 6G should be evolutionary and that the evolution should not force a complete hardware refresh. While new radio equipment is required for deployment in new frequency bands, the evolution toward 6G in existing bands should primarily occur through software upgrades, ensuring a smooth transition.

6G must demonstrate clear, tangible benefits within a realistic techno-economic framework. The network architecture must meet MNOs criteria for modularity, simplicity, openness, operational simplification, compatibility and interoperability and trustworthiness while delivering economic and social sustainability. These factors are crucial to enable fast deployment and to support the development of market-aligned services that meet user demands.

ENGINEERED FOR EXCELLENCE,
PROVEN BY PERFORMANCE
3H Comunication Systems offers RF/microwave filter solutions that are innovative, high quality, cost-effective, DC to 50 GHz, with a 5-year warranty.
LC • CERAMIC • CAVITY • PRINTED • MULTIPLEXERS •
SWITCHED FILTER BANKS • MULTI-FUNCTION ASSEMBLIES
3H Communication Systems
AS9100 & ISO9001:2015 CERTIFIED
949.529.1583 | sales@3hcomm.com
3HCommunicationSystems.com

Around the **Circuit**

Barbara Walsh, Multimedia Staff Editor

COLLABORATIONS

Anritsu Corporation announced its participation as a test and measurement partner in two pioneering demonstrations of 3GPP Rel-17 compliant non-terrestrial network (NTN) technology at the 2025 5GAA meetings in Paris. The demonstrations provided the first of their kind measurements showcasing the readiness of the technology and ecosystem to revolutionize automotive safety. In one of the collaborations with industry leaders **BMW Group**, **Deutsche Telekom**, **Viasat** and **Skylo**, **Anritsu** contributed to successful measurements of end-to-end NTN key performance indicators (KPIs). The joint effort focused on measuring NTN KPIs to demonstrate the feasibility and effectiveness of use cases, such as local hazard warning and emergency messaging.

Ericsson and **Supermicro** announced an intent to engage in a strategic collaboration to accelerate Edge AI deployment. The parties have signed a Memorandum of Understanding to explore the combination of Ericsson Enterprise Wireless Solutions' industry-leading 5G connectivity with Supermicro's industry-leading Edge AI platforms into commercial bundles that will deliver advanced Edge AI capabilities that leverage 5G network connectivity as a key value-add attribute. It will also simplify procurement and deployment with a unified solution with pre-validated AI compute and 5G connectivity. As AI becomes integrated into a wide range of business functions, many of those AI applications require low latency response times.

NEW STARTS

Greenerwave has announced the opening of new offices in Toulouse to accelerate their growth. By moving into the European capital of aerospace, the company is embedding itself within a top-tier ecosystem that brings together France's leading expertise in the sector. This strategic location within a specialized technical environment will give a strong boost to Greenerwave's ambition: to revolutionize satellite communications through a disruptive technology. Its solution, passive and low in semiconductor consumption, enables the development of a new generation of antennas that are more energy-efficient and have a lower carbon footprint.

ACHIEVEMENTS

Pixus Technologies has announced its 15th year anniversary as a provider of embedded computing and enclosure solutions. The company has been supporting the military, aerospace, industrial, HPEC, physics/research and telecom communities since its inception in 2010. The core Pixus team was created from former Kaparel/Rittal engineers who have been developing backplane-based solutions for over 30 years. Pixus is one of the few manufacturers in the industry who provide the full ecosystem of embedded subsystems from the ground up. This includes components such as card guides and rails to backplane/chassis designs, to assembled chassis platforms with integrated cooling, I/O and power solutions. The company also provides some specialty pre-integrated services. The Pixus USA office was opened in 2021.

CONTRACTS

BAE Systems has been awarded a $1.2 billion contract by **U.S. Space Systems Command** to provide the U.S. Space Force with missile tracking satellite capabilities. BAE Systems will serve as the prime contractor for the Resilient Missile Warning & Tracking medium Earth orbit Epoch 2 program and will design and build 10 spacecraft over the agreement, including a four-year delivery for the space vehicles plus another five years of operations and support. The program will provide resilient, space-based missile warning and tracking of ballistic missiles and advanced threats, such as hypersonic glide vehicles.

PEOPLE

▲ *Ulrich L. Rohde*

The Bavarian Prime Minister Dr. Markus Söder, MdL, awarded **Professor Ulrich L. Rohde** with the Bavarian Order of Merit. The Prime Minister presented the medal and award certificate to Rohde and other distinguished personalities on July 9, 2025. The Bavarian Order of Merit is awarded by the Bavarian Prime Minister on a yearly basis as "a sign of grateful recognition for outstanding scientific achievements and social service rendered to the Free State of Bavaria and the Bavarian people."

REP APPOINTMENTS

mmTron Inc. announced the appointment of **Richardson RFPD**, an Arrow Electronics company, as its authorized global distributor. This distribution agreement will expand mmTron's global reach through mmTron's innovative product portfolio and Richardson RFPD's strong technical support. Under the agreement, Richardson RFPD will represent mmTron globally while adhering to all applicable international trade restrictions and exclusions. Richardson RFPD will represent all mmTron products and will stock the products best aligned with their target markets.

RFMW announced a new distribution agreement with **Sonoma Scientific**, a U.S.-based manufacturer specializing in high-quality ferrite isolators and circulators. Sonoma Scientific's products complement RFMW's portfolio of high-power GaN and LDMOS RF and microwave amplifiers and devices, enabling customers to optimize performance in new designs. This agreement enhances RFMW's ability to deliver robust, military-grade solutions to global customers while supporting Sonoma Scientific's growth in key markets.

For More Information For up-to-date news briefs, visit mwjournal.com

EuMW 2025 Preview: Waves of Innovation

Pat Hindle, Media Director, *Microwave Journal*

The 28th edition of the European Microwave Week (EuMW 2025) will take place in Utrecht, continuing the annual series of highly successful microwave events that started back in 1998. In 2020, the event was moved from Amsterdam to Utrecht for the first time but was canceled due to the pandemic, so this will be the first year it takes place in Utrecht which is conveniently located just outside of Amsterdam. As always, EuMW 2025 is made up of three colocated conferences:

- The European Microwave Conference (EuMC)
- The European Microwave Integrated Circuits Conference (EuMIC)
- The European Radar Conference (EuRAD)

In addition, EuMW 2025 includes the Defence, Security and Space Forum; Automotive Forum; 6G Forum; and a large exhibition. EuMW 2025 provides the opportunity to participate in conferences, workshops, short courses and special events such as Women in Microwave Engineering. It is Europe's version of IMS and the largest microwave event on that continent.

EuMC

The 2025 European Microwave Conference is Europe's top conference dedicated to microwave, mmWave and terahertz devices, systems and technologies. The conference will be held from 23-25 of September and is the featured event at EuMW. A broad range of high frequency related topics, from materials and technologies to integrated circuits (ICs), systems and applications, will be addressed in all their aspects: theory, simulation, design and measurement. Examples include the latest developments of filters and passive components, modelling and design of emerging engineered materials, high frequency and high data rate microwave photonics, highly stable and ultra-low noise microwave and mmWave sources, new linearization techniques, 6G, IoT and the impact of new packaging technologies on development applications. The topic "Sustainability (including energy efficiency, eco-design) and Environmental Impact" will be a focus topic, demonstrating the conference's aim at both addressing the sustainable use of RF devices in our societies and identifying the long-term measures for mitigating the environmental impact of RF technologies.

The EuMC provides many opportunities for networking and interaction with international experts in a wide variety of specialties, attracting delegates with academic

Telonic Berkeley

1080 La Mirada Court
Vista, CA 92081

Phone
(760) 744-8350

Fax
(760) 744-8360

Web Address
www.telonicberkeley.com

email
info@telonicberkeley.com

TELONIC BERKELEY INC.

AS9100D AND ISO 9001:2015 CERTIFIED AND AN ITAR CONTROLLED COMPANY

A Pioneer of RF & Microwave Filters

…employing proven design elements (Lumped, Combline/Cavity, and Tubular) to produce high-quality Passband, Lowpass, Highpass, and Bandstop Microwave Filters… including Diplexers, Multiplexers, Filter Banks, Switches, Multipliers… also Rotary Attenuators

Telonic Berkeley **Fixed Filters** are known and used worldwide. Our impressive array of fixed filter types has evolved over the years in responding to the demanding needs of the electronic industry while offering performance parameters tailored specifically to each customer's unique requirements.

Telonic Berkeley Engineers are ready and anxious to provide innovative solutions for your RF multi-channel or **Multiplexer** needs. Our Diplexer, Triplexer or Quadraplexer designs in lumped element or combline/cavity designs may be the solution you are looking for.

Telonic Tubular Bandpass Filters are available in 2 to 12 sections. Three different and frequency sizes ranges allow for the selection of an optimal design for each requirement. Almost any type of input or output connection is available as a standard item.

Tunable Filters including Manually Tuned Bandpass Filters, Manually Tuned Bandstop Filters, Digitally Tuned Bandstop Filters, and Multi-Octave Digitally Tuned Filters up to 36 Gigahertz are available.

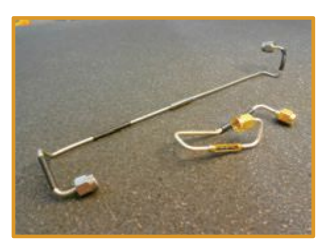

Telonic Berkeley offers a full range of **RF Cable Assemblies,** Flat Ribbon Cables, Grounding Cables, Wire Harnesses, Discrete Harnesses, and Power Cords

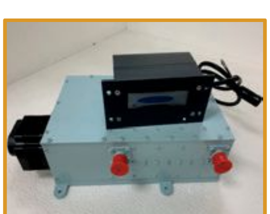

Network Managed Tunable RF Filters provide remote management, monitoring and diagnostic capabilities. High Power Tunable BSF and BPF are available as well as industrial backgrounds. With more than 50 oral and poster sessions, the conference represents an exciting forum for the presentation and discussion of cutting-edge technology in the microwave area. In addition to scientific papers, contributions on industrial applications will be presented, covering the fields of instrumentation, medical, telecommunication, radio astronomy, radar, space, automotive and defence systems.

EuMIC

The 20th European Microwave Integrated Circuits Conference will be held as part of EuMW 2025. Initiated by the GAAS Association in 1990 and renamed in 2006, the conference will take place from the 22 and 23 of September. The EuMIC conference is jointly organized by the GAAS Association and Eu*MA* and is the premier European technical conference for IC and system design ranging from RF, microwave and mmWave to terahertz electronics, ultra-fast mixed-signal circuits and optoelectronics.

The EuMIC conference is the largest scientific event in Europe related to microwave ICs. The conference aims to showcase recent notable advancements and trends from the academic and industrial fields, to exchange technical information and to provide opportunities for networking and interaction with the community. The conference covers a broad range of high frequency related topics in ICs, ranging from devices, fabrication and IC packaging technologies to the monolithic IC and complete system design, system-in-package and system-on-chip applications, encompassing all relevant aspects such as theory, modelling, simulation, fabrication and measurement.

The EuMIC conference also includes III-V-based and Si-based technologies — both strong drivers of innovation in microwave to terahertz and optical technologies, infrastructure and applications. In the emerging technology area, contributions in the field of nanotechnologies, as well as wide-bandgap devices and technologies for microwave photonics, are included. New and emerging applications of information and communication technology and sensing, megatrends such as 6G and terahertz connectivity, connected and environmental-aware vehicles, specifically automotive radar, smart and intelligent sensing, pan-global satellite coverage, smart city and smart factory developments, all rely on high frequency devices and solutions.

EuRAD

The 22nd European Radar Conference will be held from 24-26 of September in the framework of EuMW 2025. This radar conference is the most important European event for state-of-the-art and future directions in the field of radar research, technologies, system design and applications. The EuRAD conference will bring together a global network of researchers, practitioners and institutes working on radar. The paper submission includes topics clustered around four main categories:

Radar Principles and Modelling comprises a wide range of radar systems and approaches, such as ultra-wideband, noise, quantum, polarimetric, MIMO, passive, HF and over the horizon, multi-static and networked radar. It also includes as-

pects of radar electromagnetic phenomenology and modelling, such as developing digital twins of radar systems, as well as the design and characterization of radar waveforms.

Radar Technologies focuses on the various architectures and modules constituting a wide range of radar systems. Innovative research contributions are expected at multiple levels, from RF components, circuits and modules to entire multifunctional and reconfigurable architectures, from phased array technologies designed for long-range applications, to mmWave and THz systems targeting shorter ranges with high resolution. Part of these topics are also research contributions and technologies in the area of waveform synthesis, receiver architectures, synchronization and joint sensing and communication, as well as results in sustainable and energy-efficient technologies for radar manufacturing and design.

Radar Signal Processing, Algorithms and AI aims to attract research contributions in the wide areas of radar signal processing. This includes techniques, including but not limited to beamforming, MIMO, detection, compressive sensing, tracking and data fusion, radar sensor management, imaging and super-resolution techniques, radar-based automatic target classification, cognitive techniques and spectrum sharing, as well as quantum computing algorithms applied to radar.

Radar Applications will include the vast number of domains where radar systems and techniques have been recently applied, from defence and security applications, such as electronic surveillance and warfare and UAV monitoring, to civilian applications of radar in the medical, biological and industrial fields, such as human activity monitoring and gesture recognition. This category aims to attract novel contributions in the field of radar for automotive and transportation applications, as well as geoscience, environmental and weather monitoring and space surveillance and exploration.

FORUMS

The 6G Forum takes place on 22 September and is a dynamic event where industry and academic experts converge to explore the future of wireless communications. Dive into engaging presentations on system applications, standardization, spectrum management and cutting-edge microwave and antenna technologies. Enjoy a mix of technical talks, posters, demos and a lively panel discussion. Network with innovators during the demo/poster session, showcasing the latest 6G advancements.

The Automotive Forum takes place on 23 September and is


Quantic™ PMI
PLANAR MONOLITHICS
Components & Modules
to 70 GHz
▪ Modern hybrid MIC/MMIC design
▪ 4,500+ Hi-Rel Commercial, Off-the-shelf (COTS) Models
▪ Industry-leading customer and applications support
▪ Form, fit, function and custom package designs
▪ Hermetic sealing, military or aerospace screening
Quantic PMI designs and manufactures a full range of solutions for your most demanding RF and Microwave challenges.
Get a complete list of our components and module portfolio, available options, and download product features and other technical data at quanticpmi.com
Or contact us at 1-877-752-6271 or sales@quanticpmi.com
EUROPEAN MICROWAVE WEEK
JAARBEURS UTRECHT
THE NETHERLANDS
21-26 SEPTEMBER 2025
www.eumw.eu
WAVES OF INNOVATION
Visit us @ Booth #D139


Quantic™ Ohmega Ticer
Mission-Critical. High-Frequency.
Zero Compromise. Embedded Resistors.
What makes OhmegaPly® and TCR® so special?
A resistive blank slate. Visit our technical library to learn more about how we can help you with your design challenges.
Defining & delivering the future of mission-critical electronics.
QuanticOhmega.com

where industry experts gather to discuss cutting-edge radar architectures, technical aspects and market trends in automotive microwave applications and connectivity. Enjoy a blend of technical presentations, panel discussions and a poster exhibition. Network with peers during dedicated sessions and dinner. Keynote speakers will share insights on innovative solutions and regulatory challenges. This is a unique forum not available at most other events.

The 2025 Defence, Security and Space Forum is on September 24 as part of EuMW. The topics will cover space weather and its impact on military operations, critical infrastructure, GPS, GNSS navigation and communications. Learn about current and future monitoring systems and explore how to access and research open-source space weather data and meet with top experts in the field at this forum.

EXHIBITION

EuMW 2025 takes place 23 – 25 September and is the largest trade show dedicated to microwaves and RF in Europe, providing:

- 8,000 m^2 of gross exhibition space
- Around 4,000 key visitors from around the globe
- 1,500 to 1,700 conference delegates.

With more than 300 international exhibitors, the event attracts a more diverse global audience than IMS that tends to be mostly U.S.-based exhibitors. There are more European and Asian companies at EuMW, as it is much easier for them to attend in Europe. The exhibition will offer its exhibitors an unrivaled opportunity to present products, technological developments and form relationships with relevant and interested attendees including academics, professionals and industry leaders. EuMW attracts high-level, C-suite attendees, so there are more opportunities to network and discuss higher level opportunities. It also offers a forum for discussing trends and exchanging scientific and technical information. We hope to see everyone in Utrecht. ■

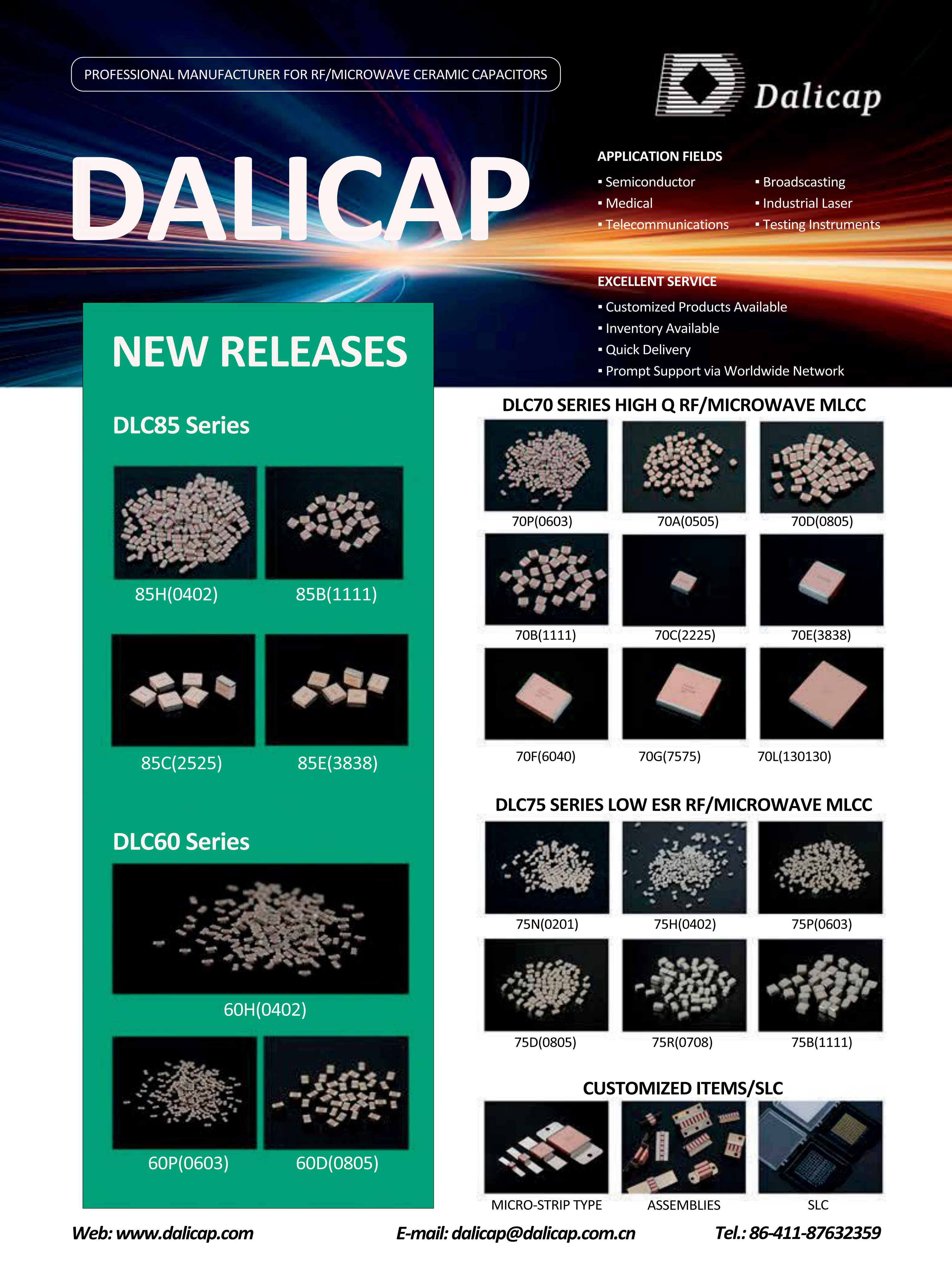

PROFESSIONAL MANUFACTURER FOR RF/MICROWAVE CERAMIC CAPACITORS
Dalicap
DALICAP
APPLICATION FIELDS
▪ Semiconductor
▪ Medical
▪ Telecommunications
▪ Broadcasting
▪ Industrial Laser
▪ Testing Instruments
EXCELLENT SERVICE
▪ Customized Products Available
▪ Inventory Available
▪ Quick Delivery
▪ Prompt Support via Worldwide Network
NEW RELEASES
DLC85 Series
85H(0402)
85B(1111)
85C(2525)
85E(3838)
DLC60 Series
60H(0402)
60P(0603)
60D(0805)
DLC70 SERIES HIGH Q RF/MICROWAVE MLCC
70P(0603)
70A(0505)
70D(0805)
70B(1111)
70C(2225)
70E(3838)
70F(6040)
70G(7575)
70L(130130)
DLC75 SERIES LOW ESR RF/MICROWAVE MLCC
75N(0201)
75H(0402)
75P(0603)
75D(0805)
75R(0708)
75B(1111)
CUSTOMIZED ITEMS/SLC
MICRO-STRIP TYPE
ASSEMBLIES
SLC
Web: www.dalicap.com
E-mail: dalicap@dalicap.com.cn
Tel.: 86-411-87632359

A Spherical Near-Field Test System for Commercial Aircraft Radome Testing

Kefeng Liu
ETS-Lindgren, Cedar Park, Texas

Anbang Liu
MJK Electronic Engineering Co. Ltd., Nanjing, China

Dennis Lewis
Boeing Company, Seattle, Wash.

Commercial aircraft weather protected radar radome certification and re-certification of repaired radomes according to the latest RTCA DO213A-Change 1A can be time-consuming in antenna pattern tests. Test systems based on three test methods, far-field, compact range and near-field (NF), have been developed to meet the requirements in the past.[1-3] However, some of these systems require improvements to comply with the latest version of RTCA DO213A Change 1A requirements, particularly with the λ/4 distance shift in test distance for the NF test methods. This paper introduces a unique, fully compliant spherical near-field (SNF) test system that meets accuracy requirements and maintains range efficiency.

DESIGN CONSIDERATIONS

The SNF test method is chosen based on the required antenna under test (AUT) test volume and the available test space for this project. However, the SNF method is time-intensive due to the need to measure the required number of test points on the NF scan surface given by the Nyquist sampling theorem:

$$N_\phi = 2N_\theta = \frac{2\pi D_{min}}{\lambda}$$
$$\Delta\phi = \Delta\theta = \frac{\lambda}{D_{min}} \quad (1)$$

The test system must also adapt to three different sizes of commercial aircraft radomes and accommodate test frequencies at 9.333 and 9.345 GHz. The largest radome will need the D_{min} at 2.2 m to fit. When λ at 9.5 GHz is chosen to calculate the sampling points, an angular sampling increment of $\Delta\phi=\Delta\theta=0.8$ degrees is required to be the common denominator to scan the sampling area. A total of 202,500 test points will need to be tested if the entire 4π solid angle is scanned in the SNF test method, which will take too long. Design parameters of the test range subsystems are considered to eliminate redundant pattern tests, thus allowing for optimal performance. Additionally, the AUT properties are utilized to shorten the test time.

Test Range Distance

In selecting test range distance, consideration is given to the minimum separation of 2λ plus the required λ/4 distance shift, which is feasible to meet in the X-Band frequency range. The probe antennas shall always be clear of the largest radome with additional test distance to meet the minimum separation. Predominantly, this test system's design is motivated to maximize test length to minimize the probe to AUT coupling to a negligible error, such that a λ/4 distance


Proven RF/MW Solutions
from Ground to
Deep Space
Commercial off-the-shelf rad tolerant parts
Complex, large format RF/MW PCBs
High power microwave solutions from L to Q-band
RF/MW components, modules and integrated assemblies
High speed IP modems with TRANSEC capability
Ultra reliable switching solutions
Microwave & high voltage ruggedized interconnects
EUROPEAN MICROWAVE WEEK
Booth E129

shift can be proven unnecessary, thus saving test time. Therefore, a nominal test distance of 2.5 m is chosen.

Anechoic Chamber

An anechoic chamber with shield-to-shield dimensions of 6.5 (L) × 6.5 (W) × 6.1 m (H) is installed to host the SNF test system and the AUT positioners. The anechoic chamber is treated with microwave absorbers to provide a floor with a reflection noise of less than -50 dB inside a 2.5 m diameter quiet zone at the center of the test range. A monorail hoist system is used to allow easy placement of the radome on the positioners.

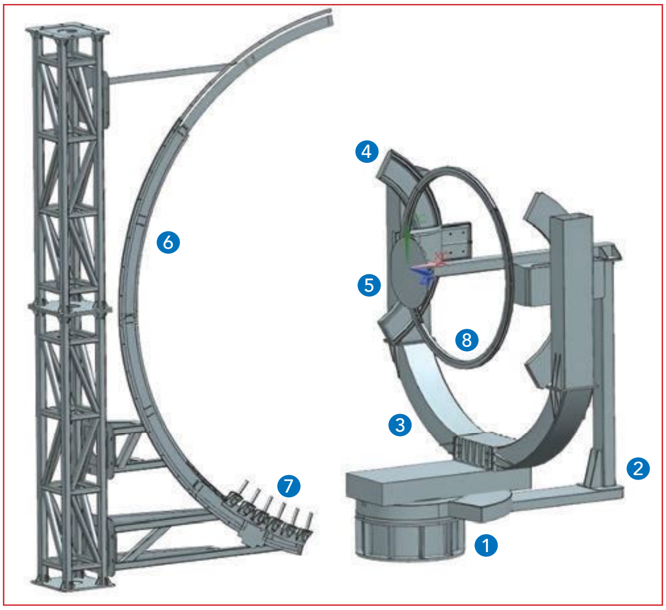

Fig. 1 AUT and probe positioner subsystems.

AUT Positioners

In designing the AUT positioner subsystem, as seen in ***Figure 1***, considerations are given to allow the SNF system scan areas and the panel antenna to be fixed throughout the test sequence. Thus, the relative angular position change between the radome and the panel antenna is implemented by changing the orientation of the radome instead of that of the panel antenna. This positioning subsystem consists of the following seven-motion axes:

1. Azimuth Positioner 1, SNF Azimuth Scan Axis (±180 degrees)
2. Azimuth Positioner 2, Radome Azimuth α Axis (±100 degrees)
3. Elevation Positioner, Radome EL ε Axis (±30 degrees)
4. Radome Roll Positioner, Radome γ Axis (±30 degrees)
5. Radome Longitudinal Linear Positioner (0 to 500 mm)
6. Panel Antenna Azimuth Over-Range Lock
7. Panel Antenna Azimuth Over-Range Counter-Act.

Axes (6) and (7) are the compensating axes that allow the radome to move to the extreme azimuth angular position while allowing the panel antenna to remain in its original center.

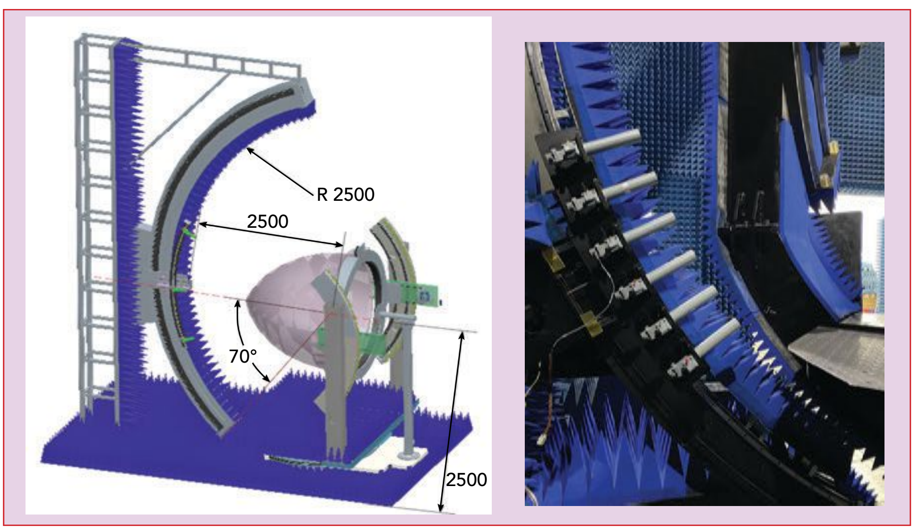

Fig. 2 Probe scanning positioner subsystems.

12-Channel Probe Subsystem

To expedite the SNF data acquisition, six dual polarized X-Band circular waveguide probes are employed with a high speed electronic switch to collect data from 12 RF channels simultaneously. The probe positioner, as shown in ***Figure 2***, has the following motions:

1. Elevation Slide Positioner, SNF Elevation Scan Axis (±80 degrees)
2. Radial Linear Slide, $\lambda/4$ Test Distance Shift (0 to 50 mm)

Notably, the RF absorbers are kept at a distance from the aperture of the six low-directivity dual polarized probes to avoid temperature and humidity variations. Changing RF absorber properties can affect the probe's calibrated path loss, which negatively affects the SNF system's stability.

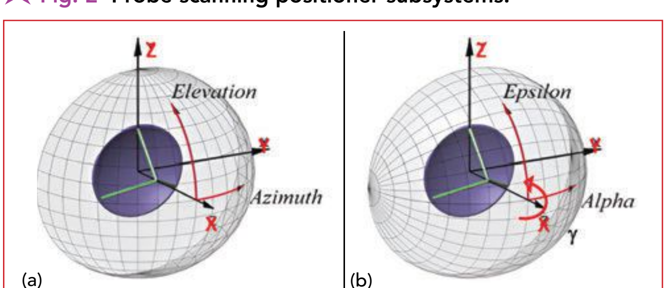

Fig. 3 Panel antenna in (a) EL/AZ (θ/ϕ) gimbal system and (b) AZ/EL (ε/α) gimbal system.

Coordinate System Conversions

The radome test labs are rarely equipped with the EL/AZ or AZ/EL panel antenna gimbals installed in commercial aircraft nose cones. Using the radome positioner to simulate relative angular motions will result in the opposite coordinate system. For example, an EL/AZ radome positioning system will simulate a relative coordinate system as if there were an AZ/EL gimbal system for the panel antenna. If one wishes to provide a radome positioning system to simulate radome testing for both EL/AZ and AZ/EL gimbal systems for the panel

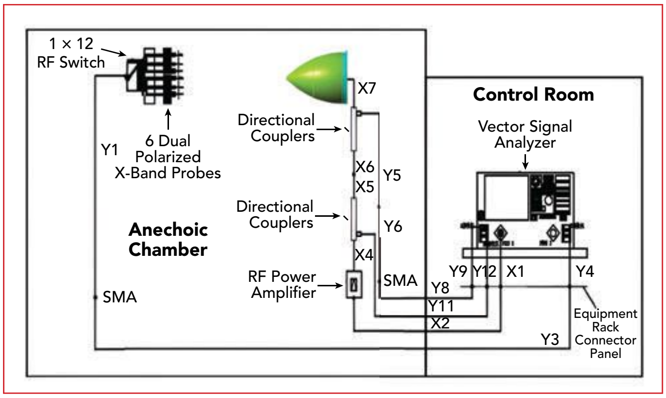

▲ Fig. 4 **RF subsystem diagram.**

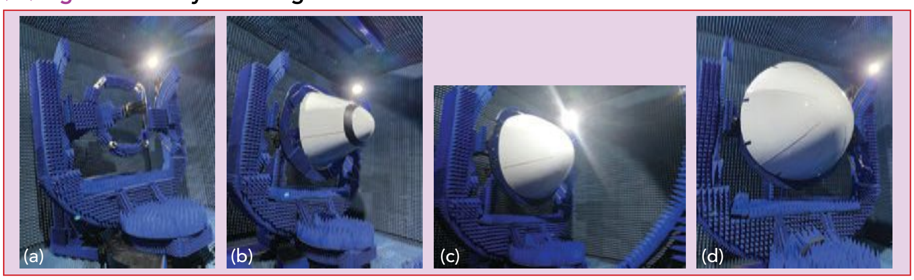

▲ Fig. 5 **AUT Setups: (a) radome-off with panel antenna, (b) radome-on with smaller radome, (c) radome-on with larger radome and (d) radome-on with the largest radome.**

antenna, a roll axis shall be added as shown in ***Figure 3***.

The EL/AZ radome positioner, as shown in Figure 1, intrinsically simulates only the AZ/EL gimbal coordinates in ***Figure 3(b)***. Using the roll axis γ, the conversion to the EL/AZ gimbal coordinate system can be calculated using a set of coordinate transformations. In the EL/AZ (θ/ϕ) gimbal coordinate system:

$$\begin{pmatrix} \hat{r} \\ \hat{\theta} \\ \hat{\phi} \end{pmatrix} = \begin{pmatrix} \cos\theta\cos\phi & \cos\theta\sin\phi & \sin\theta \\ -\sin\theta\cos\phi & -\sin\theta\sin\phi & \cos\theta \\ -\sin\phi & \cos\phi & 0 \end{pmatrix} \begin{pmatrix} \hat{i} \\ \hat{j} \\ \hat{k} \end{pmatrix} \quad (2)$$

In AZ/EL (ε/α) gimbal systems with an added roll axis γ inside of the elevation axis:

$$\begin{pmatrix} \hat{r'} \\ \hat{\varepsilon} \\ \hat{\alpha} \end{pmatrix} = \begin{pmatrix} \cos\alpha\cos\varepsilon & \sin\alpha & \cos\alpha\sin\varepsilon \\ -\sin\varepsilon & 0 & \cos\varepsilon \\ -\sin\alpha\cos\varepsilon & \cos\alpha & -\sin\alpha\sin\varepsilon \end{pmatrix} \begin{pmatrix} \hat{i'} \\ \hat{j'} \\ \hat{k'} \end{pmatrix} \quad (3)$$

$$\begin{pmatrix} \hat{i'} \\ \hat{j'} \\ \hat{k'} \end{pmatrix} = \begin{pmatrix} 1 & 0 & 0 \\ 0 & \cos\gamma & \sin\gamma \\ 0 & -\sin\gamma & \cos\gamma \end{pmatrix} \begin{pmatrix} \hat{i} \\ \hat{j} \\ \hat{k} \end{pmatrix} \quad (4)$$

By requiring that the polarization of the panel antenna be kept the same as that of the given (θ,ϕ) in EL/AZ gimbal, one can obtain the following three unique solutions of (α,ε,γ):

$$tg(\alpha) = tg\phi / \cos\theta \quad (5)$$

$$\sin(\varepsilon) = \sin\theta\cos\phi \quad (6)$$

$$tg(\gamma) = tg\theta\sin\phi \quad (7)$$

A positioning table can be established to allow fast implementation of (α,ε,γ) to simulate the required (θ,ϕ) gimbal orientation. Thus, the AUT positioning system design can implement both EL/AZ and AZ/EL gimbal coordinate systems.

RF Subsystem

Figure 4 shows the RF subsystem of the test range. The directional coupler closest to the AUT measures the reflection from the radome, while the second directional coupler is used to measure the reference input power. An RF power amplifier is used in the input port to boost the system's dynamic range, thus allowing faster data acquisition. This RF subsystem has a signal dynamic range of less than 80 dB.

Test System Control and NF2FF Software

Positioner controllers and system software, including the NF2FF transformation package, are provided by Nanjing MJK Engineering Co. LTD.

SYSTEM PERFORMANCE EVALUATIONS

Figure 5 shows the four mechanical setups for one radome-off and three radome-on RF performance evaluations to prove the validity and compliance of the installed SNF test system.

Scan Surface Truncation and Error Considerations

To expedite the SNF data acquisition, a partial scan surface shall be chosen to include a very high percentage of the AUT energy, so no sidelobe levels (SLL) above -33 dB shall appear. Since the AUT is a high gain antenna, a small portion of the solid angle is required for both radome-on and -off configurations. ***Table 1*** shows the required SLL and its allowable variation in azimuth and elevation patterns.

A scan surface with ±40 degrees in azimuth and ±28.8 degrees in elevation is chosen for this purpose. It is verified by re-scanning the AUT using the scan surface ±60 degrees in azimuth and ±38.4 degrees in elevation.

Figure 6 demonstrates that no further details of SLL above -45 dB can be seen by using the enlarged scan surface. Therefore, there is no need to further enlarge the scan surface beyond the reference scan surface. By using the reference scan surface setting, only 14,746 of the 202,500 test points are tested. Thus, an SNF pattern test for both azimuth and elevation patterns can be completed within three minutes of test time.

Stability of the Test System

Due to the required test time, test data from the SNF test system will be necessary to compare to test data acquired days ago. The stability of the test data over time is critical. ***Table 2*** shows the intercompared radome-off pattern peak values tabulated with the panel antenna fixed. ***Table 2a*** shows the values at nominal test distance, ***Table 2b*** shows the values at the nominal test distance plus a quarter wave shift and ***Table 2c*** shows the average values from Table 2a and b. These shifts simulate the radome being oriented to 21 x 11 angular positions. An SNF scan is performed and transformed to far-field at each radome positioner setup. Peak gain values are entered into the tables as the radome transmission efficiency (TE) reference data. Five days later, the same 231 SNF scans were also measured, and the

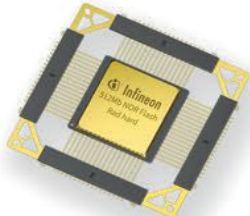

TABLE 1				
ALLOWED SSL WITH RADOME-ON				
Reference SLL		***> -21 dB***	***-21 to -40 dB***	***< -40 dB***
Category 1	Area 1: Window area within ±25 degrees in azimuth and ±10 degrees in elevation	No more than a 1 dB increase	No higher than y=Ax+B with: x=SLL radome OFF, y=SLL radome ON, A=12/19 and B= -128/19	No higher than -32 dB
	Area 2: Everywhere else	The maximum of (-23 dB, Category 1 Area 1 spec + 1 dB)		
Category 2	Everywhere	The maximum of (-23 dB, Category 1 Area 1 spec + 1 dB)		

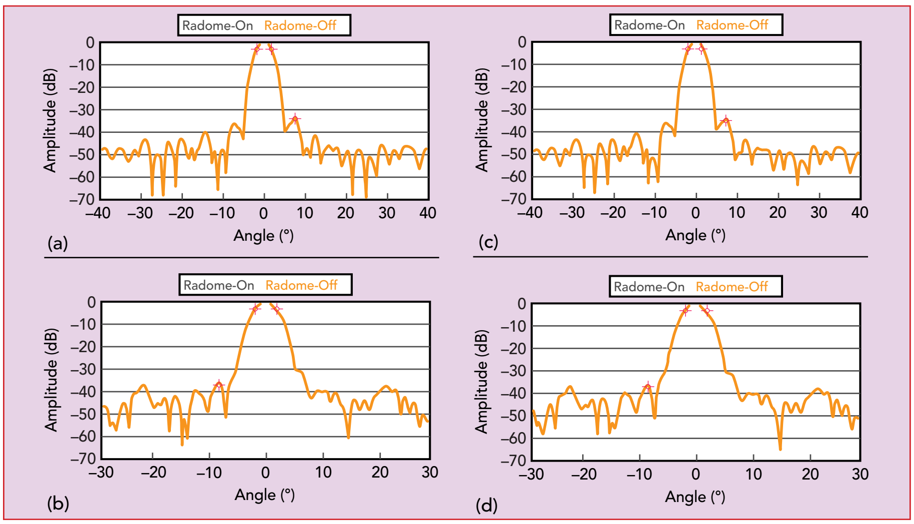

▲ Fig. 6 **Patterns from (a) azimuth reference scan, (b) elevation reference scan, (c) azimuth enlarged scan and (d) elevation enlarged scan.**

results were compared to assess the test system stability. The data includes variation due to environmental changes, such as temperature and humidity, over the six days.

It has been tested and found that the maximum difference of all peaks between two sets of pattern tests over a time span of six days is between -0.011 and +0.027 dB. Also, based on the RTCA test plan, the maximum average deviation between the two tests among 11 elevation angles is less than 0.00417 dB, or at 0.096 percent. Therefore, the overall average TE deviation due to the system stability is less than 0.0027 dB, or 0.062 percent. This test also demonstrates the potential to measure only one reference pattern peak rather than 231 repeated measurements because the variations are so small as to be negligible.

Far-Field Antenna Pattern Verification

The first verification is to evaluate the beamwidth and its SLLs by comparing the transformed far-field patterns from the SNF data to patterns obtained from a far-field range. Two pattern cuts, horizontal- and vertical-plane, are compared against far-field patterns measured at an outdoor far-field range. ***Figure 7*** shows the inter-

TABLE 2A TE DATA FOR A LARGE COMMERCIAL AIRCRAFT RADOME AT NOMINAL TEST DISTANCE

Test Frequency	9.333 GHz
Test Date	04/23/2021-04/28/2021
Normal Antenna Position	Panel Antenna Center at 2500 mm distance from the aperature of the probe antennas

		<<Left Azimuth Angle (Degrees) Right>>																						
	El Angle	-90 (%)	-80 (%)	-70 (%)	-60 (%)	-50 (%)	-40 (%)	-30 (%)	-25 (%)	-20 (%)	-10 (%)	0 (%)	10 (%)	20 (%)	25 (%)	30 (%)	40 (%)	50 (%)	60 (%)	70 (%)	80 (%)	90 (%)	Avg. (%)	Min. (%)
	-25	90.1	88.1	88.6	86.7	86.0	86.3	88.4	88.5	87.6	88.4	90.9	90.7	90.3	88.9	89.4	88.0	87.0	86.9	88.1	88.5	89.0	88.4	86.0
	-20	91.6	90.4	89.5	88.1	87.1	87.8	87.2	87.4	88.4	88.3	90.2	89.6	88.4	86.0	86.4	89.0	87.0	87.9	88.6	90.1	90.7	88.6	86.0
∧	-15	93.4	92.1	90.3	89.2	88.5	85.7	90.0	90.6	90.4	90.4	90.3	91.3	91.7	89.8	89.1	88.0	89.0	89.4	89.8	91.6	92.7	90.1	85.7
down	-10	94.4	92.7	91.0	89.4	87.5	89.9	91.4	91.6	91.2	91.0	91.7	92.0	92.5	91.0	90.7	89.0	89.0	89.3	90.9	92.8	94.2	91.1	87.5
Elev.	-5	94.7	93.4	91.8	90.3	89.4	90.8	91.9	91.9	91.7	91.5	92.2	92.2	92.4	91.5	91.4	91.0	89.0	90.0	91.1	93.2	94.7	91.7	89.0
Angle	0	94.7	93.2	91.6	89.4	88.0	90.6	91.9	92.0	91.4	91.5	92.6	92.5	91.9	91.6	92.3	91.0	90.0	89.6	91.5	93.3	94.5	91.7	88.0
(Deg.)	5	93.9	92.2	90.9	89.5	87.6	89.7	92.1	91.6	91.5	91.4	92.4	92.6	91.8	91.3	92.2	91.0	90.0	89.2	90.7	92.1	93.6	91.3	87.6
up	10	92.5	90.9	90.0	88.9	88.4	89.2	90.9	91.6	91.2	91.3	92.4	92.7	91.8	91.3	91.3	90.0	88.0	89.0	89.4	91.1	92.3	90.7	88.4
∨	15	90.8	89.6	87.9	87.1	85.7	86.8	89.5	90.7	90.6	90.8	91.2	91.7	91.1	90.8	89.8	86.0	87.0	87.6	88.1	89.9	90.7	89.2	85.7
	20	88.5	87.9	87.1	88.1	87.5	86.1	88.7	88.8	88.7	89.6	90.4	90.8	89.4	88.7	87.4	88.0	88.0	87.1	87.7	87.2	88.5	88.3	86.1
	25	88.4	88.2	87.3	85.8	86.4	87.6	88.1	87.5	87.2	87.5	88.6	88.8	88.2	88.4	89.0	87.0	87.0	85.4	87.4	88.2	88.4	87.6	85.4
	Avg.	92.1	90.8	89.6	88.4	87.5	88.2	90.0	90.2	90.0	90.1	91.2	91.3	90.9	89.9	89.9	88.9	88.1	88.3	89.4	90.7	91.7		

Overall Averge Efficiency	89.9%
Minimal Averge Efficiency	87.6%
Minimum Efficiency	85.4%
Radome Class = (A/B/C/D)	B

compared antenna patterns.

It can be observed that the two sets of patterns compare very well in both their main beams and SLL down to as low as -45 dB within the scanned azimuth and elevation angular ranges.

Test Distance $\lambda/4$ Movement

In the latest RTCA test plan, a $\lambda/4$ shift is required to average out the pattern peak variations due to the NF coupling between the probe(s) and the AUT using the SNF method. This SNF system implements the feature by providing a linear slide in the multi-probe carriage. At 9.333 GHz, the $\lambda/4$ radial shift is an 8.03 mm increase in the nominal 2500 mm test distance.

It was observed that the changes in pattern peaks with $\lambda/4$ shift present negligible changes in the TE measurement when the test distance in the SNF range is more than 75λ in electrical length.

Transmission Efficiency Verification

After the qualification of the SNF test system, the most time-consuming TE measurements are performed

TABLE 2B TE DATA FOR A LARGE COMMERCIAL AIRCRAFT RADOME AT NOMINAL TEST DISTANCE + $\lambda/4$ SHIFT

Test Frequency	9.333 GHz
Test Date	04/23/2021-04/28/2021
Normal Antenna Position	Panel Antenna Center at 2500 mm distance from the aperture of the probe antennas + 1/4 wavelength shift

		<<Left									Azimuth Angle (Degrees)						Right>>						
	El Angle	-90 (%)	-80 (%)	-70 (%)	-60 (%)	-50 (%)	-40 (%)	-30 (%)	-25 (%)	-20 (%)	-10 (%)	0 (%)	10 (%)	20 (%)	25 (%)	30 (%)	40 (%)	50 (%)	60 (%)	70 (%)	80 (%)	90 (%)	Avg. (%).	Min. (%)
	-25	90.9	89.6	89.1	86.9	86.1	86.4	88.5	88.4	87.6	88.7	90.4	90.1	89.6	88.2	88.9	86.4	87.2	86.3	88.3	87.7	88.8	88.3	86.1
	-20	92.2	91.8	90.3	88.3	87.2	88.0	85.8	87.4	88.6	88.4	89.6	88.8	87.7	85.4	85.7	87.4	86.6	87.4	88.6	89.5	90.7	88.4	85.4
∧	-15	93.8	93.4	91.1	89.7	88.3	85.8	89.2	90.6	90.6	90.6	90.0	90.5	91.2	89.1	88.4	86.5	88.4	89.0	89.7	90.7	92.6	90.0	85.8
down	-10	94.7	93.9	91.7	89.6	87.6	89.4	90.9	91.7	91.4	91.2	91.1	91.2	91.9	90.3	90.0	87.3	88.6	88.7	90.6	92.0	93.9	90.8	87.3
Elev.	-5	95.1	94.4	92.1	90.6	89.6	90.6	91.6	92.0	91.9	92.0	91.4	91.5	91.9	90.9	90.8	90.4	88.7	89.4	90.6	92.4	94.3	91.5	88.7
Angle	0	95.1	94.1	92.1	89.7	88.3	90.7	92.2	92.2	91.5	92.1	91.9	91.7	91.6	91.3	91.8	90.8	89.6	88.9	91.0	92.6	94.1	91.6	88.3
(Deg.)	5	94.3	93.3	91.5	89.6	88.0	90.0	92.2	91.7	91.8	92.0	91.6	91.9	91.2	90.7	91.5	90.5	89.2	88.8	90.2	91.5	93.2	91.2	88.0
up	10	93.0	91.8	90.5	89.1	88.5	89.2	90.7	91.7	91.4	91.9	91.6	91.9	91.3	90.9	90.6	89.7	88.1	88.7	88.8	90.5	91.9	90.6	88.1
	15	91.5	90.5	88.4	87.1	85.8	86.1	89.6	90.8	90.8	91.2	90.5	91.1	90.7	90.4	89.2	85.3	86.4	87.9	87.4	89.4	90.4	89.1	85.3
∨	20	89.6	88.8	87.4	88.2	87.6	86.4	87.3	88.7	88.9	90.1	89.8	90.2	88.8	88.2	86.7	87.4	87.3	87.8	87.0	86.5	88.1	88.1	86.4
	25	89.6	88.8	87.5	86.0	86.3	87.3	88.0	87.4	87.2	87.8	87.9	88.2	87.6	87.7	88.5	86.1	86.4	85.6	86.8	87.5	87.9	87.4	85.6
	Avg.	92.7	91.9	90.2	88.6	87.6	88.2	89.7	90.2	90.1	90.6	90.5	90.7	90.3	89.4	89.3	88.0	87.9	88.0	89.0	90.0	91.4		

Overall Averge Efficiency	89.7%
Minimal Averge Efficiency	87.4%
Maximum Efficiency	85.3%
Radome Class = (A/B/C/D)	8

TABLE 2C TE DATA FOR A LARGE COMMERCIAL AIRCRAFT RADOME AVERAGED TE DATA FROM THE TWO SETS OF TEST DATA

Test Frequency	9.33 GHz
Test Date	04/23/2021-04/28/2021
Normal Antenna Position	Averaged results of the TE data from two test distances

		<<Left									Azimuth Angle (Degrees)						Right>>						
	El Angle	-90 (%)	-80 (%)	-70 (%)	-60 (%)	-50 (%)	-40 (%)	-30 (%)	-25 (%)	-20 (%)	-10 (%)	0 (%)	10 (%)	20 (%)	25 (%)	30 (%)	40 (%)	50 (%)	60 (%)	70 (%)	80 (%)	90 (%)	Avg. (%)	Min. (%)
	-25	90.5	88.9	88.8	86.8	86.1	86.4	88.4	88.4	87.6	88.5	90.7	90.4	90.0	88.5	89.2	87.3	87.2	86.6	88.2	88.1	88.9	88.4	86.1
	-20	91.9	91.1	89.9	88.2	87.1	87.9	86.5	87.4	88.5	88.3	89.9	89.2	88.1	85.7	86.0	88.2	86.8	87.7	88.6	89.8	90.7	88.5	85.7
∧	-15	93.6	92.7	90.7	89.5	88.4	85.8	89.6	90.6	90.5	90.5	90.2	90.9	91.4	89.4	88.7	87.2	88.5	89.2	89.8	91.1	92.6	90.0	85.8
down	-10	94.6	93.3	91.4	89.5	87.6	89.6	91.1	91.7	91.3	91.1	91.4	91.6	92.2	90.6	90.4	88.0	88.7	89.0	90.7	92.4	94.1	91.0	87.6
Elev.	-5	94.9	93.9	92.0	90.4	89.5	90.7	91.8	91.9	91.8	91.8	91.8	91.9	92.2	91.2	91.1	90.9	88.8	89.7	90.9	92.8	94.5	91.6	88.8
Angle	0	94.9	93.7	91.8	89.5	88.1	90.7	92.0	92.1	91.5	91.8	92.2	92.1	91.7	91.4	92.1	91.0	89.8	89.2	91.2	92.9	94.3	91.6	88.1
(Deg.)	5	94.1	92.7	91.2	89.6	87.8	89.8	92.1	91.7	91.6	91.7	92.0	92.2	91.5	91.0	91.9	90.6	89.4	89.0	90.5	91.8	93.4	91.2	87.8
up	10	92.8	91.4	90.2	89.0	88.4	89.2	90.8	91.6	91.3	91.6	92.0	92.3	91.6	91.1	91.0	89.9	88.2	88.9	89.1	90.8	92.1	90.6	88.2
	15	91.2	90.0	88.2	87.1	85.8	86.5	89.6	90.7	90.7	91.0	90.8	91.4	90.9	90.6	89.5	85.5	86.5	87.7	87.8	89.6	90.5	89.1	85.5
∨	20	89.1	88.4	87.3	88.1	87.6	86.2	88.0	88.7	88.8	89.9	90.1	90.5	89.1	88.5	87.0	87.8	87.4	87.5	87.3	86.8	88.3	88.2	86.2
	25	89.0	88.5	87.4	85.9	86.3	87.5	88.0	87.4	87.2	87.7	88.2	88.5	87.9	88.1	88.7	86.5	86.5	85.5	87.1	87.8	88.2	87.5	85.5
	Avg.	92.4	91.3	89.9	88.5	87.5	88.2	89.8	90.2	90.1	90.4	90.9	91.0	90.6	89.7	89.6	88.5	88.0	88.2	89.2	90.4	91.6	87.5	85.5

Overall Averge Efficiency	89.8%
Minimal Averge Efficiency	87.5%
Minimum Efficiency	85.5%
Radome Class = (A/B/C/D)	B

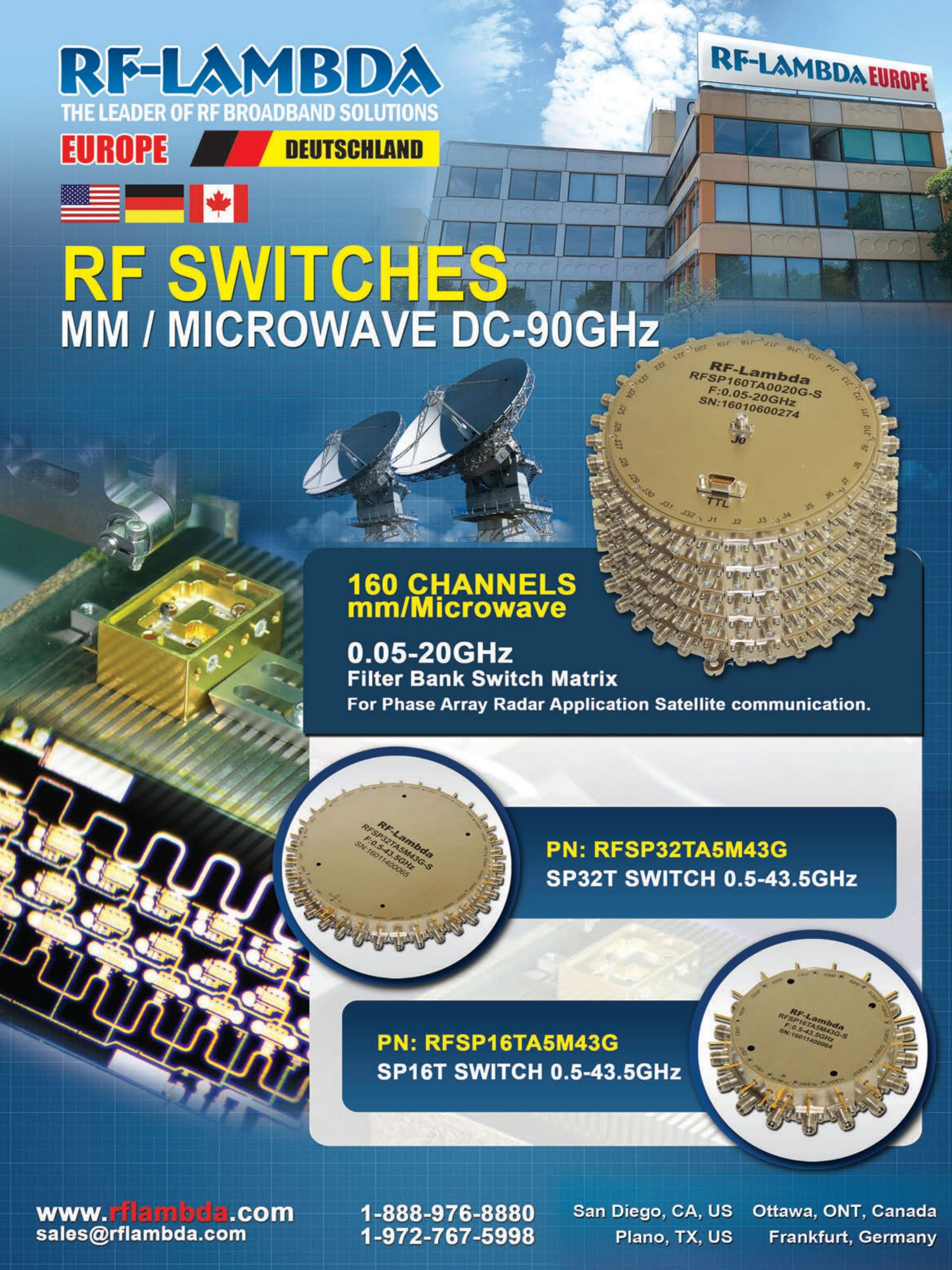
RF-LAMBDA
THE LEADER OF RF BROADBAND SOLUTIONS
EUROPE
DEUTSCHLAND
RF-LAMBDA EUROPE
RF SWITCHES
MM / MICROWAVE DC-90GHz
RF-Lambda
RFSP160TA0020G-S
F:0.05-20GHz
SN:16010600274
160 CHANNELS
mm/Microwave
0.05-20GHz
Filter Bank Switch Matrix
For Phase Array Radar Application Satellite communication.
PN: RFSP32TA5M43G
SP32T SWITCH 0.5-43.5GHz
PN: RFSP16TA5M43G
SP16T SWITCH 0.5-43.5GHz
www.rflambda.com
sales@rflambda.com
1-888-976-8880
1-972-767-5998
San Diego, CA, US
Plano, TX, US
Ottawa, ONT, Canada
Frankfurt, Germany

by completing a set of 231 panel antenna radome-off patterns. Since a λ/4 shift pattern test is not expected to be needed to average out the NF coupling error, no data for λ/4 shift in test distance are collected for radome-off measurements.

With radome-on, the pattern peaks are measured for all 231 possible radome/antenna orientations at both nominal and λ/4 shift inclusive range distances. The TE shall be obtained by comparing their pattern peak values against the corresponding radome-off reference peak values. The average TE for the nominal and the λ/4 shift inclusive range distances are then compared against results from an outdoor far-field range.

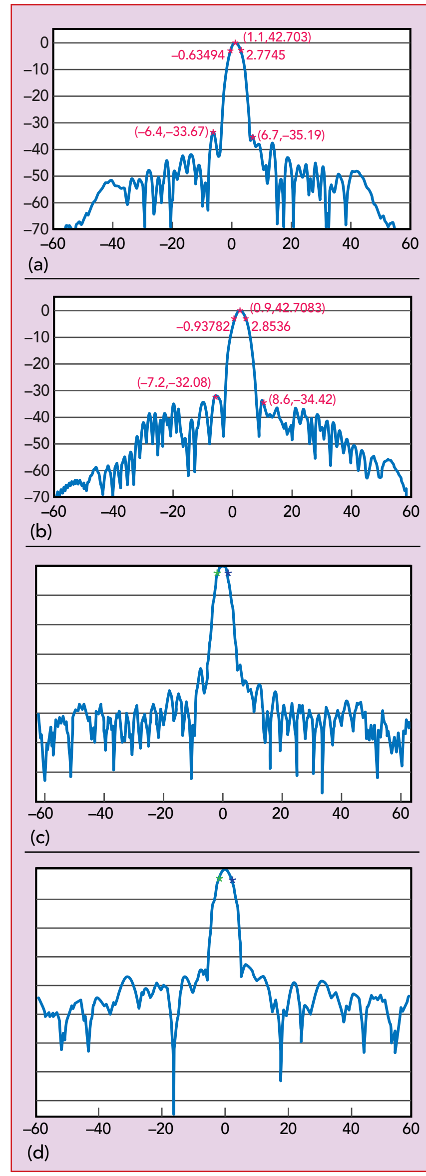

Fig. 7 Large radome-on intercompared measured far-field (a) azimuth from this SNF, (b) elevation from this SNF, (c) azimuth from an outdoor far-field range and (d) elevation from an outdoor far-field range patterns.

Table 2 presents the measured TE for a large commercial radome with a panel radar antenna; the overall average TE is 89.8 percent, and the minimum averaged TE among 11 elevation angles is 87.5 percent; the minimum TE among all 231 points is at 85.5 percent. Based on the published radome class ratings, this is a Class B radome. The same radome has been tested at an outdoor far-field range and reported at an overall average TE of 90.8 percent, a minimum averaged TE among 11 elevation angles of 88.6 percent and a minimum TE among all 231 points of 83.0 percent. The outdoor range report also rates this as a Class B radome. The two ranges, although utilizing completely different test methods with a two-month time span between the two test methods, generate less than 2.5 percent minimum TE difference in the worst case.

The TE results of all radomes of three different sizes, with two different panel radar antennas, compare well

with reported test results from two outdoor ranges in both TE reading and in radome classification. Additionally, the test results with λ/4 shift in test distance do not show any appreciable difference and demonstrate a variation for all three radomes much lower than 0.1 dB with two different system antennas. These variations do not result in any change in the radome classifications. Therefore, the TE tests with λ/4 shift in test distance should be omitted in the SNF test range if the test range distance is greater than 75λ.

Radome Incident Reflection Measurement

A response and isolation calibration can be performed at the input port of the X-Band waveguide connecting the panel antenna, and when the panel antenna is mounted at the radome-off configuration. The calibrated SNF can easily achieve a background VSWR of less than 1.02 or -40 dB in the RF system's background reflection noise. When the radome is mounted in front of the panel antenna at radome-on configuration, the incident reflection (IR) is measured with the panel antenna incident at 15 different positions to the radome. ***Table 3*** shows the sample measured IR from the largest commercial aircraft radome.

TABLE 3 INCIDENT REFLECTION OF THE LARGEST RADOME

Radome P/N & Serial Number		*41427110-51 (J089808483-0000)*		
Antenna P/N & Serial Number		*Rockwell Collins (P/N:622-5137-601)*		
Test Frequency		*9.333 GHz*		
Test Date		*2021/5/8*		
Antenna Position (reference table X in test)		*A: 37″*		*B: 35.5″*
		<<Left	*Azimuth Angle (Degrees)*	*Right>>*
	El Angle	-40 (%)	0 (%)	40 (%)
^ up Elev. Angle (Deg.)	20	0.03	0.01	0.05
	10	0.05	0.02	0.06
	0	0.03	0.01	0.02
	-10	0.01	0.03	0.03
	-20	0.02	0.03	0.02

Values shown are percentage change in S11 between Radome off and Radome on test cases. (S11_Radome+Antenna-S11_Antenna)^2*100 (Requirements is IR < 0.5%)

Beam Deflection, Pattern Distortion and SLL

Beam deflection and pattern distortion were first tested at the radome-off configuration for the pattern stability over a period of more than 48 hours. It was demonstrated that the SNF test system has a worst-case peak value difference of less than 0.003 dB and a beamwidth difference of less than 0.002, which is approximately a 0.09 per-

INTRODUCING ALTUM RF'S FAMILY OF LOW-NOISE / DRIVER AMPLIFIERS

These compact devices support a range of applications, including telecom, point-to-point radio, ISM, VSAT, SATCOM, aerospace and defense, and test and measurement.

- **ARF1200Q2:** Ka-band, 22 dB linear gain, 1.6 dB NF, ideal for phased array applications
- **ARF1205Q2:** low current consumption, single positive bias operation
- **ARF1211Q3:** ultra-low current consumption, for use in SATCOM, A&D radio systems, test and measurement
- **ARF1218Q2:** for 24 GHz applications, battery-operated applications, single positive bias

Part	Freq. Range (GHz)	Gain (dB)	NF (dB)	P1dB (dBm)	Bias Voltage (V)	Bias Current (mA)	Package
ARF1200Q2	22–31.5	22	1.6	8	3.3	15	2.5 × 2.5 QFN
ARF1201Q2	22–31.5	24	2.4	15	3.3	40	2.5 × 2.5 QFN
ARF1202Q2	37–43.5	21.5	2.5	7	3.3	15	2.5 × 2.5 QFN
ARF1203Q2	37–43.5	21	2.7	12.5	3.3	40	2.5 × 2.5 QFN
ARF1205Q2	13–25	23	1.9	16	4	65	2.5 × 2.5 QFN
ARF1211Q3	6–14	25	1.7	20	5	60	3 × 3 QFN
ARF1218Q2	22–26	29	2.6	9	3.3	6	2.5 × 2.5 QFN

LEARN MORE AT BOOTH B084B IN THE DUTCH PAVILION AT EuMW 2025 & ALTUMRF.COM

INFO@ALTUMRF.COM | +31 (0) 40 2390 888 | TWINNING CENTER, DE ZAALE 11, 5612 AJ EINDHOVEN, THE NETHERLANDS

800.348.5580 / 630.208.2200 RELLPOWER@RELL.COM RELLPOWER.COM

Richardson Electronics
POWER & MICROWAVE TECHNOLOGIES

Samples of Altum RF's low-noise / driver amplifiers are available now from Richardson Electronics, Ltd.

40W267 Keslinger Road / P.O. Box 393, LaFox, IL 60147-0393 cent change between two azimuth plane pattern results. The maximum sidelobe difference is 0.79 dB at -35 dB SSL. The tests were done for a smaller radome in the beam peak deflection between radome-off and -on. The test results show a less than ±0.2 degrees beam peak pointing error at the radome-on. The averaged small radome antenna pattern beamwidth distortion test data at both nominal and λ/4 shift inclusive test distance also shows a much less than ±0.2 degrees beam peak pointing error. The SSLs have been verified to comply with the test requirement and agree with test reports from other sites.

CONCLUSION

A multi-probe SNF test system with several unique features has been developed to perform all required antenna pattern testing fully compliant with the latest RTCA DO-213A Change 1A. The system has been verified for accuracy and repeatability and has demonstrated excellent performance. With proper selections of the SNF scanning test parameters and careful considerations of the AUT energy concentration, the multi-probe test system can also be efficient in test time.

The fixed panel antenna position and the fixed scan surface range configuration are found to be crucial factors in this test system's accuracy and repeatability. By adding the roll positioner in the radome handling, both EL/AZ and AZ/EL gimbal systems for the panel antenna can be simulated and tested for the radome-on AUT patterns. A coordinate conversion calculation has been provided.

Furthermore, by using the longer test distance in the SNF system, the NF coupling error in both radome-off and radome-on antenna pattern tests is negligible. This may allow further enhancement in test time by eliminating redundant, time-consuming TE pattern tests. ■

ACKNOWLEDGMENT

The authors would like to thank Boeing Tianjin Composite and Boeing Seattle technical staff for their help and support throughout this project. Many thanks to the engineering teams of both ETS-Lindgren China and Nanjing MJK Engineering for their effort in overcoming many unforeseen hardships, especially during the COVID times. This project could not have been completed successfully without the teamwork of these parties.

References

1. D. W. Hess, R. Luna and J. McKenna, "Electromagnetic Radome Measurements: A Review of Automated Systems," January 2005.
2. M. L. Goff, N. Adnet, N. Gross, L. Duchesne, A. Gandois and L. Durand, "A Novel and Innovative Near-Field System for Testing Radomes of Commercial Aircrafts," *Proc. AMTA 2017*, October 15-20, 2017.
3. J. Wilbur, "Low Cost Automated RTCA DO/213 Compliant Radome Test System," *Proc. AMTA 2011*, October 16-21, 2011.

MiCable

6~40GHz

16-WAY ULTRA WIDEBAND POWER DIVIDER/COMBINER

5G / Testing / Instruments & others

NEW

Low VSWR / Low I. L. / High Isolation

Excellent Amplitude & Phase Unbalance

P/N	P16N060400
Way	16
Freq. Range	6~40GHz
Sum VSWR	1.7:1 (Max.)
Distri. VSWR	1.7:1 (Max.)
Insertion Loss*	5.5 dB(Max.)
Amplitude Unbal.	±0.8 dB(Max.)
Phase Unbal.	±12 Deg.(Max.)
Isolation	15 dB(Min.)
Dimension	44.5×210×12.7(mm)

* Above Theoretical Loss 12dB

Test Curve

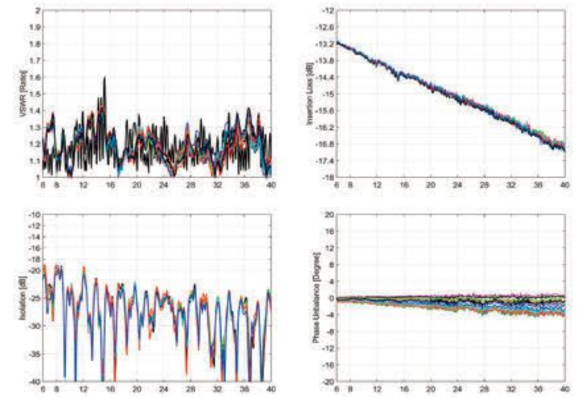

More Information-
Scan the QR Code

MIcable Inc.

www.micable.cn   sales@micable.cn   +86-591-87382856


ERZIA
Setting the standard for RF excellence
INTEGRATED ASSEMBLIES
ERZIA
Engineered, manufactured, and tested
at our state-of-the-art facility.
RF Front Ends
EW, Radar, and NewSpace
Fully Customized
EUROPEAN
MICROWAVE WEEK
JAARBEURS UTRECHT
THE NETHERLANDS
21-26 SEPTEMBER 2025
www.eumw.eu
WAVES OF INNOVATION
Visit us at booth C084
erzia.com

mmWaves SPECIAL FOCUS

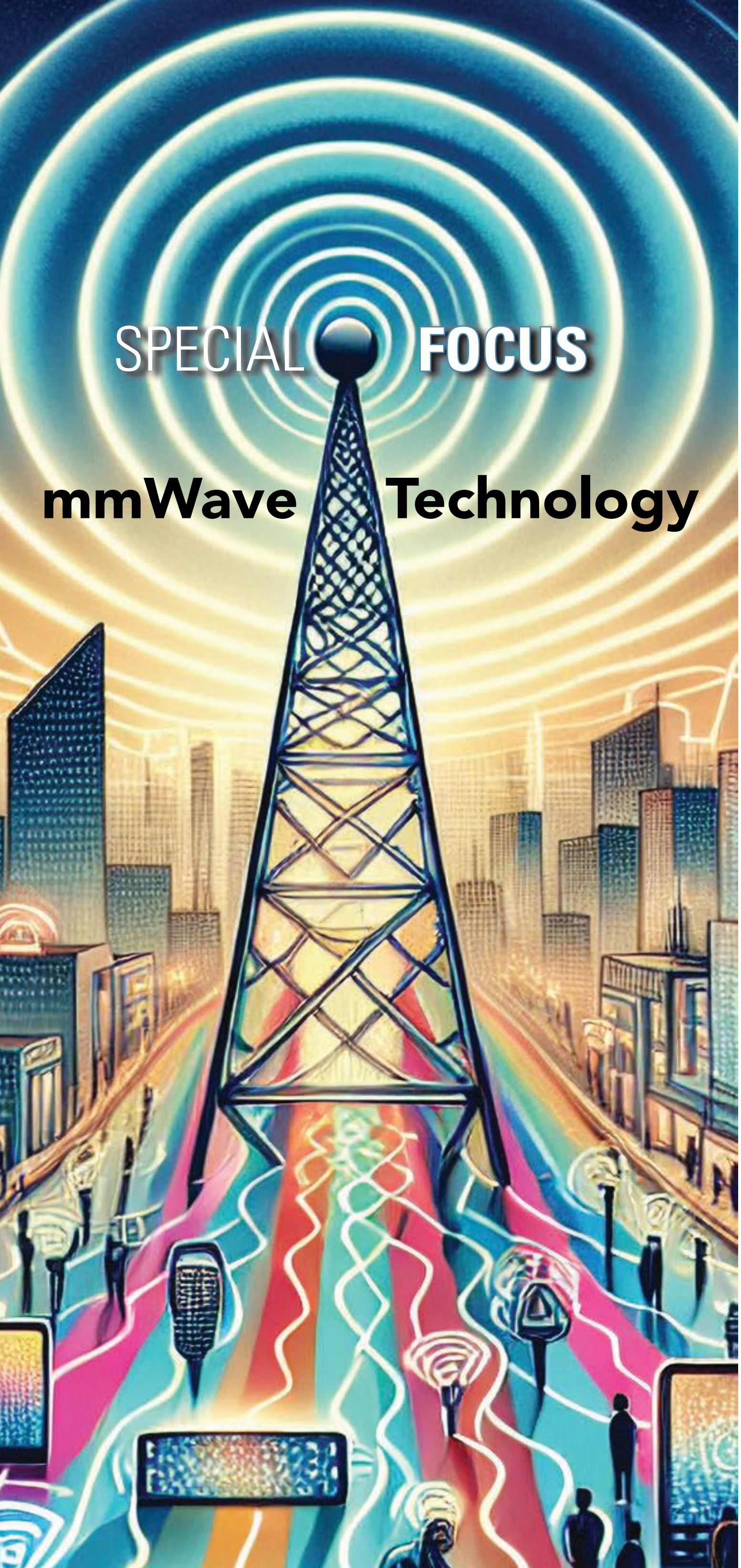

Table of Contents

Custom Uni-Guide Connectors Service Dual-Ridged Waveguides

Alex Chen and Andrew Laundrie
Eravant, Torrance, Calif.

Hermetically sealed electronic packages with waveguide interfaces can be challenging to design and costly to produce. Direct transitions from a microstrip circuit to a standard waveguide typically require a sealed dielectric window embedded in the waveguide channel. A common alternative with fewer design and manufacturing challenges uses a coaxial glass bead embedded in the package wall. The outside end of the bead's center conductor is mated with a coaxial bulkhead connector, and a separate coaxial-to-waveguide adapter is added to complete the hermetically sealed waveguide interface.

Fig. 1 **Uni-Guide waveguide connector.**

Eravant's Uni-Guide™ waveguide connectors introduce a combined packaging approach, as seen in ***Figure 1***. Several standard models provide full waveguide band coverage, with rectangular waveguide sizes ranging from WR-42 (18 to 26.5 GHz) through WR-10 (75 to 110 GHz). By sharing the same electrical and mechanical interfaces used by standard coaxial connectors, Uni-Guide connectors enable more direct transitions from microstrip circuits to waveguide ports, while taking advantage of the relative simplicity and low cost of a glass bead embedded in the electronic package. Depending on the Uni-Guide model, the angular orientation of the waveguide interface can be rotated in increments of either 45 or 90 degrees. Field-replaceable and field-configurable Uni-Guide connectors can reduce the costs and delays associated with component design and production. They also provide a means of repairing and maintaining equipment that requires frequent waveguide connections. Common applications include antenna test ranges, portable test equipment and production test stations. Many common wave-

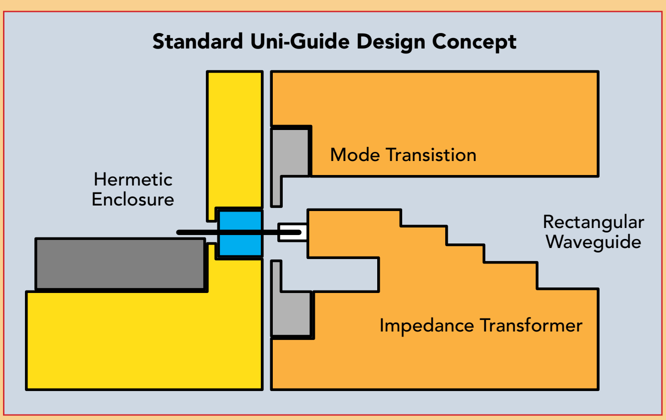

Fig. 2 **Design concept of waveguide and coax connector interface.**

YOUR PARTNERS IN 6G TESTING.

While 6G standards continue to evolve, ETS-Lindgren is already developing innovative solutions to help our customers prepare for 2030—and beyond. As the industry works to define the next generation of wireless technology, ETS-Lindgren is actively supporting early 6G research with advanced test environments, precision measurement systems, and next-gen OTA (Over-the-Air) validation tools.

With a proven track record in supporting every generation of wireless standards, we're committed to empowering researchers, developers, and manufacturers with the tools they need to accelerate breakthroughs for tomorrow. Our work ensures our customers stay ahead of the curve—ready for the challenges and opportunities 6G will bring in the next decade. We remain *Committed to a Smarter, More Connected Future*.

For more information on our Wireless Solutions, visit our website at www.ets-lindgren.com or contact your local ETS-Lindgren office or representative.

Connect with us at:

COMMITTED TO A SMARTER, MORE CONNECTED FUTURE

ETS·LINDGREN®
An **ESCO Technologies** Company

Offices Worldwide | **ets-lindgren.com**

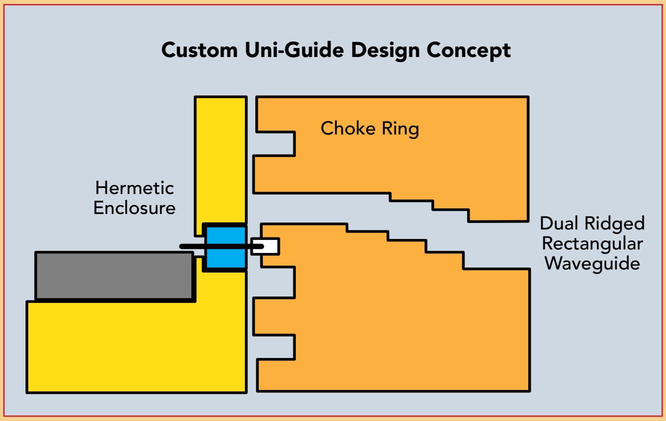

▲ Fig. 3 Removal of back-short usually included in design.

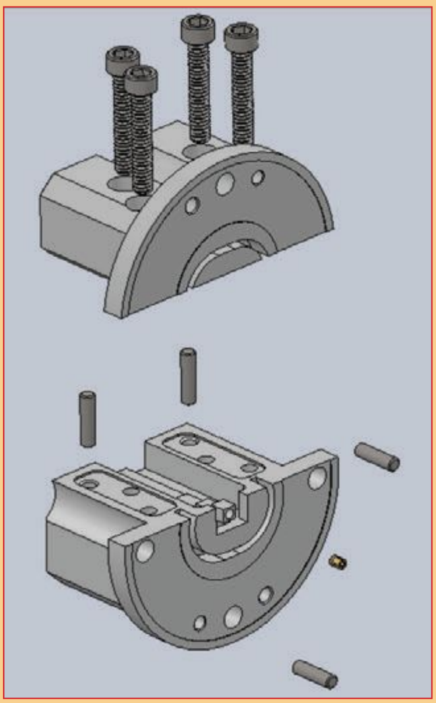
▲ Fig. 4 Split block connector design.

guide components such as amplifiers, mixers, frequency multipliers and noise sources, can also benefit from the versatility and effectiveness of Uni-Guide connectors.

The design concept behind Uni-Guide connectors is a waveguide interface that matches that of a standard coaxial connector, as demonstrated in ***Figure 2***. The pin protruding from a coaxial glass seal passes through a small hole in the waveguide connector and terminates inside a receptacle embedded in the mode transition section of the connector assembly. An impedance transformer bridges the span between the mode transition and the waveguide flange. Hole patterns in the waveguide connector match those of a standard coaxial connector, making Uni-Guide waveguide connectors fully interchangeable with industry-standard coaxial connectors. By avoiding a pair of mated coaxial connectors in the signal path, Uni-Guide connectors achieve lower insertion loss and improved impedance matching when compared to other realizations.

Standard Uni-Guide waveguide connectors include model SUF-1009-280-S1, spanning 75 to 100 GHz with a WR-10 waveguide flange. Its coaxial port is compatible with 1 mm flanged connectors that accept a pin diameter of 9 mils and mounting holes separated by 0.28 in. Other Uni-Guide connectors with the same 1 mm coaxial interface use WR-12 and WR-15 flanges. Additionally, Eravant offers models that interface to waveguide sizes WR-19, WR-22 and WR-28, covering full waveguide bands from 24 to 60 GHz. These models are compatible with 1.85 mm flanged coaxial connectors that accept a pin diameter of 12 mils and have mounting holes spaced 0.48 in. apart.

Additional Uni-Guide models include one that operates from 18 to 28 GHz using a WR-42 waveguide interface, and another that covers 22 to 33 GHz through a WR-34 flange. Both models accept a pin diameter of 12 mils and require mounting holes spaced 0.750 in. apart on either side of the glass bead. To accommodate standard coaxial connector types, an additional pair of mounting holes may be added to the component package to make these waveguide connectors fully interchangeable with commonly available coaxial connectors.

CUSTOM DESIGN EXAMPLES

A customer who recognized the benefits of field-replaceable and field-configurable waveguide ports presented a set of unique requirements. Their needs were not fully addressed by any standard Uni-Guide connector. In particular, the customer required a WRD-180 dual-ridged waveguide interface that covers 18 to 40 GHz with a maximum insertion loss of 0.25 dB and a minimum return loss of 15 dB. For comparison, the standard Uni-Guide connector model SUF-2812-480-S1 provides an insertion loss of 0.3 dB and a return loss of 20 dB from 24 to 44 GHz.

Eravant engineers were confident they could modify the mode transition and impedance transformer of a standard Uni-Guide connector to achieve the wider bandwidth of a WRD-180 waveguide interface. However, the customer also presented an existing, non-standard coaxial interface that could not be modified. The greatest challenge was a glass seal with a center pin that was shorter than what a standard Uni-Guide connector requires. The shorter pin forced the removal of the back-short typically included with a standard connector design, as seen in ***Figure 3***. Because a back-short is essential for impedance matching and mode conversion, the component package's outer surface would have to serve as the back-short in the new design. The proposed arrangement increased the risk of signal leakage and spurious resonances caused by small gaps between the package and the waveguide connector. As a result, a choke ring was included in the proposed design to reduce signal leakage and suppress resonances.

To demonstrate feasibility and optimize the dimensions of the mode converter and impedance transformer, electromagnetic simulations were performed using CST Studio. The optimized design predicted a minimum return loss of 20 dB from 18 to 40 GHz. The base material selected for the custom connector is 6061-T651 aluminum, with silver plating to minimize losses. Designed to accept pin lengths from 0.044 to 0.060 in., a pressed-in receptacle was fabricated from beryllium copper and plated with a hard gold alloy. The custom design uses a split block construction approach to accommodate the greater

complexity of the design. The split block also enables the use of economical fabrication methods while supporting a straightforward assembly process, as seen in ***Figure 4***.

CONNECTOR TESTING

Measurements of the connector's insertion loss and return loss faced the same challenges presented by any adapter that couples one connector type to another. Usually, two identical adapters are connected back-to-back and measured as a combined assembly. The performance of one adapter is determined from measurements of the combined adapters. This approach is commonly used to test coaxial adapters, coaxial to waveguide transitions and waveguide mode converters.

Two of the custom WRD-180 connectors were connected at their waveguide ports, with their combined electrical response measured at their coaxial ports. Due to their lack of an integrated back-short, the waveguide connectors could not accept a standard coaxial connector at their coaxial ports. A pair of cylindrical test fixture pieces was fabricated, with the ends of each piece accommodating either a 2.92 mm coaxial connector or the coaxial interface of a WRD-180 waveguide connector, as seen in ***Figure 5***. A hole passing through each fixture piece provided a coaxial transmission path between the custom waveguide connector and the coaxial connector. A Teflon sleeve served as a dielectric insulator for the connecting coaxial line. The insertion loss of each center piece was estimated as approximately 0.2 dB. The insertion loss of the two coaxial connectors was measured separately.

The waveguide connectors were clamped together during back-to-back measurements to determine their combined insertion loss and return loss. Insertion loss for a single connector was estimated to be one-half of the measured attenuation. This approximation assumes

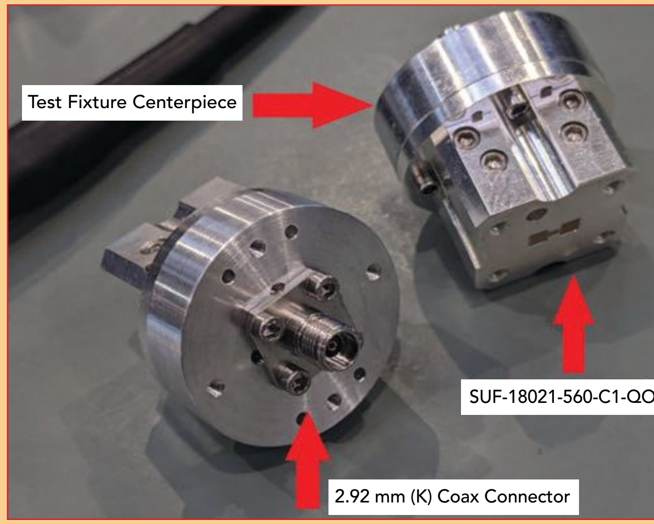

Fig. 5 **Test fixture for Uni-Guide connectors.**

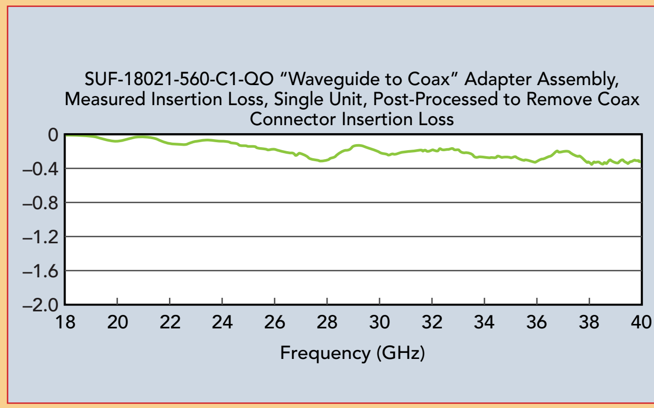

Fig. 6 **Insertion loss of a single waveguide connector.**

that mismatch effects have a negligible impact on overall insertion loss. The attenuation of the fixture center pieces and the 2.92 mm coaxial connectors were sub-

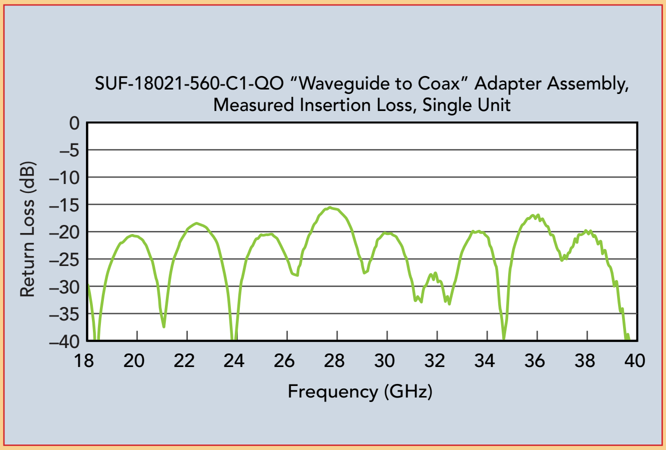

Fig. 7 **The estimated return loss of a single waveguide connector.**

tracted from the measured insertion loss to yield the insertion loss of a single waveguide connector, as shown in ***Figure 6***.

The return loss of the combined assembly was also measured. Noting that mismatch effects are additive for low loss pairs of identical components connected back-to-back, the estimated return loss of a single waveguide connector was estimated as the return loss of the combined connectors, offset by 4 dB to compensate for the additive effects of cascaded components, as demonstrated in ***Figure 7***.

Overall, the first iteration of the custom design nearly meets all requirements presented by the customer. Electromagnetic simulations predicted that the custom connectors would handle at least 200 W. Although the measured insertion loss of 0.4 dB (average) exceeded the desired goal of 0.25 dB, return loss met or exceeded the goal of 15 dB. The connectors thus demonstrated the feasibility and practicality of expanding the Uni-Guide product family to include dual-ridged waveguide interfaces.

Based on the success of the WRD-180 design, another Uni-Guide waveguide connector was developed for the same customer to cover frequencies from 6 to 18 GHz using a WRD-650 waveguide interface. This custom design was not required to mate with an unusually short center pin, to allow the use of an integrated back-short similar to those used in standard Uni-Guide connectors. The WRD-650 Uni-Guide connector accepts a standard 36-mil pin and supports power levels up to 400 W. Maximum insertion loss is 0.3 dB and minimum return loss is 15 dB from 6.5 to 18 GHz.

By using Uni-Guide waveguide connectors, component manufacturers can offer a wide range of waveguide sizes and orientations using a reduced number of package designs. As drop-in replacements for existing industry-standard coaxial connectors, they are field-replaceable and field-configurable. When customers require a specific waveguide size and orientation on an electronic component, Uni-Guide waveguide connectors reduce or eliminate the need for non-recurring engineering and its associated dual costs and delays. Custom designs utilizing dual-ridge rectangular waveguides have been developed, with more designs and new applications on the horizon.

Eravant applies design modifications to standard components and develops integrated assemblies for specific applications. They typically have turnaround times from two days to eight weeks for complex assemblies. Custom solutions are based on a design library of over 5,000 components. Using mature designs as a foundation not only reduces uncertainty but also ensures that design reviews are completed faster and hardware is manufactured sooner. Eravant works closely with customers through an interactive development process that makes prototypes more compact, robust and affordable with each new revision. ■

Q- and V-Bands for Next-Gen Communications

Tudor Williams
Filtronic, Sedgefield, U.K.

In today's world, communication must be instant and reliable, regardless of location. Operating from 37 to 52 GHz, Q- and V-Bands open the door to significantly larger data pipelines; however, reaching these higher frequencies presents a new set of technical challenges. While many feeder links in the satellite communications (satcom) market today operate at Ka-Band, the push toward Q- and V-Bands is gaining momentum. This shift is being driven by the ever-growing need to move larger volumes of data, especially in satcom and Earth observation.

The Q- and V-Bands open far more spectrum, with bigger and more continuous bandwidths than Ka-Band, enabling higher data rates and more efficient transmission between satellites and ground stations. However, moving to higher frequencies presents challenges. For example, design becomes significantly more complex, and today, few commercial products operate effectively at 50 GHz and above. High-power systems are particularly challenging and typically rely on traveling-wave tube amplifiers (TWTAs). Although TWTAs are effective, they are expensive, complex to manufacture and have a limited lifetime.

This is where solid-state alternatives come into play, thanks to advances in semiconductor processes. The shift from GaAs to GaN, the industry migration to shorter wavelengths and the combination of low loss and waveguide combining make solid-state amplifiers a rival to TWTAs. In addition to similar performance, solid-state amplifiers offer advantages in cost, scalability, production speed and lifetime.

The Q- and V-Bands are also attractive due to the structure of the available spectrum. The Q- and V-Bands complement each other, and using both together maximizes spectral efficiency and ensures operators benefit from the available bandwidth.

ARTES PROGRAM AND SATELLITE NETWORKS

A new development in satcom is the ARTES program, a European Space Agency (ESA)-backed initiative designed to push the envelope in satcom technology. Filtronic recently secured a contract with ESA to develop RF solutions for next-generation satellite networks at Q- and V-Bands, as well as K- and Ka-Bands.


qorvo
Connecting the World Through Space
With system-level expertise and a broad product portfolio, Qorvo enables seamless connectivity across ground, airborne and space-based SATCOM platforms.
LEARN MORE at
qorvo.com/go/satcom
© 07-2025 Qorvo US, Inc. | QORVO is a trademark of Qorvo US, Inc.

As part of ESA's ARTES 4.0 program, Filtronic will design high-power RF solutions for next-gen satellite networks. The networks focus on cost-effective feeder links for 'new space' satellite payloads to enable high-throughput communications and efficient transmission. The satellite uses Q-Band for transmitting and V-Band for receiving, accessing a large bandwidth for higher data rates. This approach is key to enhancing broadband communication for satellite constellations, which are increasingly relied upon to meet the growing demand for data.

One key aspect of this project is its adaptability. While it is focused on LEO applications, the technology being developed can be adapted for use in medium Earth orbit (MEO) and geostationary Earth orbit (GEO) satellites. This flexibility can support a range of applications from commercial satellite networks to military communications, making it a resource for both civilian and defence sectors.

A persistent challenge in the industry is the volume of data these networks need to handle. While the K- and Ka-Band systems are currently sufficient, they are increasingly strained as data demands grow. With recent developments in higher frequency solutions, such as Q- and V-Bands, the work being done in this program is laying the groundwork for advancements.

The project's goal is to create a flexible, high performance system that can operate across different orbits. By blending LEO, MEO and GEO satellite networks, it is possible to create a more resilient and efficient communication system that can better handle the increasing data load. Additionally, the potential defence applications expand the importance of the program. As the demand for secure and reliable space-based communications rises, technologies that can adapt to both commercial and military needs are becoming more valuable.

This program is setting the stage for future satcom systems that will meet the growing data demands of today's connected world. It is an exciting time for space communications, and this initiative is a step forward in making commercially viable, robust satellite networks a reality.

SECURE BATTLEFIELD COMMUNICATIONS

Unlike lower frequencies, which tend to spread signals over a broader area, the narrower beam widths produced at higher frequencies are harder to intercept or jam. This makes mmWave frequencies like Q- and V-Bands particularly attractive for secure battlefield communications.

Although tactical communications using mmWave are still emerging, their potential for secure, high data rate transmissions is undeniable. With growing interest in using Q- and V-Band frequencies for military satcoms, a clear trend is emerging toward higher frequency solutions to enhance secure communications in both tactical and strategic settings. Additionally, they are more resistant to jamming, as the power required would exceed that of conventional systems.

The advances in semiconductor technology, particularly with GaN, have enabled improvements in the power density of devices operating at high frequencies. This has enabled Filtronic to push the boundaries of power output, providing solid-state solutions capable of supporting high-power applications, such as those required in defence communications.

mmWave technology is also making an impact in missile systems, particularly with mmWave seekers. These systems utilize high frequency signals to achieve superior spatial resolution, thereby enhancing the accuracy of target detection and tracking while maintaining the same level of protection from jamming in contested and congested environments. In the U.K., the defence sector is exploring high frequency solutions, displaying the military and government sectors' increasing focus on next-gen systems to enhance secure communications. By combining GEO, MEO and LEO satellite systems with Q- and V-Band frequencies, these advancements will increase the security and resiliency of communications.

CHALLENGES AT Q- AND V-BANDS

High frequency systems bring many benefits but introduce thermal management challenges. As operating frequencies rise, device efficiency typically declines. While lower frequency devices may reach efficiencies of 40 to 50 percent, systems in V-Band often see efficiencies drop to just 10 to 20 percent. This means much of the input energy is converted into heat, creating a significant engineering challenge, especially in compact satellite and defence systems where space and weight are limited.

Historically, GaAs devices at these frequencies offered modest output power, helping mitigate thermal issues. However, with advances in semiconductor technology and a move to GaN, power output has increased significantly. Filtronic, for example, has increased power output by 4x to 5x within the same footprint compared to earlier designs. While this boost is essential to overcome atmospheric attenuation at Q- and V-Band frequencies, it damages the manageability of the thermal load.

Addressing these challenges requires a holistic approach. High performance thermal interface materials, die attach solutions and heat spreaders are all crucial for optimising heat extraction while maintaining mechanical reliability. Additionally, system-level design plays a key role. Combining multiple smaller devices into a module can evenly distribute heat and improve overall thermal stability. Continuous improvements in thermal management — from advanced materials to precision assembly techniques — will be key in enabling the reliable operation of high frequency, high-power systems in space and defence applications.

Scaling up production introduces a layer of complexity. Scaling from prototype to high volume manufacturing presents significant challenges since high frequency mmWave devices require precision at every step. Tiny imperfections in materials or interconnects can have a substantial impact on RF performance.

Because of this, manufacturing techniques must be precise and require advanced processes that can handle the tight tolerances necessary for these high frequency applications. Additionally, supply chain security is a risk. Currently, many high-reliability packaging facilities are offshore, which raises security concerns, especially regarding critical applications in defence and infrastructure.

PROMISES AND CHALLENGES OF GAN

GaN is gaining traction in high-power and high frequency applications. With its properties such as a high breakdown voltage, excellent electron mobility and superior thermal conductivity, it is proving to be a disruptor in industries such as satcoms, radar and defence systems. Unlike materials such as silicon or GaAs, GaN enables more efficient and higher-power output, which opens up new possibilities for next-gen technologies.

However, as with most breakthroughs, these advantages come with challenges. One of the biggest hurdles, similar to Q- and V-Band challenges, is thermal management. GaN devices, especially those operating at mmWave frequencies, generate intense power densities. GaN devices tend to generate high heat densities with hot spots around transistor gates, creating a significant heat dissipation problem. Managing that heat is crucial for maintaining peak performance and extending the lifespan of devices.

The challenges are applicable in defence and space as well. These systems are designed to endure extreme conditions, from wide temperature fluctuations to exposure to radiation and mechanical stress. As a result, GaN packaging must do more than protect the device — it must keep things running smoothly in harsh environments. The packaging must ensure that thermal stability and signal integrity are maintained, even in harsh conditions such as the vacuum of space or on the battlefield.

Lastly, the heat generated by GaN demands a packaging solution that strikes the right balance. The materials used must withstand the intense thermal load while also accounting for the differences in thermal expansion between the device and traditional packaging materials. Without striking this balance, the device could face mechanical stress, cracking or delamination during thermal cycling, therefore disrupting its performance.

> **"This program is setting the stage for future satcom systems that will meet the growing data demands of today's connected world.**

MATERIALS AND TECHNIQUES FOR HIGH FREQUENCY

To tackle the challenges of high frequency systems, the industry is exploring advanced materials and techniques. Technologists are testing sintered silver, particularly in die attach methods. This material offers high conductivity, void-free bonds that effectively draw heat away from the device, ensuring better performance while maintaining mechanical robustness. Sintered silver is especially appealing for industries such as aerospace, defence and satcoms, where high-reliability performance is crucial, particularly under extreme conditions like high temperatures and mechanical stress. It also has advantages in high volume production environments. For mission-critical applications, eutectic gold-tin (AuSn) bonding is the preferred choice. Its ability to handle rapid thermal cycling and vacuum environments makes it a reliable material for systems where stability and reliability are non-negotiable.

Additionally, substrate materials have a high impact on performance. For example, copper-tungsten (CuW) and copper-molybdenum (CuMo) are great choices because they offer a thermal expansion match to GaN and provide high thermal conductivity. This helps reduce stress at the interface and prolongs device life. Meanwhile, diamond heat spreaders can be used alone or combined with innovative cooling techniques, such as liquid cooling. Another popular choice is aluminium nitride (AlN), which balances thermal performance, electrical insulation and manufacturability — increasingly crucial as systems become more compact and power-dense.

The techniques used for packaging are also evolving to meet the demands of high frequency systems. Traditional wire bonding remains reliable; however, it can introduce inductance and loss, which limits bandwidth and efficiency. These limits are especially detrimental at mmWave frequencies. As a result, newer methods such as flip-chip mounting, embedded passive structures and 3D packaging are gaining traction. These approaches reduce interconnect lengths, minimise parasitic losses and optimise thermal paths, making modules more compact, lightweight and efficient. With the communication demands of today's world, industries such as satcoms and defence are pushing further into the high frequency Q- and V-Band ranges.

As industries pursue these higher frequencies, challenges around thermal management, packaging and device reliability are becoming more pronounced. Yet Q- and V-Bands also open the door to advancements, with the potential to expand data capacity and spectrum, improving global connectivity and secure communications.

Pushing into these higher frequencies will continue to challenge the industry, especially from a design perspective. However, the progress underway today is laying the foundation for the next generation of high performance, resilient satellite networks, thanks to more data bandwidth capacity. ■

Leveraging the Potential of 5G mmWaves

Rajesh Kumar Manish
MarketsandMarkets, Pune, India

MmWave, commonly called extremely high frequency or very high frequency, is the band of spectrum between 30 and 300 GHz. Their wavelengths range from 1 to 10 mm. Previously, mmWaves were mainly used in military and satellite communication applications; however, this technology has been gaining traction in mobile and telecom applications, including 5G. In the context of wireless communication, mmWave generally refers to bands of the spectrum centered at 38 GHz, 60 GHz and 94 GHz. According to MarketsandMarkets, and as shown in ***Figure 1***, the mmWave technology market is expected to grow at a CAGR of 20.1 percent between 2024 and 2029, driven by

Fig. 1 **Overview of mmWave technology growth.**

increasing mobile data traffic, growing demand for bandwidth-intensive applications and high adoption in small cell backhaul networks. Mobile and telecommunication is one of the most significant end-use segments for mmWave technology, as mmWaves are widely used in small cell backhaul networks to ensure fast connectivity. Thus, mmWave backhaul equipment is an integral part of the deployment of 5G, which is expected to create avenues for future growth. In addition, the aggregate data rates supported by the upcoming 5G technology are expected to be 1000x and 100x more than those of the existing 3G and 4G data rates, respectively. Thus, there would be a growing need for the mmWave spectrum to provide an increased data rate and enhanced quality of the received signal.

INCREASING USE OF MMWAVE TECHNOLOGY IN VARIOUS INDUSTRIES

mmWave is a preferred technology across various industries. The mmWave technology market has experienced significant growth over the past decade. Currently, mmWave finds use in mobile and telecom, consumer and commercial, aerospace and defense, imaging, commercial and industrial segments, with many additional potential applications. The mmWave ecosystem comprises product manufacturers, component manufacturers, network infrastructure designers and network operators, as shown in ***Figure 2***. mmWave products are emerging in the microwave provider market; however, they differ from other RF products in terms of their end uses and functionalities. Moreover, the integration of mmWave products with 5G connectivity makes them suitable for a wide range of applications. The component and product manufacturers use technologies offered by mmWave solution providers to develop comprehensive solutions. These solutions are then distributed and supplied by either distributor channels or specialized digital product suppliers through online and offline marketing channels.

KEY PARTICIPANTS IN MMWAVE MARKET

mmWave bands meet the high-capacity needs of 5G enhanced mobile broadband. They provide a high-capacity wireless backhaul solution, which can benefit the rapidly growing number of cell sites, particularly in densely populated urban areas. mmWave technology is becoming increasingly prevalent in wireless backhaul networks due to the growing demand for high speed internet and 5G networks. This translates to faster data transfer rates between base stations and the core network, which is crucial for supporting the massive data traffic generated by applications like 5G, virtual reality and IoT.

"The mmWave technology market is expected to grow at a CAGR of 20.1 percent between 2024 and 2029. "

With the increase in congestion levels of global data traffic, the need for mmWave technologies in mobile networks is expected to rise significantly, particularly in macrocell and microcell backhaul. In the past three to four years, LTE rollouts have increased worldwide. In turn, mmWave technology increased rapidly because LTE networks are denser than 2G and 3G networks. E-Bands and V-Bands are widely used for mmWave backhaul solutions, as they can provide a high bandwidth through a single channel, with the capability to secure about 400 Mbps transmission for a single 250 MHz channel. With the availability of equipment that supports high bandwidth, wireless networks will face increasingly heavy congestion over the next five years. This will drive the shift from the existing 3G and 4G technologies to 5G. As previously mentioned, the aggregate data rates supported by 5G technology are expected to be 1000x and 100x faster than the existing 3G and 4G data rates, respectively.

According to the Ericsson Mobility Report 2023, during the last quarter of 2023, there was a significant increase in the number of 5G subscribers, with more 5G devices becoming available.

Fig. 2 **mmWave technology market participants.**

More than 50 service providers worldwide announced commercial 5G service launches. A significant upsurge in 5G subscriptions has been witnessed in South Korea, where all service providers launched commercial 5G services in April 2022. 5G network deployments increased globally in 2023, laying the foundation for the massive adoption of 5G subscriptions. Over the next five years, the adoption of 5G subscriptions is expected to be significantly faster than that of LTE. A key factor in this is China's early involvement in 5G. This early adoption is in contrast with LTE, where the country was not one of the early markets to launch, although devices were available earlier. China is expected to hold a significant share in the 5G IoT market in Asia Pacific due to the high investments in network infrastructure and the presence of major telecom players. The rise in industrial automation is expected to accelerate the deployment of 5G networks in China, as it will provide single wireless access to large industrial facilities instead of using different short-range wireless standards, thereby minimizing signal interferences caused by obstacles. The rise in implementation of 5G networks for various applications, including manufacturing, would create a significant opportunity for mmWave technology to develop 5G infrastructure.

AI AND ML ADVANCEMENTS

Artificial intelligence (AI) and machine learning (ML) are two emerging trends in the technology industry that continue to impact various sectors. The demand for high data rate communication and the scarcity of available spectrum in existing microwave bands have been the catalysts for the introduction of 5G. To fulfill these demands, mmWaves with large bandwidths have been proposed to enhance the efficiency and stability of the 5G network. In mmWave communication, the concentration of the transmission signal from the antenna is conducted by beamforming and beam tracking.

AI and ML can be used to optimize mmWave network performance by analyzing real-time data on traffic patterns, signal strength and interference. This allows for dynamic adjustments to beamforming, resource allocation and network management, maximizing efficiency and user experience. In 5G mmWave, the process of initial beam selection, i.e. finding an appropriate beam pair between transmitter and receiver, is time-consuming. AI and ML can play a significant role in reducing the beam selection time during initial access.

THZ WAVES

With 5G efforts ongoing, in 2019, the Federal Communications Commission (FCC) opened the gates to a potential 6G future by allowing companies to begin experimenting with terahertz (THz) and submillimeter waves. These are radio bands that fall in the spectrum of 95 GHz to 3 THz.

THz waves have higher frequencies than mmWaves, addressing network congestion and bandwidth limitations. Advanced versions of 5G rely on mmWave bands to carry vast amounts of data at ultrafast speeds with minimal response time, making it possible to achieve milestones such as autonomous cars and remote surgeries. mmWaves work only over short distances, requiring a line of sight between the transmitter and the user, and THz waves have an even weaker range. However, if THz waves can be harnessed with innovative networking approaches, they may unlock more capacity for applications over a 6G wireless network.

While mmWaves boast advantages over other radio frequencies, they also have disadvantages. For example, mmWaves are not capable of bouncing off physical objects. Obstacles such as tree branches and walls can interfere with and absorb the transmission or halt the signal. In addition, mmWave technology is often more expensive than other commonly used frequencies. This makes the technology difficult for smaller companies to access. Currently, mobile network providers are focused on building mmWave ready 5G infrastructure. This includes setting up micro base stations in open

land with technology that supports mmWaves and redesigning the structure of devices that will run using the 5G network.

The limited range of mmWave technology forces telecom operators to increase the number of towers and other equipment. This range can also be expanded by increasing the transmitting power. However, increased transmitting power can result in increased fuel consumption and radiation. Transmission towers also consume a significant amount of space, leading to large-scale deforestation, primarily in rural areas. In addition, several materials used for mmWave circuits are toxic, and their prolonged use can be hazardous to the surrounding environment. These materials include SiGe, GaAs, InP and GaN.

mmWaves open more spectrum; however, until recently, only a few electronic components could generate or receive mmWaves. This gap in available electronic components caused the spectrum to remain unused. Generating and receiving mmWaves is challenging, but the traveling media is the bigger challenge associated with these high frequencies. Other challenges include atmospheric and free-space path loss, as well as poor foliage penetration. mmWaves are governed by the same physics that governs the rest of the radio spectrum, and as such, they have limitations related to their wavelength. The shorter the wavelength, the shorter the transmission range for a given power. The signal properties remain constant, regardless of factors such as antenna gain at the transmitter and receiver ends or reflection, absorption and diffraction during signal transmission. mmWaves, sub-mmWaves and THz waves will continue to have an impact on the telecom and other industries, starting with 5G growth and moving towards the introduction of 6G.

GAN TRANSISTORS

GaN high-electron-mobility transistors (HEMTs) are a viable option for mmWave applications because they can operate simultaneously at high voltage and high frequency. GaN HEMTs are used in mmWave power amplifiers, which require a gate length of less than 150 nm to control short-channel effects. These transistors offer superior performance at high frequencies compared to traditional silicon transistors. Advancements in GaN technology are crucial for developing efficient mmWave power amplifiers, a key component for mmWave systems.

As 5G expands and 6G gets closer on the horizon, mmWave and THz wave technologies will become an increasing priority for network providers. This growth will usher in new products, materials and network designs, enabling faster speeds and more usable bandwidth. ■

Nxbeam

Ku/ Ka/ V/ E-Band Power Amplifier MMICs

Maximized performance for linear power applications

Ku/Ka-Band MMIC Die and Packaged MMICs

MMIC Die:

NPA1020-DE	12.5 - 14.5 GHz	15 W
NPA2020-DE	23.0 - 25.0 GHz	10 W
NPA2001-DE	26.5 - 29.5 GHz	35 W
NPA2002-DE	27.0 - 30.0 GHz	35 W
NPA2003-DE	27.5 - 31.0 GHz	35 W
NPA2004-DE	25.0 - 27.5 GHz	40 W
NPA2030-DE	27.5 - 31.0 GHz	20 W
NPA2040-DE	27.5 - 31.0 GHz	10 W

QFN Packaged MMICs:

NPQ2101-SM	27.5 - 31.0 GHz	5 W
NPQ2103-SM	27.5 - 31.0 GHz	8 W
NPQ2105-SM	27.5 - 31.0 GHz	12 W
NPQ2107-SM	27.5 - 31.0 GHz	15 W

Contact Nxbeam for Flange Packaged Options

V-Band MMICs

MMIC Die:

NPA4000-DE	47.0 - 52.0 GHz	1.5 W
NPA4010-DE	47.0 - 52.0 GHz	3.0 W

E-Band MMICs

MMIC Die:

NPA7000-DE	65.0 - 76.0 GHz	1.0 W

mmWave and Sub-THz Antenna Testing

MilliBox
San Jose, Calif.

FEATURES OF AN ANTENNA TEST SETUP

Antenna test setups play a critical role in the design and optimization of wireless systems. When designing an antenna, the engineer typically starts by using electromagnetic (EM) software simulators to optimize the antenna's specifications for parameters such as gain, efficiency, bandwidth, beamwidth and polarization. Once the antenna is manufactured, it must be tested over-the-air (OTA) to validate that the fabricated antenna performance matches its specifications.

An antenna test setup for OTA qualification is composed of an anechoic chamber, an antenna positioner and a probe attached to an instrument with software recording the measurements, as shown in ***Figure 1***.

THE BOTTLENECK FOR MMWAVE ANTENNA TESTING

mmWave technology was traditionally defined to cover the radio frequencies from 30 to 300 GHz. At these mmWave and sub-THz frequencies, the short wavelengths have several implications.

First, the signal routing from the MMIC to the antenna with length > λ/10 cannot be neglected or treated as a lumped component. At lower frequencies, the antenna can be measured in isolation from the rest of the RF chain at the port. However, at mmWave, the MMIC and antennas cannot be accurately measured independently, and any testing will require a radiated OTA test measurement.

Secondly, to overcome path loss, phased array antennas are commonly used at mmWave frequencies to increase gain and directivity. These can be fixed passive arrays, but usually are active beamforming phased arrays with dynamic phase shifters to steer the radiating energy. In the latter case, the antenna is no longer a simple device, and the radiation pattern of the antenna array cannot be isolated from the rest of the system.

When large engineering teams work on such complex wireless systems, nearly every single design iteration can directly impact the gain, radiation pattern and directivity. If the team has one traditional chamber to share or go offsite to test, the design progress grinds to a halt.

SOLVING THE BOTTLENECK AT MMWAVE AND SUB-THZ

Antenna performance is typically characterized in the far field. The far-field distance (d) is the boundary after which the wave patterns become relatively uniform with fields that fall off in amplitude by 1/r. The far-field distance can be calculated using ***Equation 1***, where D is the diameter of the antenna and λ is the wavelength.

$$d = \frac{2D^2}{\lambda} \qquad (1)$$

For example, if engineers have a 4 × 4 antenna array with antennas spaced λ/2 apart, the far-field boundary can be calculated as d = 9λ, since D is the distance between the farthest elements of the array. At 28 GHz, this yields a far-field boundary of 9.6 cm. In the sub-THz range, this distance is even shorter.

Consequently, a small benchtop mmWave chamber on a lab bench is adequate for most antenna arrays. With multiple team members having access to their own antenna test setup, the iterative effort becomes easier. Sharing one resource cannot compete with a multitude of small team-allocated antenna test

Fig. 1 **mmWave and sub-THz antenna test setup.**

benches. This is when getting small, affordable OTA antenna test setups for mmWave and sub-THz performance is the solution.

COMPACT MMWAVE AND SUB-THZ ANECHOIC CHAMBERS

Because the wavelength at mmWave is small, the far-field distance is generally reduced when the array size stays small. With this, the overall dimension of the system can be adjusted to something 1 to 2 meters in length and remain in the far field. The compact chambers are portable, more convenient and lower cost than traditional microwave chambers.

The isolation strategy also changes when considering requirements for higher frequencies, such as mmWave and sub-THz. Lower frequencies have a longer range and penetrate obstacles more easily, causing interference. In contrast, for mmWave and sub-THz frequencies, outside interference is minimal. For one, the propagation at those frequencies is low. In addition, the spectrum is very wide, lowering the chance of accidental interference. Furthermore, because higher frequencies need a higher gain directional antenna to propagate further, the chance for internal stray reflection increases significantly. In other words, in microwave frequencies, the chance for outside interference is high and internal reflection is low, whereas in mmWave and sub-THz frequencies, the opposite is true — the chance of outside interference is low, but internal stray reflection is much higher. Therefore, MilliBox uses non-metal enclosures since they reduce internal reflections and introduce a minimal risk of outside interference.

Fig. 2 **Radiation pattern from a 28 GHz 8 x 8 phased array system.**

AUTOMATED POSITIONER FOR RADIATION PATTERN MEASUREMENTS

When the antenna under test is placed on a positioner, the transmitted power can be measured from a distant point where a probe or a feed horn is placed. As the antenna is rotated, additional points are captured, creating a clear graph of the power level at different angles, constituting a radiation pattern.

Radiation patterns verify that the antenna is propagating its power in the desired direction. Elaborate antennas, such as horns and phased arrays, are directional and intended to transmit power in a specific direction. A 3D positioner becomes indispensable for these measurements.

3D antenna positioners have two or more rotation axes with motors controlled by software. This controls the antenna position on one side and connects to an instrument on the other end, allowing it to plot a 3D image of the radiation pattern directly. A typical 3D radiation pattern from a phased array is shown in ***Figure 2***.

CHARACTERISTICS OF AN MMWAVE ANTENNA POSITIONER

Generally, a positioner is defined by its size and weight capacity, its number of rotation axes and its angular resolution. ***Figure 3*** shows a MilliBox 3-axis antenna positioner. MilliBox aims to reduce the risk of stray reflection, so they manufacture the body of the positioner with non-metal materials. Positioner bodies

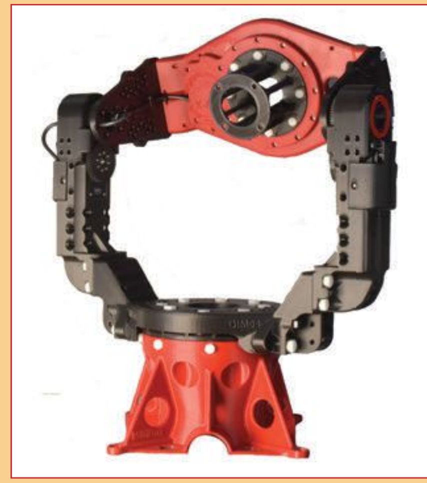

Fig. 3 **mmWave 3-axis antenna positioner.**

can be made of organic material, such as plastic or foam, or covered in absorbing material.

Capturing OTA data can be done in many ways; therefore, the flexibility of having the positioner's controller in source code is a great advantage. Python, a free and well-known program, is the first choice to control the positioners. Additionally, having the data capture output in a portable format, such as CSV, helps broaden the choice of data visualization tools.

Wiring and signal routing are often afterthoughts that can have disastrous consequences. Having all rotation axes hollowed such that the cables can be routed through reduces cable length and torsion stress on those cables. For instance, low-profile cable assemblies are compatible with automated 3D antenna positioners, and when waveguide is the only practical device under test connectivity, embedding frequency extenders into the 3D positioners is a solution.

OPTIMIZED ANTENNA TEST SOLUTIONS

The needs for antenna test solutions at mmWave frequencies and beyond differ from those of lower frequency microwave testing, and having multiple test setups available to design engineers increases throughput and efficiency. MilliBox offers a line of anechoic chambers and antenna positioners that cater to the specific requirements of the mmWave and sub-THz wireless markets. ■

PA MMIC Extends the Reach of Ka-Band Satcom

Next-generation broadband satellite systems require exceptionally linear and high-power RF links to support "anywhere, anytime" connectivity. mmTron's TMC215 MMIC power amplifier (PA) extends the linear power benchmarks for Ka-Band satcom. Covering 27 to 31 GHz, the TMC215 delivers 45 W of output power at 1 dB compression (P1dB) with 34 percent power-added efficiency (PAE).

In linear operation, the PA achieves –32 dBc spectral regrowth at 25 W output and a 21 dBc noise power ratio (NPR) at 22 W. With a 5G NR signal, the error vector magnitude (EVM) remains below 3 percent up to an output power of 10 W, and the adjacent channel leakage ratio (ACLR) exceeds –40 dBc. The three-stage architecture provides 23 dB linear gain.

The TMC215 is typically biased at 28 V drain voltage and 3 A current draw. To support flexible system integration, the drain bias can be reduced to 18 V, enabling power scaling while maintaining linearity and PAE.

Built using space-qualified GaN-on-SiC technology, the TMC215 was engineered for demanding environments. The transistor layout, matching networks and backside metallization were optimized for high reliability. When assembled according to mmTron's guidelines, the mean time to failure (MTTF) exceeds 10^7 hours at a junction temperature below 210°C.

The amplifier is available as bare die (4.9 × 4.0 × 0.1 mm), die-on-tab (CuMoCu, CuW or Ag-Diamond) with bypass capacitors or in a flange package. An evaluation module is also available for prototyping and testing.

The TMC215 is just one of mmTron's high-linearity, high-power MMICs that cover frequency bands between 22 and 42 GHz. Datasheets are available at mmtron.com/products/.

mmTron, Inc.
Redwood City, Calif.
www.mmtron.com
contact@mmtron.com

WIDEBAND RF UP-CONVERTER

VENDORVIEW

The ADRF6780S is a wideband RF up-converter, qualified for high-reliability aerospace applications and sold in a compact plastic package. This IC has an RF output from 6 to 24 GHz and a selectable multiplier LO covering 5.4 to 28 GHz. The ADRF6780S integrates mixers, VVAs, multipliers, buffers and log detectors into one chip and has the flexibility to support zero IF or superheterodyne architectures.

Analog Devices
www.analog.com

MMWAVE OTA ANTENNA TEST SYSTEM

VENDORVIEW

The mmWave OTA Antenna Test System is a turnkey solution for customers needing to make far-field antenna measurements up to 220 GHz. The measurement system is anchored by a CMT VNA and includes a 3D antenna positioner (Gimbal), sophisticated but intuitive measurement software, frequency extender modules and accessories to set up a chamber for far-field antenna measurements. Each OTA bundle can be configured with a set of two, three or four anechoic chamber cubes, depending on far-field measurement requirements.

Copper Mountain Technologies
www.coppermountaintech.com

PLO PRODUCES +15 DBM AT 34 GHZ

VENDORVIEW

Based on high performance voltage-controlled dielectric resonator oscillator (DRO) technology, model SOP-34310115-KM-BB is a phase-locked oscillator (PLO) that generates 34 GHz at +15 dBm. Using either an internal or external reference signal, typical phase noise is -85 dBc/Hz at a 10 kHz offset. Phase-lock and phase-error output signals are provided.

Eravant
www.eravant.com

AMP20052, 20 – 500 MHZ, 1000 W

VENDORVIEW

Exodus AMP20052 is designed for EW/ECM, EMI/RFI, lab and general communications applications.

It has a Class A/AB linear design and 1000 W minimum with 60 dB gain. It features high-power advanced technology devices for instantaneous bandwidth. Optional monitoring for forward/reflected/VSWR indication as well as voltages and currents is available. It provides high efficiency with unprecedented reliability and ruggedness in a 6U chassis.

Exodus Advanced Communications
www.exoduscomm.com

ULTRA-BROADBAND HIGH PERFORMANCE POWER DIVIDERS

The HYPERLABS power divider lineup includes 2-way and 4-way resistive dividers with models operating up to 110 GHz. The broadband Wilkinson power divider product line offers 2-way models operating up to 67 GHz designed to provide highly symmetrical amplitude and phase division with high isolation. HYPERLABS is a global provider of ultra-broadband amplifiers, baluns, pick-off tees, bias tees, DC blocks, power dividers, pick-off tees attenuators and more.

HYPERLABS
www.hyperlabs.com

HIGH POWER SURFACE-MOUNT 90° HYBRID

VENDORVIEW

MIcable released the new 0.225 to 2 GHz high power surface-mount 90-degree hybrid. It has low insertion loss (0.8 dB max.), excellent VSWR (1.30:1 max.), extremely good amplitude unbalance (±1 dB max.) and phase unbalance (±5 degrees max.), high isolation (17 dB min.) and 200 W power handling capability with excellent stability and heat dissipation ability in a small package. It is suitable for power amplifier, power combining network, antenna feed network, modulator and phase shifter applications.

MIcable Inc.
www.micable.cn

958 SERIES GUI-CONTROLLED WIDEBAND SYNTHESIZERS

The 958 Series offers high performance, GUI-controlled wideband synthesizers with +20 dBm typical output power. Operate remotely via Wi-Fi or Ethernet and choose from five versatile modes: CW, sweep, hop, PWM and external trigger. Features include ultra-fast < 10 µs switching, 0.01 Hz resolution, low phase noise, FSK modulation support and customizable CW filtering. With built-in attenuators (up to 70 dB), wide reference compatibility (10 to 250 MHz) and single-supply 8 to 15 VDC operation, it delivers precision and flexibility for demanding RF applications.

Millimeter Wave Products, Inc.
www.miwv.com

W-BAND DUAL-MODE SOLID-STATE POWER AMPLIFIER

This W-Band dual-mode solid-state power amplifier (QPP) is engineered for high performance radar and communication systems. Offering both variable pulses and CW mode in a compact package, it delivers consistent output power and stable gain across 92 to 96 GHz. With rugged construction and precision-tuned performance, it is ideal for lab development or system integration where space and thermal management are critical.

Quinstar Technology
www.quinstar.com

WIRELESS INSITE® 3D WIRELESS PREDICTION SOFTWARE

VENDORVIEW

Remcom delivers cutting-edge mmWave solutions through its Wireless InSite® 3D wireless prediction software, supporting advanced 3D ray tracing, diffuse scattering and atmospheric absorption modeling to accurately simulate high frequency propagation scenarios in urban, indoor, vehicular and FWA environments. Its hybrid massive MIMO beamforming and adaptive steering tools analyze mmWave path loss and blockage, enabling SINR, throughput and Doppler prediction for dynamic networks. With unique optimizations preserving full 3D fidelity and efficient performance, Remcom equips engineers to design and deploy next-generation 5G/6G mmWave systems.

Remcom
www.remcom.com

ASL-50B SERIES AMPLIFIERS

The ASL-50B series of products consists of gain blocks with +25, +30 and +35 dB. The noise figure levels are +3.5 dB typical and +5.5 dB max. at 50 GHz. The output P-1 dB is +11 dBm typical and +8 dBm min. at 50 GHz. Like all WT products, the ASL-50B series amplifiers are battle-tested and backed with the four-year warranty program. This type of service gives customers the support they need for long-term uses, reducing costly replacements. All WT Products are RoHS compliant and burn-in tested for 48 hours at +50°C.

Wright Technologies
www.wrighttec.com

European Microwave Week 2025

The only European event dedicated to the Microwave and RF industry

The European Microwave Week 2025 takes place in the city of Utrecht. Bringing industry and academia together, the European Microwave Week 2025 is a SIX day event, including THREE cutting edge conferences, THREE Forums and ONE exciting trade and technology Exhibition featuring leading players from across the globe. EuMW 2025 provides access to the very latest products, research and initiatives in the microwave sector. It also offers you the opportunity for face-to-face interaction with those driving the future of microwave technology. EuMW 2025 will see an estimated 1,600 conference delegates, over 4,000 attendees and in excess of 300 international exhibitors (inc. Asia & US).

The Exhibition

Registration to the exhibition is FREE!

- Over 300 International Companies - meet the industry's biggest names and network on a global scale
- Cutting-edge Technology - exhibitors showcase their latest product innovations, offer hands-on demonstrations and provide the opportunity to talk technical with the experts
- Industrial Workshops - get first hand technical advice and guidance from some of the industry's leading innovators

Entry to the exhibition is FREE.
Register at: www.eumw.eu

Be There

Exhibition Dates	Opening Times
Tuesday 23 September 2025	09:30 - 18:00
Wednesday 24 September 2025	09:30 - 17:30
Thursday 25 September 2025	09:30 - 16:30

The Conferences

The EuMW 2025 consists of three conferences, three forums and associated workshops:

- European Microwave Integrated Circuits Conference (EuMIC) 22-23 September 2025
- European Microwave Conference (EuMC) 23-25 September 2025
- European Radar Conference (EuRAD) 24-26 September 2025
- Plus Workshops and Short Courses (From 21 September 2025)
- In addition, EuMW 2025 will include the Defence, Security and Space Forum, the Automotive Forum and the 6G Forum

The three conferences specifically target ground breaking innovation in microwave research. The presentations cover the latest trends in the field, driven by industry roadmaps. The result is three superb conferences created from the very best papers submitted. For the full and up to date conference programme including a detailed description of the conferences, workshops and short courses, please visit www.eumw.eu. There you will also find details of our partner programme and other social events during the week.

TO SEE THE CONFERENCE SESSION MATRIX please visit: www.eumw.eu

How to Register

Registering as a Conference Delegate or Exhibition Visitor couldn't be easier. Register online and print out your badge in seconds onsite at the Fast Track Check In Desk. Online registration is open now, up to and during the event until 26 September 2025.

- Register online at **www.eumw.eu**
- Receive an email receipt with QR code attached
- Bring your email, QR code and photo ID with you to the event
- Go to the Fast Track Check In Desk and print out your badge
- Alternatively, you can register onsite at the self service terminals during the registration.

Please note: NO badges will be mailed out prior to the event.

On-site registration opening times:

- Saturday 20 September 2025 (16:00 - 19:00)
- Sunday 21 - Thursday 25 September 2025 (08:00 - 17:00)
- Friday 26 September 2025 (08:00 - 10.00)

Registration Fees

Full Week ticket:

Get the most out of this year's Microwave Week with a Full Week ticket. Combine all three conferences with access to the Defence, Security and Space Forum and the 6G Forum (the Automotive Forum and the Schools are not included) as well as all the Workshops or Short Courses.

Registration at one conference does not allow access to the sessions of the other conferences.

Reduced rates are offered if you have society membership to any of the following: EuMA✪, GAAS, IET or IEEE. Reduced rates for the conferences are also offered if you are a Student/Senior (Full-time students 30 years or younger and Seniors 65 or older as of 26 September 2025). The fees shown below are invoiced in the name and on behalf of the European Microwave Association. All payments must be in € Euros – cards will be debited in € Euros.

ALL FEES ARE EXEMPT OF DUTCH VAT.

Lunches are included with all conference/forum and workshop registrations:

– Sunday: lunch boxes provided to delegates

– Monday–Friday: delegates receive a seated 3 course lunch

CONFERENCES REGISTRATION	ADVANCE DISCOUNTED RATE (FROM NOW UP TO & INCLUDING 22 August 2025)				STANDARD RATE (FROM 23 August 2025 & ONSITE)			
	Society Member ✪		Non-Member		Society Member ✪		Non-Member	
1 Conference	Standard	Student/Sr.	Standard	Student/Sr.	Standard	Student/Sr.	Standard	Student/Sr.
EuMC	€ 710	€ 200	€ 1,000	€ 280	€ 1,000	€ 280	€ 1,400	€ 400
EuMIC	€ 540	€ 180	€ 760	€ 250	€ 760	€ 250	€ 1,060	€ 350
EuRAD	€ 490	€ 170	€ 680	€ 240	€ 680	€ 240	€ 950	€ 330
2 Conferences	Standard	Student/Sr.	Standard	Student/Sr.	Standard	Student/Sr.	Standard	Student/Sr.
EuMC + EuMIC	€ 1,000	€ 250	€ 1,400	€ 350	€ 1,400	€ 350	€ 1,970	€ 450
EuMC + EuRAD	€ 960	€ 250	€ 1,340	€ 350	€ 1,340	€ 350	€ 1,880	€ 450
EuMIC + EuRAD	€ 820	€ 250	€ 1,150	€ 350	€ 1,150	€ 350	€ 1,610	€ 450
3 Conferences	Standard	Student/Sr.	Standard	Student/Sr.	Standard	Student/Sr.	Standard	Student/Sr.
EuMC + EuMIC + EuRAD	€ 1,220	€ 300	€ 1,710	€ 400	€ 1,710	€ 400	€ 2,390	€ 500
Full Week Ticket	€ 2,070	€ 500	€ 2,680	€ 600	€ 2,680	€ 600	€ 3,510	€ 700

✪ BECOME A MEMBER – **NOW!**

EuMA membership fees: Professional € 25 / year, Student € 15 / year.

One can apply for EuMA membership by ticking the appropriate box during registration for EuMW. Membership is valid for one year, starting when the subscription is completed. The discount for the EuMW fees applies immediately. Members have full e-access to the International Journal of Microwave and Wireless Technologies.

EUMA KNOWLEDGE CENTRE

The EuMA website has its Knowledge Centre which presently contains over 24,000 papers published under the EuMA umbrella. Full texts are available to EuMA members only, who can make as many copies as they wish, at no extra-cost.

SPECIAL FORUMS AND SESSIONS REGISTRATION		ADVANCE DISCOUNTED RATE (UP TO & INCLUDING 22 August 2025)		STANDARD RATE (FROM 23 August 2025 & ONSITE)	
	Date	Delegates*	All Others**	Delegates*	All Others**
Automotive Forum	23 September 2025	€ 365	€ 515	€ 510	€ 720
Defence, Security & Space Forum	24 September 2025	€ 180	€ 250	€ 250	€ 350
6G Forum	22 September 2025	€ 365	€ 515	€ 510	€ 720
Design School	21 September 2025	€ 40	€ 40	€ 55	€ 55
Radar School	22 September 2025	€ 40	€ 40	€ 55	€ 55
EuMW Experience	24 September 2025	€ 60	€ 60	€ 60	€ 60

*those registered for EuMC, EuMIC or EuRAD **those not registered for a conference

Workshops and Short Courses

Despite the organiser's best efforts to ensure the availability of all listed workshops and short courses, the list below may be subject to change. Also workshop numbering is subject to change. Please refer to www.eumw.eu at the time of registration for final workshop availability and numbering.

Sunday 21 September 2025			
SS-01	Full day	EuMIC	Fundamentals of Microwave PA Design
SS-02	Half-day	EuMC	Wearable Antenna Systems for Joint Body-Centric Communication, Powering and Sensing
WS-01	Full day	EuMC/EuMIC	Advancements in Technologies and Circuits Leading to 6G
WS-02	Full day	EUMC	Polymer Microwave Fiber (PMF) Communication for Sub-THz, Low-Cost High Data Rate Short-Range Systems
WS-03	Full day	EuMC	Acoustic Wave Filters for Space Applications
WS-04	Full day	EuMC	Additive Manufacturing for Microwave Components and Systems
WS-05	Full day	EuMC/EuMIC	Opportunities and Challenges for the Cryogenic Microwave Control of Quantum Processors
WS-06	Full day	EuMC/EuMIC	RFIC Design, Packaging and Antenna Solutions for mm-Wave and Sub-THz Communication and Radar
WS-07	Full day	EuMC	Integrated Microwave Photonics
WS-08	Full day	EuMC/EuMIC	Thermal Effects and Heat Management in Active Phased Arrays: Chip, Package and Antenna Level Concepts
WS-09	Full day	EuMC/EuMIC	Innovations in Load-Pull Techniques for Wideband and High-Frequency Applications
WS-10	Full day	EuMC/EuMIC	Advanced mm-Wave IC Design: A Step Ahead
WS-11	Half-day	EuMC/EuMIC	The Path to 2030: Joint Communication and Sensing in the 6G Internet-of-Everything Era
WS-12	Half-day	EuMC/EuMIC	AI and Data-Driven Modeling for RF/MW Design
WS-13	Half-day	EuMC	Microwave Carbon Footprint of Wireless Commuincations - From Energy Efficiency to Embedded Emissions

Monday 22 September 2025			
SM-01	Half-day	EuMC	Architecture and Applications for Emerging SATCOM and NTN Communication Networks
SM-02	Half-day	EuMC	Radiative Wireless Power Transfer Basics and Implementation
WM-01	Full day	EuMC	Photonic Technologies and Systems for RF Applications
WM-02	Full day	EuMC	Latest Advancements in Microwave Measurement Techniques for Future Communications and Quantum Applications
WM-03	Half-day	EuMC/EuRAD	Standard, Prototype, and Measurement for Integrated Sensing and Communications in the COST Action INTERACT

Wednesday 24 September 2025			
SW-01	Full day	EuMC/EuMIC	Embedding Sustainability into RF Technologies
WW-01	Half-day	EuMC	Innovative Semiconductor Device Architectures and Accurate Modeling for Emerging Applications - Bridging the Gap Between Circuit Design Challenges and Practical Commercialization
WW-02	Half-day	EuMC/EuRAD	High Resolution Radar Technologies for Future Automotive Systems
WW-03	Half-day	EuMC/EuMIC	RF & Sub-THz Heterogeneous Integration
WW-04	Half-day	EuMC	Recent Progress in Compact, Ultra-Low Phase Noise Microwave-Photonic Frequency Synthesis

Thursday 25 September 2025			
STh-01	Full day	EuMC/EuRAD	Basics of Systems Engineering for the Microwave Engineering Community
STh-02	Half-day	EuRAD	Synchronization in Distributed Radar – Prospective and Problems
WTh-01	Full day	EuRAD	Automotive Radar Research Trends
WTh-02	Half-day	EuRAD	Multistatic/Distributed Radar Systems

Friday 26 September 2025			
SF-01	Half-day	EuRAD	Integrated Sensing and Communications: Fundamentals, State-of-the-Art and the Road Ahead
SF-02	Half-day	EuRAD	Nonlinear Radar: From Concepts to Applications

WORKSHOPS AND SHORT COURSES	IN COMBINATION WITH CONFERENCE REGISTRATION				WITHOUT CONFERENCE REGISTRATION			
	Society Member		Non-Member		Society Member		Non-Member	
	Standard	Student/Sr.	Standard	Student/Sr.	Standard	Student/Sr.	Standard	Student/Sr.
Half Day	€ 120	€ 90	€ 170	€ 120	€ 170	€ 120	€ 220	€ 170
Full Day	€ 180	€ 130	€ 240	€ 180	€ 240	€ 180	€ 320	€ 240

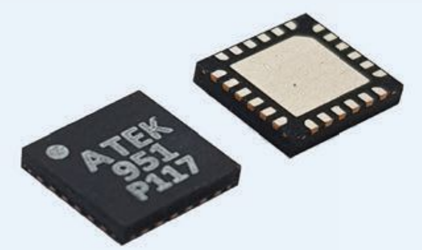

10 MHz to 8 GHz LNA with Bypass MMIC

ATEK Midas, a designer and supplier of high performance mixed-signal silicon ASICs and RFICs and advanced GaAs and GaN MMICs, introduces ATEK951P4. ATEK951P4 is a 10 MHz to 8 GHz wideband LNA with bypass MMIC in a 4 x 4 mm QFN SMT plastic package.

The ATEK951P4 wideband LNA integrates a bypass option that provides a flat 18 dB gain and a noise figure of 2 to 3 dB. This LNA offers P1dB drive at +17 dBm while maintaining +30 dBm output IP3 and requiring only 82 mA from its +5 V single supply. The bypass state is enabled with a single positive control input, eliminating the need for negative voltage rails. The ATEK951P4 offers an outstanding combination of functionality, noise figure, drive and linearity for a wide range of SDR, UWB, IoT, test instrument, satcom, counter-UAS and EW/ECM receiver applications. RF inputs and outputs are matched to 50 Ω. ATEK951P4 LNA products and evaluation boards are available from stock.

ATEK Midas applies expertise, creativity and passion to design analog and mixed-signal silicon ASICs and RFICs, along with GaAs and GaN MMICs and modules for aerospace, automotive, 5G/6G telecom, data center, defense, industrial/IoT, medical, scientific and test and measurement markets. ATEK Midas partners with customers to provide focused, custom IC design and development services that deliver IP blocks to engineering prototypes and turn-key production solutions. These solutions are complemented by ATEK Midas' line of MMIC standard products for communication and sensor applications, extending up to 100 GHz.

ATEK's North American sales and applications partner, ViNo Waves LLC, works closely with ATEK technical representatives to provide sales, marketing and technical support. ViNo Waves can be reached at sales@vinowaves.com.

ATEK Midas
Istanbul, Türkiye
info@atekmidas.com
For further information contact Norm Hildreth
+1 781-789-8454
normh@vinowaves.com

Analog Devices Introduces: Apollo MxFE

Check out ADI's most advanced software-defined, direct RF-sampling, wideband mixed signal front-end platform.

Analog Devices Inc.

https://players.brightcove.net/706011717001/VwMdg0a0kC_default/index.html?videoId=6328949464112

Introducing FSWX - World's First Multi-Channel Signal & Spectrum Analyzer with Cross-Correlation

Measure signals that were once out of reach with the FSWX Rohde & Schwarz's new, groundbreaking signal and spectrum analyzer that is set to revolutionize the field of signal and spectrum analysis.

Rohde & Schwarz

https://www.youtube.com/watch?v=kUVj9682OcY

Pixus Technologies Celebrates Its 15th Anniversary

Pixus Technologies has announced its 15th year anniversary as a provider of embedded computing and enclosure solutions. The company has been supporting the military, aerospace, industrial, HPEC, physics/research and telecom communities since its inception in 2010.

Pixus Technologies

https://pixustechnologies.com/

SP145 + Spike: Master RF Mapping in Minutes!

Master RF mapping in minutes with the SP145 and Spike software. This dynamic combination offers comprehensive signal analysis, enabling precise spectrum analysis and signal visualization for RF engineering professionals and enthusiasts alike.

Signal Hound

https://www.youtube.com/watch?v=qUcp8qF901c

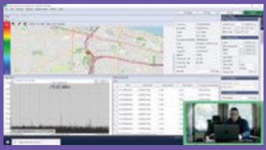

Unboxing SV Microwave's VITA 67.3 Developer Kit

SV Microwave introduces a rugged, all-in-one solution for prototyping and testing VITA 67 designs.

SV Microwave

https://www.youtube.com/watch?v=lVewhn8Mzbo

Werlatone Celebrates 60 Years

Werlatone is celebrating its 60th year. Started as a "garage-shop" operation, Werlatone has evolved its engineering and manufacturing strategies to become a leading supplier of high-power, passive wideband RF/microwave solutions for major aerospace and defense contractors for communications, EW and radar systems.

Werlatone

https://werlatone.com

NEW PRODUCTS

FOR MORE NEW PRODUCTS, VISIT WWW.MWJOURNAL.COM/BUYERSGUIDE
FEATURING VENDORVIEW STOREFRONTS

AEM RENAISSANCE

SEE US @ EUMW

Ka-Band Coaxial Isolator

2A9BDP is a Ka-Band coaxial isolator that covers three separate sub-bands between 27.5 to 31 GHz. It offers a unique interface of a 2.9 mm female connector for input and a feedthrough pin for the output. With its low insertion loss, high isolation, compact size and stability over a wide temperature range, it is an ideal choice for military environmental conditions.

www.rec-usa.com

ALTUM RF

SEE US @ EUMW

E-Band Solutions

Altum RF's new E-Band PA GaAs MMICs support today's demanding mmWave telecom and satcom applications by offering high output power and gain for longer-range links. The ARF1018, 71 to 76 GHz with 1.8 W Psat (including bonding transitions from die) and 27 dB small-signal gain. The ARF1019, 81 to 86 GHz with 1.6 W Psat (including bonding transitions from die) and 24 dB small-signal gain. The die size for both MMICs is 3.5 x 4.1 x 0.05 mm^3 and include an on-chip integrated power detector.

www.altumrf.com

AMPHENOL RF

Cable Assemblies

Amphenol RF introduced the SMPM to SMPM assembly on RG-178 cable into their portfolio of cable assemblies. The compact size of these assemblies makes them highly suited for use in applications where space is at a premium. With a 50 Ω impedance and the ability to operate from DC to 6 GHz, the SMPM to SMPM cable assembly on RG-178 is equipped to provide reliable RF performance in the most demanding applications.

www.amphenolrf.com

COPPER MOUNTAIN TECHNOLOGIES

SEE US @ EUMW

V0902 2-Port 9 GHz VNA

VENDORVIEW

CMT's V0902 delivers highly accurate measurements up to 9 GHz with the ideal feature set for many production and field service applications in a cost-effective package. V0902 has a 100 kHz starting frequency, 300 kHz maximum IF bandwidth, 135 dB typical dynamic range and 25 µs per point measurement speed.

www.coppermountaintech.com

ERAVANT

SEE US @ EUMW

COTS-Powered Custom Solutions

VENDORVIEW

From 1 to 330 GHz and beyond, Eravant's custom design capability is supported by a vast design library based on decades of industry-leading innovation and manufacturing expertise. Offering a wide array of proven designs that include signal sources, power amplifiers, control components and antennas, Eravant can work with your team to quickly transform system requirements into working prototypes ready for volume production. Contact us today to gain traction and accelerate your projects with Eravant COTS.

www.eravant.com

JFW INDUSTRIES, INC.

SEE US @ EUMW

8-channel USB Programmable Attenuator

VENDORVIEW

JFW Industries, Inc model 50P-2140 SMA is an 8-channel USB programmable attenuator. It operates from 200 to 6000 MHz with attenuation range 0 to 95 dB in 1 dB steps. All eight attenuators are individually controlled. Test software is provided with the USB attenuator. If you would like to integrate the USB attenuator into your script testing, a JFW Python library is offered upon request.

www.jfwindustries.com

26.5-40GHz 500W

Solid State Power Amplifier

Features

- Ultra Wide Band: 26.5-40GHz
- Gain: 57dB Min •
- Output Power: 57.5dBm Min
- High-efficiency GaN technology
- Low power consumption
- Low spurious signal
- Forward/reverse power monitoring
- Over voltage, over temperature, over current protection
- Optional overdrive protection

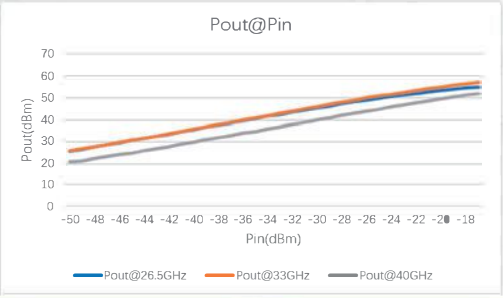

DC solid state power amplifier Modules

Fast Delivery!

- 26.5-40GHz Output Psat：47dBm
- Model：TLPA26.5G40G-47-47

- 6-18GHz Output Psat：48dBm
- Model：TLPA6G18G-47-48

AC Type Benchtop Power Amplifier up to 50KW

Three Years Warranty

- 0.5-6GHz 500W CW Solid State Power Amplifier
- C band 10KW CW Solid State Power Amplifier
- 1-4GHz 20KW Pulse Solid State Power Amplifier
- 4-8GHz 2000W CW Solid State Power Amplifier
- 6-18GHz 1000W CW Solid State Power Amplifier
- 2-18GHz 100W CW Solid State Power Amplifier
- 8-18GHz 2500W Pulse Solid State Power Amplifier
- 26-40GHz 500W CW Solid State Power Amplifier
- 40-60GHz 100W CW Solid State Power Amplifier
- 75-110GHz 10W CW Solid State Power Amplifier

MICABLE INC.

Wideband Solid-State Switch Matrices

VENDORVIEW

The newly launched solid-state switch matrices operate across a broad frequency range of 0.5 to 8 GHz, offering low insertion loss, high isolation, fast switching and high reliability. Engineered for precision, the matrices provide excellent consistency in both amplitude and phase across all output ports through meticulous design and thorough optimization. Available in configurations from 1×16 up to 1×64, the largest 1×64 matrix delivers insertion loss ≤ 5 dB and isolation ≥ 70 dB. The product includes control software and supports multiple interface options — USB, Ethernet and TTL — enabling smooth integration into systems for 5G RRU, Wi-Fi 6E, antenna arrays and phased array applications.

www.micable.cn

MICABLE INC.

8-Way Ultra-Wideband Power Divider/Combiner

VENDORVIEW

MIcable's 18 to 67 GHz 8-way ultra-wideband power divider/combiner can accept an 18 to 67 GHz signal and deliver eight output signals with equal amplitude and phase. Due to extremely wide bandwidth, excellent VSWR, insertion loss and isolation, it can be widely applied in 5G, high speed data communication, testing, instruments and other related fields.

www.micable.cn

MPG

Full Comms Whilst Jamming

MPG's ECM Deconfliction System enables reliable VHF/UHF communication whilst simultaneously operating on-platform broadband jammers. Designed for integration with armored vehicles, infrastructure or manpack deployments, the system incorporates two bolt-on modules that interface with the ECM and radio, allowing continuous jamming across 225 to 400 MHz, but with no impact to frequency hopping radio operation. The system enhances mission resilience and avoids the frequently encountered compromise between electronic force protection and availability of communications.

www.mpgdover.com

PICO TECHNOLOGY

High Bandwidth Sampling Oscilloscopes

Pico Technology announced the extension of its PicoScope 9400A Series of high bandwidth sampling oscilloscopes. The products are engineered to meet the demanding needs of high speed electronics, communications, semiconductor research and high-energy physics applications. The PicoScope 9400A Series is built on Pico's SXRTO technology and, with this launch, adds three models to the previously announced 25 GHz version, giving users a choice of 6 GHz, 16 GHz, 25 GHz and a flagship 33 GHz bandwidth model.

www.picotech.com

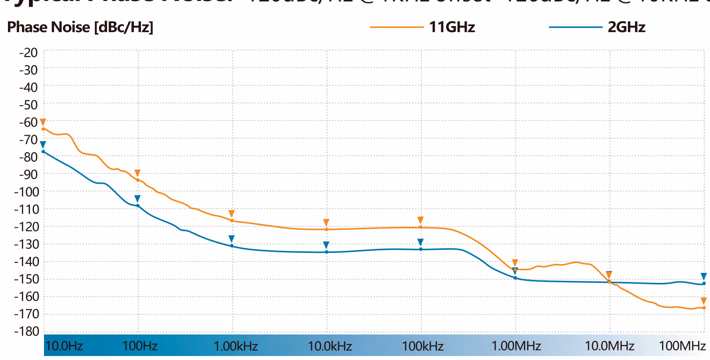

NewProducts

QORVO
Connecting the World Through Space

SEE US @ EUMW

VENDORVIEW

Qorvo's QPA1722 is the latest addition to their growing K-Band space portfolio, delivering 3x instantaneous bandwidth in a 38 percent smaller footprint to meet the demands of modern LEO satellite payloads. Housed in a compact SMT package, this high-efficiency GaN PA enables greater data throughput and flexible system integration. With over 40 years of space expertise and a portfolio spanning Ku, K- and Ka-Band solutions, Qorvo delivers the performance and reliability that enable the next generation of satcom systems.

www.qorvo.com

QUANTIC PMI
Solid-State Digital and Analog Controlled Attenuators

SEE US @ EUMW

VENDORVIEW

Quantic PMI's solid-state digital and analog controlled attenuators are designed for commercial, industrial and military applications including transmission loss simulation, signal fading/handover system evaluation and telecom network infrastructure. Choice of attenuation ranges with resolution as low as 0.005 dB and frequency ranges to 70 GHz. Either voltage variable or digitally variable programmable versions are available. Quantic PMI's attenuators offer the industry's best attenuation flatness versus frequency. Form, fit, function and custom designs are their specialty. COTS availability.

www.quanticpmi.com

REACTEL
Filters, Multiplexers & Multifunction Assemblies

SEE US @ EUMW

VENDORVIEW

Reactel will feature its full line of filters, multiplexers and multifunction assemblies covering up to 67 GHz at EuMW 2025 in Utrecht. Supporting military, commercial, industrial and research needs, Reactel can design the right unit for you. From small, lightweight units suitable for flight or portable systems to high power units capable of handling up to 25 kW, connectorized or surface-mount, large or small quantities, Reactel's engineers can design a unit specifically for your application. Visit them in stand B131 to discuss your requirements.

www.reactel.com

RFMW
Low Loss, High-Rejection 2–18 GHz Filter Bank

SEE US @ EUMW

VENDORVIEW

The ED2 FB010BW16SG is an 8-way bandpass filter bank covering 2 to 18 GHz with 2 GHz-wide bands. Optimized for low SWaP systems, it offers a typical insertion loss of 4 dB, > 12 dB return loss and 20 ns switching speed in a compact 9 × 9 mm SMT package. With internal 50 Ω matching and +30 dBm CW input handling, it's ideal for EW, SIGINT and broadband communications systems operating across harsh temperature ranges.

www.rfmw.com

NewProducts

RFMW

SEE US @ EUMW

110 GHz Performance in a Compact, Rugged Connector Solution

VENDORVIEW

Now available at RFMW, Smiths Interconnect's high frequency mini-lock connector delivers outstanding 110 GHz performance in a compact, lightweight, PFAS-free design. Engineered for space, EW and defense systems, it combines excellent electrical performance, low insertion force and a robust locking mechanism for secure, reliable signal transmission in harsh environments. Qualified to MIL-STD shock and vibration standards.

www.rfmw.com

SMITHS INTERCONNECT

SEE US @ EUMW

K2TVA Thermopad® Temperature Variable Attenuator Series

Temperature effects can wreak havoc on system performance. Smiths Interconnect's Thermopad® temperature variable attenuators utilize patented-technology in a passive solution which is smaller, less complex and less costly than active compensation alternatives. High reliability versions are available for mission critical applications. For over 50 years, Smiths Interconnect's solutions have been trusted by the industry's smartest engineers.

www.smithsinterconnect.com

SOUTHWEST MICROWAVE

SEE US @ EUMW

0.8 mm Connector

Visit Southwest Microwave at EUMW, stand E096, to discover their groundbreaking 0.8 mm (145 GHz) high performance thread-in connector. This cutting-edge design ensures exceptional signal integrity while delivering low VSWR, RF leakage and insertion loss. The company will also present their 0.8 mm vertical launch connector for microstrip and CPW, currently in the prototyping phase. Southwest Microwave remains committed to surpassing previous milestones, cementing their reputation as a performance leader in microwave connectors.

www.southwestmicrowave.com

SPECTRUM CONTROL

SEE US @ EUMW

Miniaturized, Integrated RF+Digital Solutions

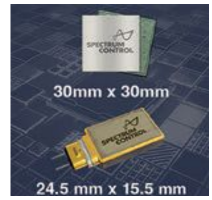

Spectrum Control is accelerating RF+digital integration and miniaturization with their SiP platform that simplifies development and significantly reduces size. See live demos at EUMW featuring software-instrumented mmWave block converters that extend 2 to 18 GHz systems to 40 GHz and board-mount micro-optical transceivers that convert digital output to high speed optical signals for extreme environments. Also on display, ultra-miniature high Q filters for compact RF front-ends. Now available are multiplexers and filter banks for smart antenna modules. Stop by stand C106.

www.spectrumcontrol.com

TAOGLAS

SEE US @ EUMW

Patriot Series

Taoglas has released the Patriot series, a compact, multi-function combination roof mount antenna designed for connected vehicle fleets across emergency services, utilities and commercial sectors. Integrating up to 18 antenna elements into a single low-profile enclosure, the Patriot delivers robust multi-network connectivity while reducing vehicle roof clutter and simplifying installation. Originally developed for the Ford Interceptor, the existing vehicle OEM antenna can simply be replaced with the Patriot, while keeping the original antenna functionality, but also adding multi-radio connectivity.

www.taoglas.com

TELEDYNE LABTECH

Thermal Management in GaN PCBs

Teledyne Labtech, a top supplier of PCBs with integrated thermal management, has developed an innovative technique of embedding copper coins to enhance the thermal path for high power GaN devices. By directly mounting the device to the ground plane, the temperature of the GaN device junction will decrease, improving efficiency and increasing MTBF.

www.teledynelabtech.com

MICRO-ADS

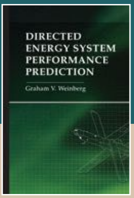

Bookend

Review by Reena Dahle

Directed Energy System Performance Prediction
Graham V. Weinberg

"Directed Energy System Performance Prediction" provides a thorough, high-level overview of directed energy systems. In the first few chapters, the author explains the necessary background to understand the fundamentals of performance modeling for high-power RF (HPRF) and high-energy laser (HEL) systems. Each chapter provides a summary and current references for further details, allowing readers to research specific topics in more depth. The explanations of the mathematical models used to predict and analyze the performance of the two types of directed energy weapons (DEW) systems are clear and helpful.

The author explores different threat modeling scenarios, ranging from a single threat to a multitude of threats, to examine the DEW system performance prediction using the power density functions derived. Multiple threats were explored for narrowband HPRF systems based on their arrival time, including simultaneous arrival, arrival through a renewal process and linear arrival. The author shares simulation plots that predict the success of the HPRF DEW in eliminating threats for different case scenarios of the multiple threats' arrival time and lifetime as a function of time. For the simulation, the threats were assumed to arrive in a linear trajectory toward the HPRF DEW but were delayed in time. The book also touches on the differences between HPRF and HEL systems. This book could benefit from a more in-depth description of the electronic vulnerability levels on electronic systems for HPRF DEWs.

Finally, the book takes it a step further by providing readers with future research directions in Chapter 7, allowing them to understand the gaps in this field and identify areas of research interest. This book is a valuable resource for a wide range of industry professionals, including defense contractors and government security groups. Additionally, the book's thorough compilation of mathematical modeling frameworks makes it useful for research in universities and labs.

Copyright: 2023
Pages: 230
ISBN: 9781685690274
To order this book, contact:
Artech House
us.artechhouse.com

Advertising**Index**

ADVERTISERS ARE HIGHLIGHTED IN BLUE

Sales Representatives

Microwave Journal

Eastern and Central Time Zones
Carl Sheffres
Group Director
(New England, New York, Eastern Canada)
Tel: (781) 619-1949
csheffres@mwjournal.com

Michael Hallman
Associate Publisher
(NJ, Mid-Atlantic, Southeast, Midwest, TX)
Tel: (301) 371-8830
Cell: (781) 363-0338
mhallman@mwjournal.com

Pacific and Mountain Time Zones
Brian Landy
Western Reg. Sales Mgr.
(CA, AZ, OR, WA, ID, NV, UT, NM, CO, WY, MT, ND, SD, NE & Western Canada)
Tel: (831) 426-4143
Cell: (831) 713-9085
blandy@mwjournal.com

International Sales
Michael O'Kane
Tel: +44 (0) 1875 825 700
Cell: +44 (0) 7961 038 245
mokane@horizonhouse.com

Germany, Austria, and Switzerland (German-speaking)
Victoria and Norbert Hufmann
victoria@hufmann.info
norbert@hufmann.info

France
Gaston Traboulsi
Tel: +44 207 596 8742
gtraboulsi@horizonhouse.com

Korea
Jaeho Chinn
JES MEDIA, INC.
Tel: +82 2 481-3411
corres1@jesmedia.com

China
Shanghai
Linda Li
ACT International
Tel: +86 136 7154 0807
lindal@actintl.com.hk

Wuhan
Phoebe Yin
ACT International
Tel: +86 134 7707 0600
phoebey@actintl.com.hk

Shenzhen
Annie Liu
ACT International
Tel: +135 9024 6961
anniel@actintl.com.hk

Beijing
Cecily Bian
ACT International
Tel: +86 135 5262 1310
cecilyb@actintl.com.hk

Hong Kong
Floyd Chun
ACT International
Tel: +852 28386298
floydc@actintl.com.hk

Taiwan, Singapore
Simon Lee
ACT International
Tel: +852 2838 6298
simonlee@actintl.com.hk

Japan
Katsuhiro Ishii
Ace Media Service Inc.
Tel: +81 3 5691 3335
amskatsu@dream.com

Submitting ad material?
Visit: www.adshuttle.com/mwj
(866) 774-5784
outside the U.S. call
+1-414-566-6940

Ed Kiessling
(781) 619-1963
ekiessling@mwjournal.com

Corporate Headquarters: 685 Canton Street, Norwood, MA 02062 • Tel: (781) 769-9750

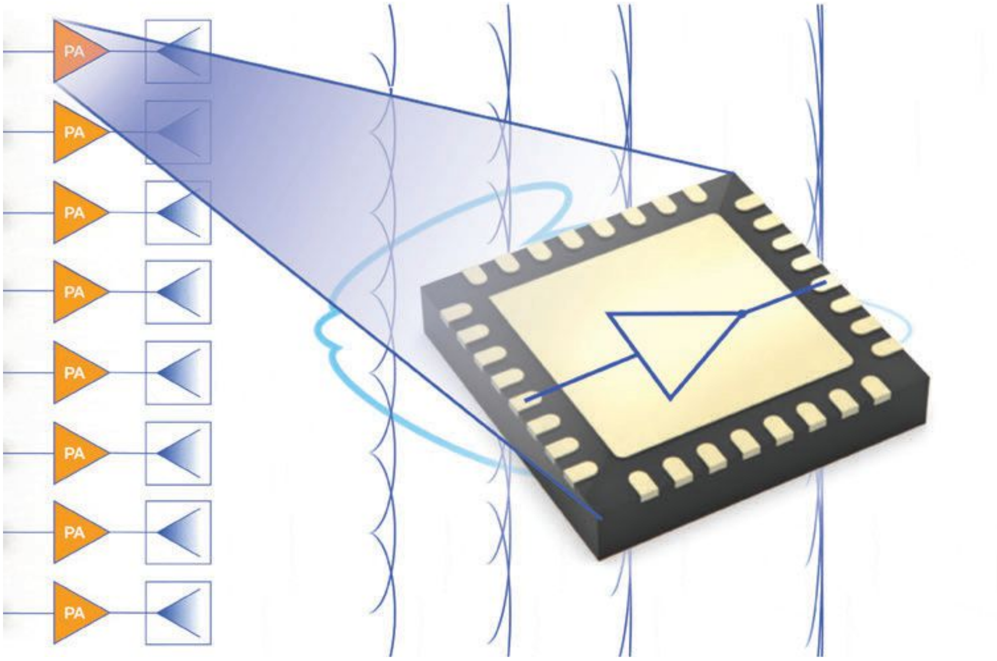
PA
PA
PA
PA
PA
PA
PA
PA

FABS and LABS

NXP Semiconductor: Bringing Bright Minds Together





NXP was founded in 2006, leveraging decades of experience in semiconductors under the Philips name. In the nearly 20 years since they spun off, NXP has become a prominent name and innovator in healthcare, wearables, automotive, avionics and autonomous home technologies. NXP has grown and expanded into these industries through partnerships, mergers and acquisitions. One key merger took place in 2015 when NXP and Freescale merged and became the world's fourth-largest semiconductor company and largest automotive supplier. Four years later, NXP acquired Marvell's Wi-Fi connectivity business unit. In addition to these mergers and acquisitions, NXP has opened a variety of labs around the world, including the AIoT Applications Innovation Center in Tianjin, China, focused on driving innovation across smart city, smart mobility and smart home applications. In 2020, NXP opened a GaN fab in Arizona and in 2024, NXP opened its new Smart Home Innovation Lab in Austin, Texas. Today, NXP is present in over 30 countries and employs more than 33,000 people.

The Smart Home Innovation Lab demonstrates NXP's dedication to autonomous home technology design and testing. It is built to resemble a modern, active household, complete with a bedroom, kitchen, media room, home gym and garage. This design enables NXP to more efficiently pursue collaboration with industry and accurate, timely testing. The lab is over 5,200 square feet and employs nearly 30 system engineers. In addition to the dedicated rooms, the lab has fully equipped engineering benches and a showcase of finished projects to spark creative ideation.

In addition to enhancing comfort and style, the Smart Home Innovation Lab prompts engineers to enhance safety, security and ease of use. For example, it provides a space to test voice control in noisy areas and energy efficiency during standard household use. Two key features of NXP's smart home product family are ultra-wideband (UWB)-enabled chipset "anchors" designed to track for precise location, and edge-based intelligence, including data processing, privacy and security. The NXP UWB sensors enable precise tracking of a device throughout a home. As the device, such as a phone or smart watch, moves throughout the home, it is tracked by the UWB sensor/anchor to prompt changes such as turning lights on or off and thermostats up or down. NXP can enable preset features, such as closing a valve when a sensor detects a water leak; however, presets are not mandatory. As users move throughout the house, the system detects patterns for each individual and applies them to automatically meet their needs. These options enable a safe and comfortable home with true customization.

Some common concerns with autonomous homes are bandwidth, data privacy and connectivity challenges, such as internet outages. NXP's localized devices eliminate those concerns by removing the dependency on the cloud connection. Information is no longer reliant on cloud access; the information is directly processed and managed on the edge. In addition to maintaining operability through internet outages, the disconnection from the cloud increases safety by making autonomous homes less susceptible to security breaches and protects the users' data.

The Smart Home Innovation Lab is a new, exciting addition to the NXP portfolio; however, it is only a sliver of their capabilities and industries. NXP continues to be a trusted partner for innovative solutions – including microcontrollers, processors, sensors and connectivity solutions – in the automotive, industrial & IoT, mobile and communications infrastructure markets. NXP's core belief that we are brighter together is omnipresent in their innovative team, advanced facilities and close partnerships.

www.nxp.com

eXclusive Digital Content >>>

REVIEW BOARD MWJ APPROVED

Low-Profile Quad-Band AMC-Backed Antenna for Gain Enhancement

Z. Mordi, University Blida-1, Institute of Aeronautics and Spatial Studies, Aeronautical Science Laboratory, Blida, Algeria

Z. Hamouda, High School of Aeronautical Techniques, Algiers, Algeria

P. Laly, University of Lille, IEMN Lille, France

M. Lagha, University Blida-1, Institute of Aeronautics and Spatial Studies, Aeronautical Science Laboratory, Blida, Algeria

T. Lasri, University of Lille, IEMN Lille, France

A low-profile quad-band coplanar waveguide (CPW)-fed antenna backed by an artificial magnetic conductor (AMC) is suitable for various applications, including WLAN, Bluetooth, WiMAX and satellite communications. The initial design is a rectangular slotted quad-band antenna, which features a low gain across all frequency bands of interest. To enhance performance, a circular AMC ring with four zero-phases of the reflection coefficient is added as a reflector. AMC incorporation results in a gain improvement of 4, 5.3, 5.1 and 4.7 dBi in the four bands of interest centered at 2.5, 3.5, 5.4 and 7.7 GHz, respectively. Measurements agree closely with simulation.

Planar antennas are widely used in modern electronic applications, where compactness, cost-effectiveness and high performance are critical considerations. These antennas play a key role in various fields, including wireless communication,[1] medical devices[2] and telecommunications.[3]

Among planar antennas, multi-band designs are particularly advantageous due to their ability to operate across multiple frequency bands, supporting diverse functionalities. Compared to wideband antennas, which require more complex structures to maintain consistent performance across a broad frequency range, multi-band antennas are often simpler in design. This simplicity facilitates the manufacturing process and can potentially reduce costs. Moreover, they are designed to operate within specific frequency bands, minimizing the risk of outside interference.

While planar antennas are recognized for versatility and affordability, they are limited by narrow bandwidth, moderate gain and surface wave issues. Utilizing metamaterials presents a promising approach to addressing these limitations and enhancing performance.

Metamaterials are engineered materials that exhibit properties not found in nature.[4] Their unique characteristics arise from their structures rather than their compositions,[5] allowing them to control electromagnetic waves in unique and advanced ways.[6] Frequency selective surfaces (FSS),[7-9] electro-

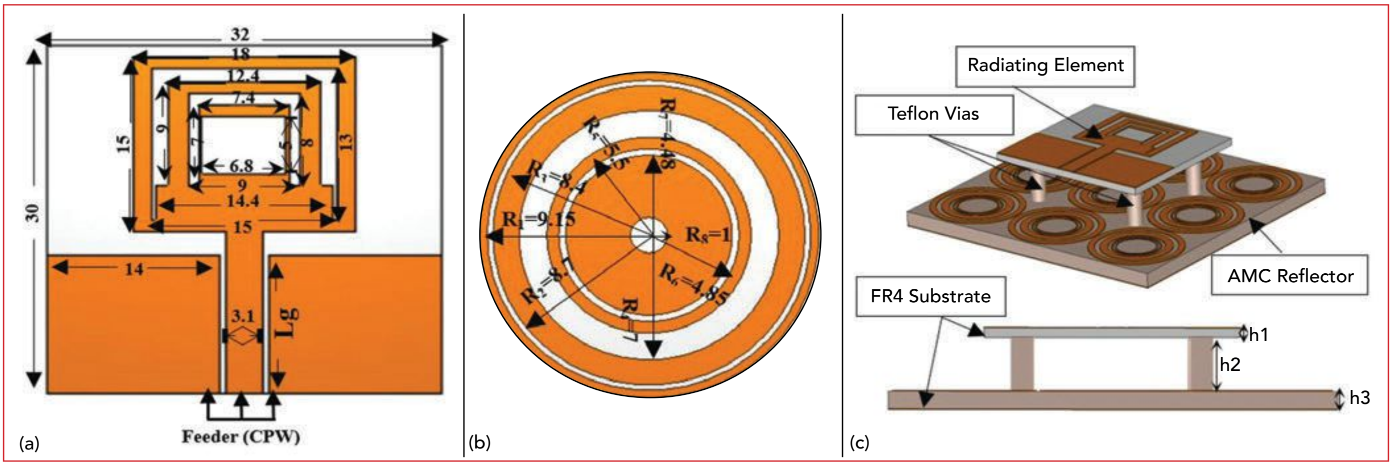

Fig. 1 AMC-backed antenna: (a) antenna top view, (b) AMC unit cell and (c) integrated structure. Dimensions are in mm.

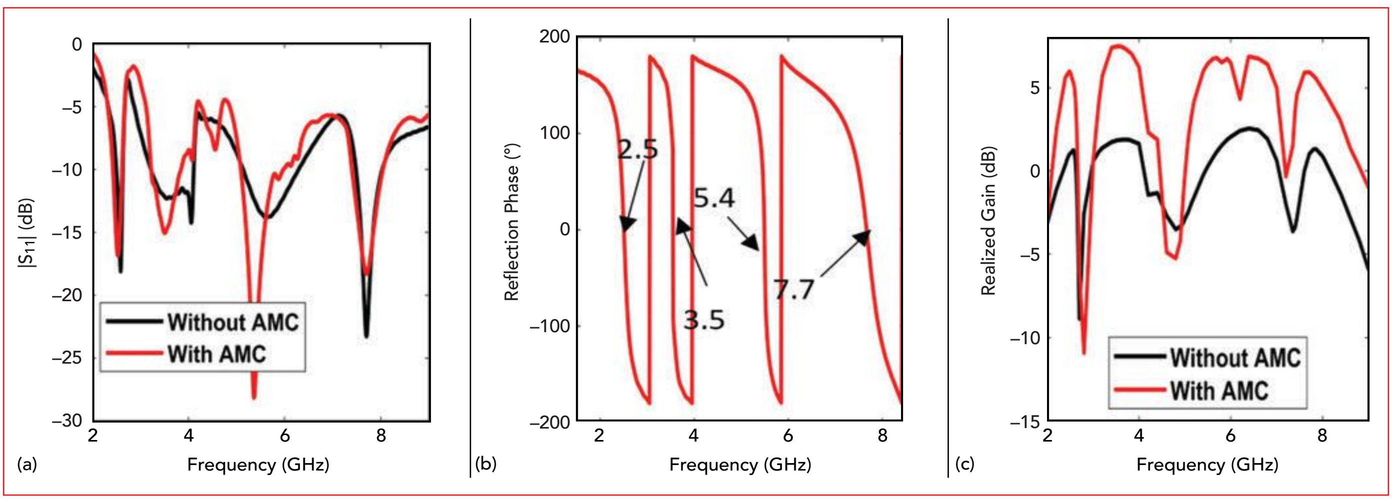

Fig. 2 Simulation: (a) reflection coefficient magnitude (b) reflection coefficient phase and (c) realized gain.

magnetic band gap (EBG) structures[10,11] and AMCs[12,13] are examples of metamaterials that have demonstrated the ability to enhance antenna performance in terms of directivity, gain, impedance, bandwidth and efficiency.

Achieving high gain is a crucial factor in many situations where long-range communications, signal quality and efficiency are priorities. Particularly, wireless applications such as antennas for mobile satellite communication systems[14] and Wi-Fi networks (IEEE Std 802.11-2020) demand high gain to meet performance requirements.

To meet this demand, the quad-band, low-profile, CPW-fed, slotted rectangular AMC-backed antenna described in this work operates across frequency bands centered at 2.5, 3.5, 5.4 and 7.7 GHz, making it suitable for WLAN, Bluetooth, WiMAX and satellite communications.

DESIGN AND ANALYSIS

Figure 1 shows the AMC-backed antenna structure. The radiating element (see Figure 1a) is rectangular and features slots designed to achieve quad-band performance. The antenna is mounted on a 32 × 30 mm (0.26 × 0.25 λ_0) FR4 substrate, where λ_0 represents the free-space wavelength corresponding to the lowest operating frequency. The substrate has a thickness (h_1) of 1.6 mm, a relative permittivity (ε_r) of 4.5 and a loss tangent of 0.002. The antenna is fed via a coplanar waveguide (CPW), as shown in Figure 1a.

The AMC unit cell, as seen in Figure 1b, is characterized by four circular rings and serves as a fundamental component of the design. A 3 × 3 AMC array of these unit cells serves as a reflector, positioned beneath the antenna to improve its gain. AMCs are known as high impedance surfaces (HIS)[15] that can mimic perfect magnetic conductors (PMCs) within a certain frequency range.[16] Figure 1c shows the AMC array integrated with the antenna.

Simulated performance is shown in ***Figure 2***. Antenna $|S_{11}|$ with and without the AMC array (see Figure 2a) indicates quad-band behavior. The reflection phase simulation (see Figure 2b) exhibits four zero-phase transitions of the reflection coefficient. Realized gain (see Figure 2c) is simulated at boresight. All simulations are performed using CST Studio Suite software. The antenna gain simulation highlights the gain enhancement achieved by integrating the AMC array. Specifically, gain is improved by 4.8, 5.6, 6.1 and 5 dBi at 2.5, 3.5, 5.4 and 7.7 GHz, respectively.

PARAMETRIC STUDIES

Figure 3 summarizes parametric studies used to optimize the antenna structure. The parameter Lg (see Figure 1a) is critical to the antenna's

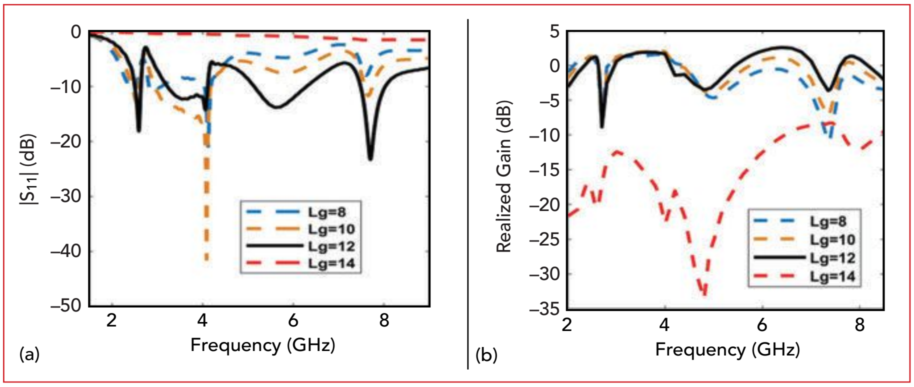

Fig. 3 Parametric study of the antenna parameter Lg: (a) $|S_{11}|$ and (b) realized gain. Dimensions are in mm.

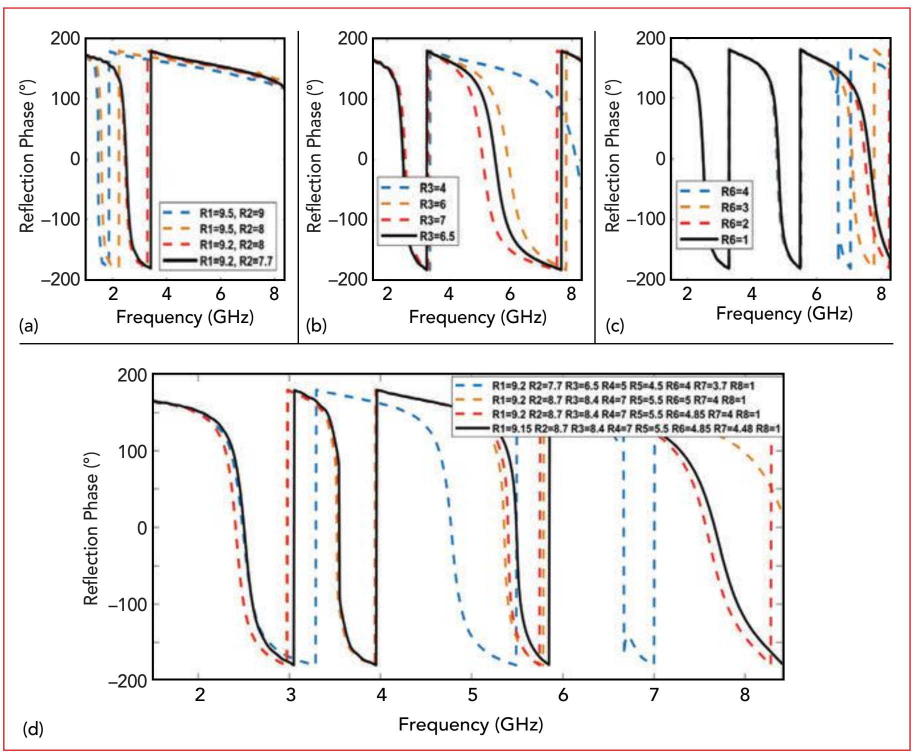

Fig. 4 Parametric study of AMC reflection phase for unit cells with different radius values: (a) R_1, (b) R_3, (c) R_6 and (d) R_1 through R_8. Dimensions are in mm.

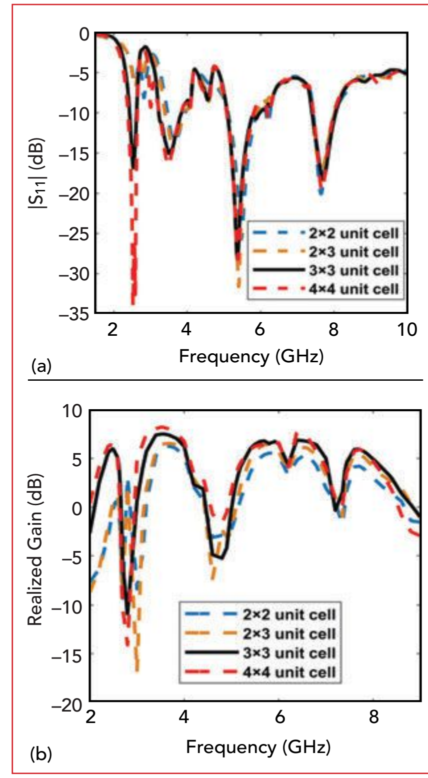

Fig. 5 Parametric studies of AMC array size: (a) $|S_{11}|$ and (b) realized gain.

performance. Figure 3a and Figure 3b show the effects of Lg on reflection coefficient and realized gain, respectively. As Lg increases but remains below 14 mm, a good impedance match is achieved, particularly in the third band. A similar trend is noted for gain. After optimization, Lg = 12 mm is chosen to achieve the desired performance.

The AMC unit cell is optimized as well (see ***Figure 4***). Initially, a simple circular ring patch is designed, exhibiting a zero-reflection phase at 2.5 GHz. To achieve quad-band behavior, additional rings are incrementally incorporated, each achieving the desired zero-reflection phase at a specific frequency.

Additional parametric studies are conducted after integrating the AMC reflector behind the antenna. The AMC array size significantly affects both the antenna reflection coefficient and realized gain, as demonstrated in ***Figure 5a*** and ***Figure 5b***. The first two configurations fail to achieve an acceptable $|S_{11}|$ in the first frequency band. Optimal impedance matching is achieved with the 3 × 3 and 4 × 4 AMC unit cell configurations. Similarly, realized gain for the first two configurations (2 × 2 and 2 × 3) is lower than that of the 3 × 3 and 4 × 4 configurations, which are nearly identical. Based on matching, gain and overall dimensions, 3 × 3 is chosen as the optimal array size.

The separation distance (h_2) between the antenna and the AMC structure, as seen in ***Figure 6***, also affects the performance of the AMC-backed antenna. Increasing h_2 decreases$|S_{11}|$, particularly in the second frequency band. However, this improvement does not extend to gain (see Figure 6b), especially in the highest frequency band, where increasing h_2 leads to a decrease in gain. After analyzing the results, an air gap of h_2 = 9 mm is selected to maintain a low-profile structure while optimizing performance. Notably, 9 mm corresponds to 0.075 λ_0, which is significantly smaller than the typical 0.25 λ_0 (30 mm) for a perfect electric conductor (PEC) reflector.

Figure 7 shows $|S_{11}|$ and realized gain for different values of the angle ϕ. The angle ϕ has no effect on the performance of the proposed prototype and is, therefore, chosen to be 0 degrees.

RESULTS AND DISCUSSION

The fabricated AMC-backed

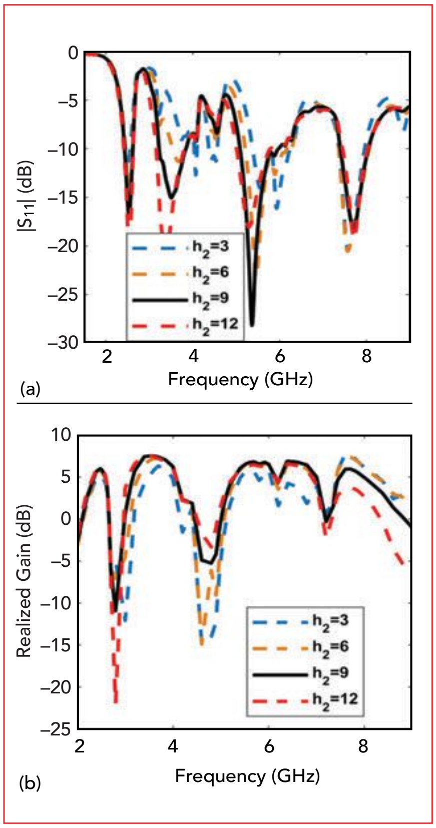

▲ Fig. 6 Parametric study of parameter h_2: (a) $|S_{11}|$ and (b) realized gain. Dimensions are in mm.

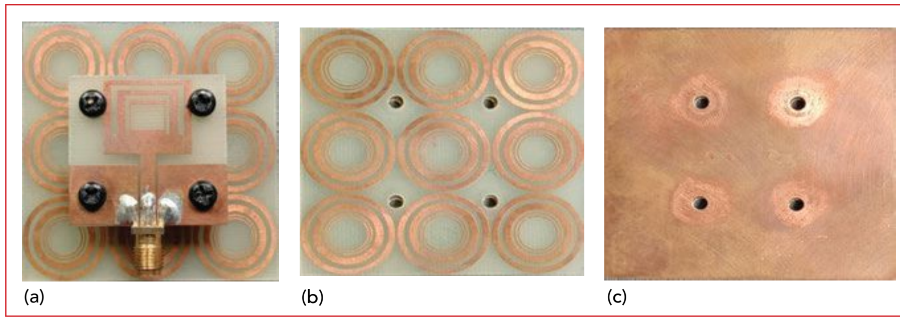

▲ Fig. 8 Fabricated AMC-backed antenna: (a) assembly, (b) AMC reflector front side and (c) AMC reflector back side.

antenna (see ***Figure 8***) is tested in an anechoic chamber using an A. H. Systems SAS-200/571 standard gain horn antenna and an Agilent PNA–X series N5242A network analyzer covering a frequency range of 10 MHz to 26.5 GHz. Teflon fixing screws are added to the structure to ensure stability during the measurement. These screws are strategically placed in the middle of the structure to avoid contact with the AMC cells, preventing any interference or attenuation.

Figure 9 shows $|S_{11}|$ of the quad-band antenna without (see Figure 9a) and with (see Figure 9b) the AMC back plane, respectively. Without the AMC, the antenna performs effectively across the four frequency bands where $|S_{11}| \leq -10$ dB from 2.42 to 2.61, 3.08 to 4.4, 5.2 to 6.2 and 7.3 to 8.17 GHz, with a minimum less than −15 dB in all frequency bands.

With the AMC reflector (see Figure 9b), the antenna demonstrates quad-band operation that not only confirms but surpasses the simulation results. The simulated bandwidths are 2.43 to 2.62, 3.23 to 3.84, 5 to 5.84 and 7.39 to 8.03 GHz, while the measured bandwidths are 2.39 to 2.6, 3.17 to 4.51, 4.84 to 5.5 and 7.25 to 8.38 GHz. The slight deviation observed in the frequency bands is attributed to fabrication tolerances

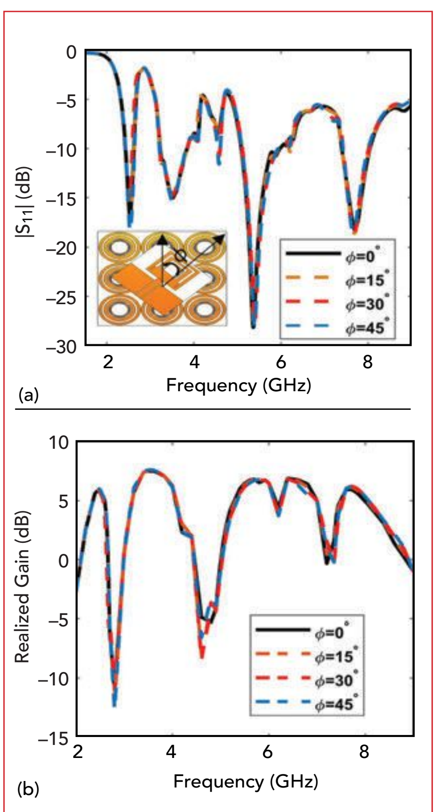

▲ Fig. 7 Parametric study of parameter f: (a) $|S_{11}|$ and (b) realized gain.

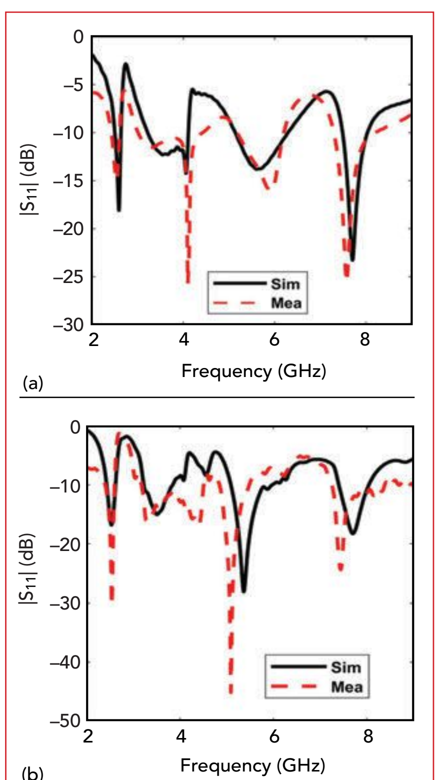

▲ Fig. 9 Antenna $|S_{11}|$: (a) without AMC reflector and (b) with AMC reflector.

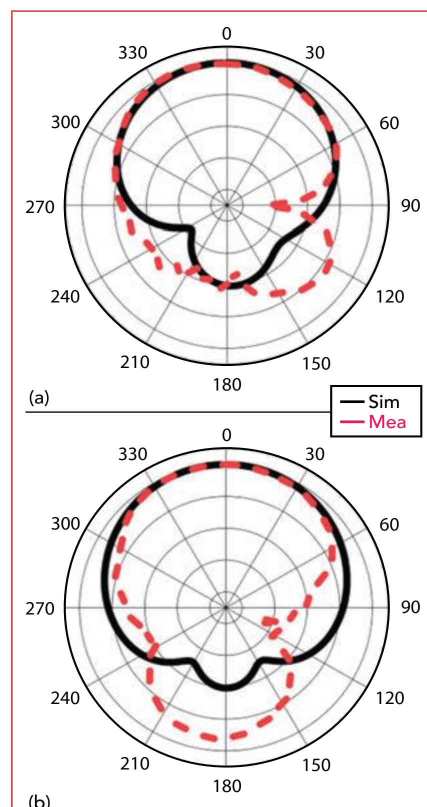

▲ Fig. 10 Antenna radiation patterns at 2.5 GHz: (a) E-plane and (b) H-plane.

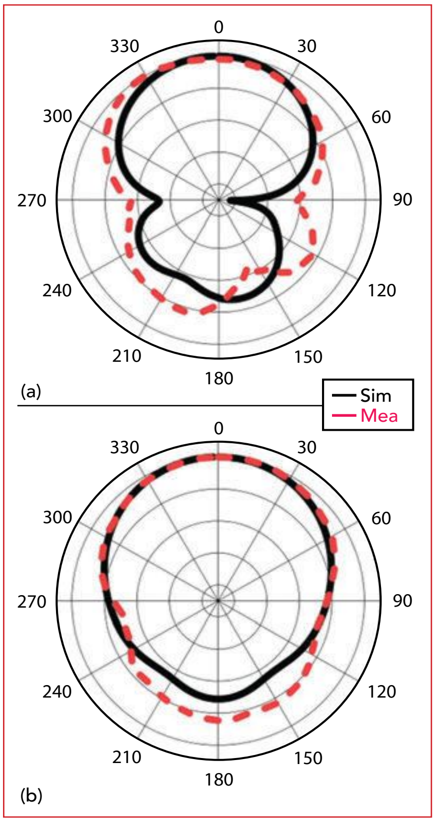

Fig. 11 **Antenna radiation patterns at 3.5 GHz: (a) E-plane and (b) H-plane.**

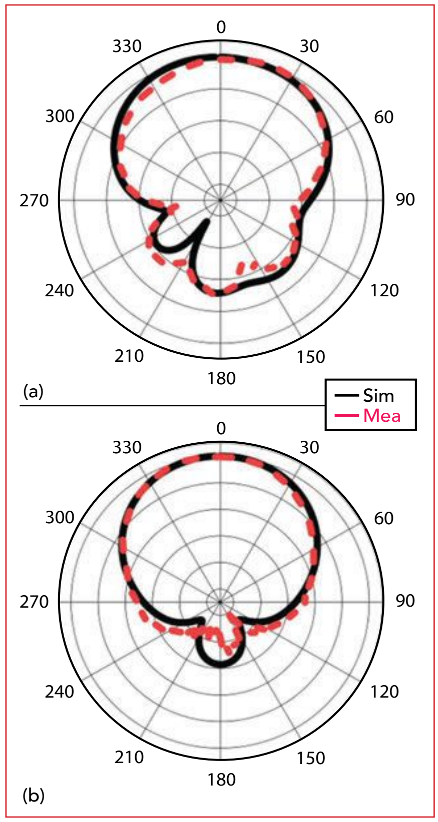

Fig. 12 **Antenna radiation patterns at 5.4 GHz: (a) E-plane and (b) H-plane.**

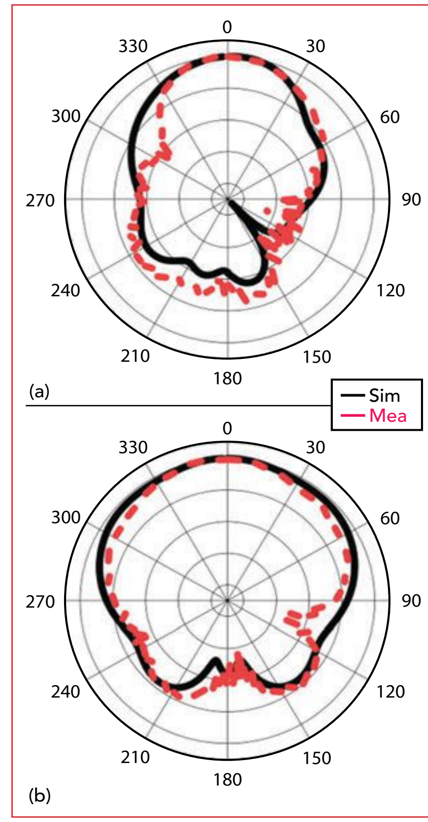

Fig. 13 **Antenna radiation patterns at 7.7 GHz: (a) E-plane and (b) H-plane.**

and assembly techniques. Note that the measured bandwidths cover the entire simulated bandwidths in three of the four bands. Only the third frequency band is slightly shifted toward lower frequencies when compared to the simulation.

Figure 10 through ***Figure 13*** are simulated and measured E- and H-plane radiation patterns at the four operational frequencies: 2.5, 3.5, 5.4 and 7.7 GHz. There is close agreement between simulation and measurement, with minor deviations due to manufacturing and soldering imperfections. Moreover, the performance improves with increasing frequency. The radiation patterns exhibit a directional nature in both simulation and measurement, attributed to integration with the AMC surface.

Realized gain measured at several operational frequencies with and without the AMC reflector is shown in ***Figure 14***. Even if a slight difference of up to 1 dBi is observed, a strong correlation is clearly demonstrated between measurement and simulation. The measured results of the antenna with the AMC reflector show gain enhancements of 4, 5.3, 5.1 and 4.7 dBi at 2.5, 3.5, 5.4, and 7.7 GHz, respectively, confirming that the AMC reflector performs effectively with the quad-band antenna.

Table 1 shows a comparison with other recent work. Note that this design demonstrates several advantages, particularly in terms of size and performance. It has a compact size of $0.46 \times 0.46 \times 0.11\ \lambda_0$, which is smaller or comparable to the majority of the designs listed in the table. Despite its smaller size, it supports multi-band operation covering several key bands, including ISM, WLAN, Bluetooth, WiMAX and satellite communications, which makes it highly competitive compared to other designs. Furthermore, the use of FR4 as substrate material offers a distinct economic advantage compared to felt[19] and polyimide[21] that have flexibility but at a substantially higher cost. Moreover, it achieves a gain enhancement of 5.3 dB, higher than several of the designs listed.

Although its maximum gain of 7.1 dBi is not the highest among the designs listed, the AMC-backed antenna offers a balance of compactness,

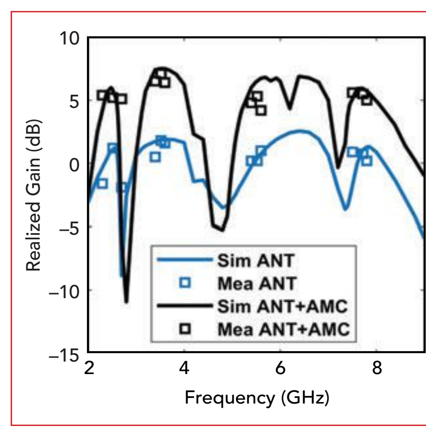

Fig. 14 **Antenna simulated and measured realized gain with and without the AMC reflector.**

cost-efficiency, multi-band operation and enhanced gain. These factors make it a better choice for multi-band applications, particularly in scenarios where space, cost and performance are critical considerations.

CONCLUSION

This article describes a low-profile quad-band antenna backed by an AMC reflector. The design process starts with the development of the quad-band antenna, which exhibits

TABLE 1
COMPARISON WITH OTHER WORK

Reference	Size ($\lambda_0 \times \lambda_0 \times \lambda_0$)	Substrate	Bandwidth (GHz)	Maximum Gain (dB) (dBi)	Gain Enhancement (dBi)
17	0.58 × 0.58 × 0.16	FR4	3.1 to 3.7	5.5	3.8
18	0.62 × 0.62 × 0.10	FR4	2.36 to 2.51	3.3	5.4
			5.03 to 6.12	7.4	4.3
19	0.83 × 0.83 × 0.062	Felt	2.07 to 3.23	6.8	4.3
			5.23 to 6.13	3.9	0.8
20	0.67 × 0.67 × 0.10	FR4	2.4 to 2.484	3.9	5.4
			3.4 to 3.5	5.5	4.5
			5.15 to 5.825	2.6	0.8
21	0.62 × 0.77 × 0.04	Polyimide	1.34 to 1.67	6.1	3.4
			2.33 to 2.47	5.4	1.8
			3.55 to 3.7	7.5	4
22	0.77 × 0.82 × 0.17	FR4	2.19 to 2.54	7.2	4.7
			3.06 to 5.25	8	5.4
			6.43 to 6.96	7.4	4.4
			7.71 to 8.29	7.5	3.9
This Work	0.46 × 0.46 × 0.11	FR4	2.39 to 2.6	5.2	4
			3.17 to 4.51	7.1	5.3
			4.84 to 5.5	5.3	5.1
			7.25 to 8.38	5.5	4.7

a low gain (< 2 dBi) across the four frequency bands. To enhance the gain, an AMC is placed behind the antenna to function as a reflector.

Measurements confirm quad-band behavior, with enhanced gains of 4, 5.3, 5.1 and 4.7 dBi at the four operational frequencies, respectively. These results highlight the performance improvements provided by the AMC reflector and demonstrate close agreement between simulation and measurement.

This AMC-backed antenna is characterized by its simplicity, high gain, multi-band operation and low-profile, making it an excellent candidate for multi-band applications, especially where space is limited. Specifically, it is suitable for WLAN, Bluetooth and WiMAX applications thanks to its operation across the 2.39 to 2.6, 3.17 to 4.51 and 4.84 to 5.5 GHz bands, as well as for military and satellite communication in the 7.27 to 8.38 GHz range. ■

References

1. K. Li, T. Sato and N. Kajitani, "Wideband Planar Antennas for Millimeter-Wave Wireless Communications," *IEEE Antennas and Propagation Society International Symposium*, July 2008.
2. S. Q Xiao and R. Q. Lee, "Antennas Design for Implantable Medical Devices," *IEEE International Conference on Computational Electromagnetics*, February 2015.
3. A. Diallo, C. Luxey, P. L. Thuc, R. Staraj and G. Kossiavas, "Enhanced Two-Antenna Structures for Universal Mobile Telecommunications System Diversity Terminals," *IET Microwaves, Antennas & Propagation*, Vol. 2, No. 1, March 2008, pp. 93–101.
4. B. P. Smyth, S. Barth and A. K. Iyer, "Dual-Band Microstrip Patch Antenna Using Integrated Uniplanar Metamaterial-Based EBGs," *IEEE Transactions on Antennas and Propagation*, Vol. 64, No. 12, December 2016, pp. 5046–5053.
5. A. Sihvola, "Metamaterials: A Personal View," Radioengineering, Vol. 18, No. 2, June 2009.
6. S. Chen, Zhi Li, Y. Zhang, H. Cheng and J. Tian, "Phase Manipulation of Electromagnetic Waves with Metasurfaces and its Applications in Nanophotonics," *Advanced Optical Materials*, Vol. 6, No.13, July 2018.
7. M. Y. Zeain and M. Abu, A. A. Althuwayb, H. Alsariera, A. J. Abdullah Al-Gburi, A. Abdulateef Abdulbari and Z. Zakaria, "A New Technique of FSS-Based Novel Chair-Shaped Compact MIMO Antenna to Enhance the Gain for Sub-6GHz 5G Applications. *IEEE Access*, Vol. 12, March 2024, pp. 49489–49507.
8. S. Peddakrishna and T. Khan, "Performance Improvement of Slotted Elliptical Patch Antenna Using FSS Superstrate," *International Journal of RF and Microwave Computer-Aided Engineering*, Vol. 28, No. 9, May 2018.
9. H. A. Mohamed, M. Edries, M. A. Abdelghany and A. A. Ibrahim, "Millimeter-Wave Antenna with Gain Improvement Utilizing Reflection FSS for 5G Networks," *IEEE Access*, Vol. 10, July 2022, pp. 73601–73609.
10. K. Payandehjoo and R. Abhari, "Employing EBG Structures in Multiantenna Systems for Improving Isolation and Diversity Gain," *IEEE Antennas and Wireless Propagation Letters*, Vol. 8, October 2009, pp. 1162–1165.
11. S. Ghosh, T. -N. Tran and T. Le-Ngoc, "Dual-Layer EBG-Based Miniaturized Multi-Element Antenna for MIMO Systems," *IEEE Transactions on Antennas and Propagation*, Vol. 62, No. 8, August 2014, pp. 3985–3997.
12. H. Malekpoor and M. Hamidkhani, "Performance Enhancement of Low-Profile Wideband Multi-Element MIMO Arrays Backed by AMC Surface for Vehicular Wireless Communications," *IEEE Access*, Vol. 9, December 2021, pp. 166206–166222.
13. U. Ali, S. Ullah, A. Basir, B. Kamal, L. Matekovits and H. Yoo, "Design and SAR Analysis of AMC-Based Fabric Antenna for Body-Centric Communication." *IEEE Access*, Vol. 11, July 2023, pp. 73894–73911.
14. S. Ye, X. Liang, W. Wang, R. Jin, J. Geng, T. S. Bird and Y. J. Guo, "High-Gain Planar Antenna Arrays for Mobile Satellite Communications [Antenna Applications Corner]," *IEEE Antennas and Propagation Magazine*, Vol. 54, No. 6, December 2012, pp. 256–268.
15. S. Clavijo, R. E. Diaz and W. E. McKinzie, "Design Methodology for Sievenpiper High-Impedance Surfaces: An Artificial Magnetic Conductor for Positive Gain Electrically Small Antennas," *IEEE Transactions on Antennas and Propagation*, Vol. 51, No. 10, October 2003, pp. 2678–2690.
16. H. R. Raad, A. I. Abbosh, H. M. Al-Rizzo and D. G. Rucker, "Flexible and Compact AMC Based Antenna for Telemedicine Applications," *IEEE Transactions on Antennas and Propagation*, Vol. 61, No. 2, February 2013, pp. 524–531.
17. A. Verma, R. K. Arya and S. N. Raghava, "Metasurface Superstrate Beam Steering Antenna with AMC for 5G/WiMAX/WLAN Applications," *Wireless Personal Communications*, Vol. 128, January 2023, pp.1153–1170.
18. C. Du, L. -R. Pei, J. Zhang and C. -X. Shi, "A Gain Enhanced Dual-Band Low SAR AMC-Based MIMO Antenna for WBAN and WLAN Applications," *Progress in Electromagnetics Research M*, Vol. 115, 2023, pp. 21–34.
19. U. Ali, A. Basir, M. Zada, S. Ullah, B. Kamal and H. Yoo, "Performance Improvement of a Dual-Band Textile Antenna for On-Body Through Artificial Magnetic Conductor," *IEEE Access*, Vol. 11, July 2023.
20. M. Ameen, O. Ahmad and R. K. Chaudhary, "Bandwidth and Gain Enhancement of Triple-Band MIMO Antenna Incorporating Metasurface-Based Reflector for WLAN/WiMAX Applications," *IET Microwaves, Antennas & Propagation*, Vol. 14, No. 13, October 2020, pp. 1493–1503.
21. S. Yang, C. Yu, X. Yang and J. Zhao, "A Tri-Band Flexible Antenna Based on Tri-Band AMC Reflector for Gain Enhancement and SAR Reduction," *AEU-International Journal of Electronics and Communications*, Vol. 168, August 2023.
22. S. Yang, F. Tong, J. Chu, Y. Chen, Z. Zhao, Z. Fang, Y. Zheng and W. Wang, "Compact Tetracyclic Nested AMC-Backed Multi-Band Antenna with High OoB Rejection and Enhanced Gain Radiation for IIoV-Based Sensing and Communication," *IEEE Internet of Things Journal*, Vol. 11, No. 2, January 2024, pp. 2819–282.

A Dual-Band Doherty Power Amplifier with an Enhanced Back-Off Range

Yuezhi Wu, Guohua Liu and Huabang Zhong
School of Electronics and Information, Hangzhou Dianzi University, Hangzhou, China

This article presents a design method for a dual-band Doherty power amplifier (DPA) with a large back-off range. The method uses a composite right-/left-handed (CRLH) transmission line structure. Using the phase nonlinearity of a CRLH transmission line, the phase shift of two frequency points can be realized. CRLH transmission lines are used for the phase compensation structure of the peak power amplifier (PA) to achieve accurate phase control and a large frequency ratio. The drain termination of the peak PA is kept infinite at the back-off point and the back-off range is improved.

With the development of modern communication technology, more complex modulation methods are gradually increasing the signal's peak-to-average power ratio (PAPR), requiring the PA to maintain high efficiency over a wide dynamic range.[1] The drain efficiency of a traditional RF PA declines exponentially in its back-off range.[2] To satisfy communication requirements, efficiency in the power back-off range must be improved. The DPA maintains a high efficiency at the output back-off (OBO) level and has been widely used.[3] However, the traditional DPA back-off range and linearity are limited because the drain termination of the peak PA cannot satisfy the absolute open condition.[4] Achieving dual-band operation for a large frequency ratio is also challenging.[5]

CRLH transmission lines enable greater design freedom for dual-band circuits. CRLH transmission lines have been used to design a phase compensation line in a dual-band DPA to digitally control the phase of the main and auxiliary amplifiers[6] A DPA based on E-CRLH transmission lines with improved adjacent channel power ratio) and efficiency was proposed by Keshavarz et al.[7] However, the multi-octave design of dual-band PAs still has some problems. The design described in this article employs a CRLH transmission line phase shifter to adjust the drain termination of the peak PA to the open condition at low power with a large frequency ratio.

THEORETICAL ANALYSIS AND DESIGN

Compared with the traditional DPA, the asymmetrical DPA uses a higher power peak PA to address the insufficient output current and poor load modulation effect of the peak PA at saturation.[8-10] However, because the carrier and peak PAs have different saturation powers, the optimal termination impedance must be changed according to traditional theory. The design parameters of a DPA are given by ***Equation 1*** through ***Equa-***

tion 3:

$$\alpha^2 = \frac{1-\beta}{\beta} \quad (1)$$

$$R_T = \alpha R_{opt} \quad (2)$$

$$R_L = \frac{\alpha^2}{1+\alpha^2} R_{opt} \quad (3)$$

Where:

β is a given back-off level related to back-off level *X*, in dB, as *X* = -20 log(β).[11,12] For example, β = 0.33 for 9.54 dB back-off

$\alpha = |I_{Pmax}|/|I_{Cmax}|$ and it is the ratio of peak PA current to carrier PA current at peak output power

R_{opt} is the optimum output impedance of the devices

R_T is the characteristic impedance of the impedance inverters in the load combiner network

R_L is the combined point impedance

In this design, the power divider is an asymmetric structure that enables the carrier PA and the peak PA to reach saturation with the same input power. Based on the CRLH transmission line, the phase shifter adjusts the S_{22} phase of the peak circuit to the open condition. A CRLH is added to the peak circuit as a phase compensation line to match the phase between the carrier circuit and the peak circuit at the junction point. The dual-band DPA is designed to operate in the 0.7 to 0.8 GHz and 2.6 to 2.8 GHz frequency bands with a back-off level of 11 dB and a large frequency ratio.

Composite CRLH Transmission Line Theory

A dual-band device can work at two different frequencies, ω_1 and ω_2.[13] A multi-frequency device composed of multiple microstrip lines has the same displacement at two arbitrary frequency points: $\Phi_1 = -\beta_1 l$ and $\Phi_2 = -\beta_2 l$, where *l* is the electrical length of the multi-segment transmission line. The dispersion relation of the dual-band device should satisfy ***Equation 4*** and ***Equation 5***:

$$\beta(\omega_1) = \beta_1 \quad (4)$$

$$\beta(\omega_2) = \beta_2 \quad (5)$$

Where β_1, β_2 and ω_1, ω_2 are arbitrary values.

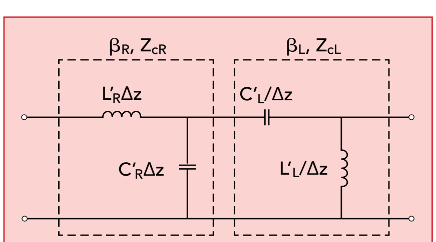

Fig. 1 Simplified equivalent circuit model of an ideal CRLH transmission line.

The equivalent circuit model of an ideal balanced CRLH transmission line is shown in ***Figure 1***, where the propagation constants of the lossless right-handed transmission line and the left-handed transmission line are given in ***Equation 6*** and ***Equation 7***:

$$\beta_L = -\frac{1}{\omega\sqrt{L'_L C'_L}} \quad (6)$$

$$\beta_R = -\sqrt{L'_R C'_R} \quad (7)$$

Where C'_R, L'_R, C'_L and L'_L are the distributed capacitance and inductance per unit length.

In the balanced case, the propagation constant of an ideal CRLH transmission line can be expressed as the direct addition of the propagation constants of the left-handed and right-handed lines. Its characteristic impedance is the same as the separate left-handed and right-handed lines. They are shown in ***Equation 8*** and ***Equation 9***:

$$\beta = \beta_R + \beta_L = \omega\sqrt{L'_R C'_R} - \frac{1}{\omega\sqrt{L'_L C'_L}} \quad (8)$$

$$Z_c^{CRLH} = \sqrt{\frac{L'_R}{C'_R}} = \sqrt{\frac{L'_L}{C'_L}} \quad (9)$$

If the CRLH transmission line matches the port impedance and the phase shift of the first frequency, ***Equation 10*** and ***Equation 11*** must be satisfied:

$$Z_c^{CRLH} = Z_t \quad (10)$$

$$\beta^{CRLH}(\omega = \omega_1) = \beta_1 \quad (11)$$

Equations 9, 10 and 11 are three independent equations containing unknown variables C'_R, L'_R, C'_L, L'_L, which increases the design freedom. Therefore, the second frequency is satisfied easily and the frequency ratio is extended widely. The parameters of the CRLH transmission line are given in ***Equation 12*** through ***Equation 15***:

$$L'_R = \frac{Z_t[\beta_2 - \beta_1(\omega_1/\omega_2)]}{\omega_2[1-(\omega_1/\omega_2)^2]} \quad (12)$$

$$C'_R = \frac{\beta_2 - \beta_1(\omega_1/\omega_2)}{Z_t\omega_2[1-(\omega_1/\omega_2)^2]} \quad (13)$$

$$L'_L = \frac{Z_t[1-(\omega_1/\omega_2)^2]}{\omega_1[\beta_2(\omega_1/\omega_2) - \beta_1]} \quad (14)$$

$$C'_L = \frac{1-(\omega_1/\omega_2)^2}{Z_t\omega_1[\beta_2(\omega_1/\omega_2) - \beta_1]} \quad (15)$$

The previous discussion is based on an ideal CRLH transmission line. An LC ladder network is typically used to construct a composite left-/right-handed transmission line in practical applications. The complex LC network can be equivalent to the ideal CRLH transmission line. A CRLH transmission line with a physical length *l*, composed of *N* structural units of length *p*, has *l* = *Np*. Since the phase shift of each unit structure is ΔΦ, the total phase shift of N unit structures is Φ = NΔΦ. With β = -Φ/*l*, the relationships in ***Equation 16*** and ***Equation 17*** are obtained:

$$L_R = L'_R p,\ L_L = L'_L/p \quad (16)$$

$$C_R = C'_R p,\ C_L = C'_L/p \quad (17)$$

It is necessary to consider the inductance and capacitance of the LC component of the dual-band phase-shifted CRLH transmission line. The relation $\beta_i = -\Phi_i/(Np)$, (i = 1, 2) and Equations 16 and 17 are introduced into Equation 12 through Equation 15. The parameters of the dual-band CRLH transmission line are given in ***Equation 18*** through ***Equation 21***:

$$L_R = \frac{Z_t[\phi_1(\omega_1/\omega_2) - \phi_2]}{N\omega_2[1-(\omega_1/\omega_2)^2]} \quad (18)$$

$$C_R = \frac{\phi_1(\omega_1/\omega_2) - \phi_2}{NZ_t\omega_2[1-(\omega_1/\omega_2)^2]} \quad (19)$$

$$L_L = \frac{NZ_t[1-(\omega_1/\omega_2)^2]}{\omega_1[\phi_1 - \phi_2(\omega_1/\omega_2)]} \quad (20)$$

$$C_L = \frac{N[1-(\omega_1/\omega_2)^2]}{Z_t\omega_1[\phi_1 - \phi_2(\omega_1/\omega_2)]} \quad (21)$$

A symmetrical structure is adopted to obtain the same input and output impedance of the CRLH transmission network. This is done by determining the impedance and phase of the right-handed line based on Equations 8 and 10, then converting it into a traditional microstrip line, as shown in ***Figure 2***.

Phase Shifter Design

For the center frequency points of the two operational bands, phase

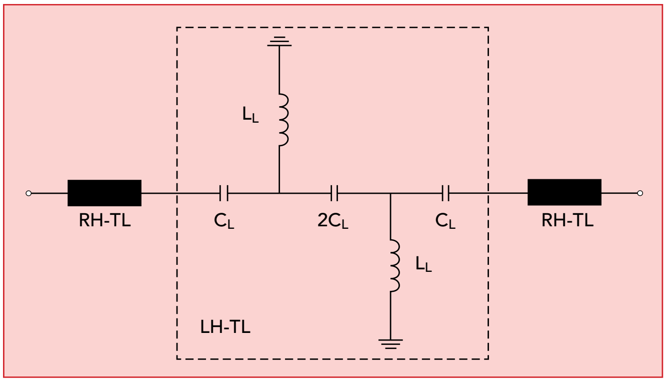

Fig. 2 **CRLH circuit model.**

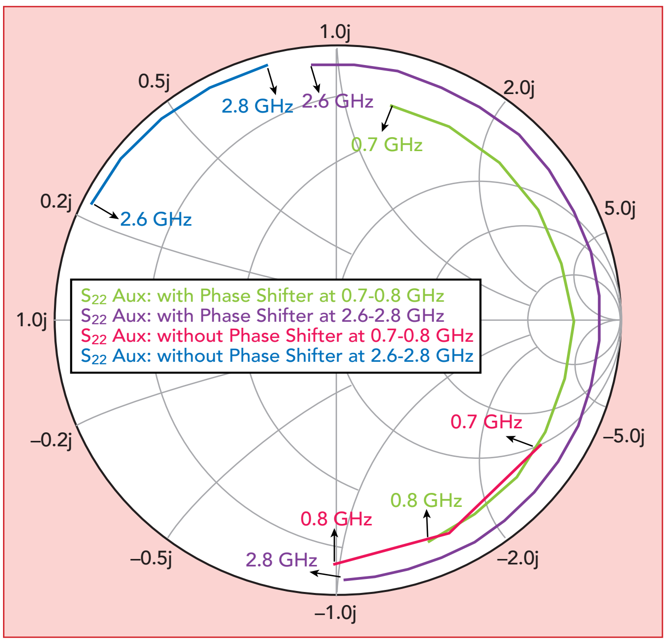

Fig. 3 **Peak power amplifier S_{22}.**

shifts with complementary absolute values are required to adjust the phase of S_{22} to the open condition. The S_{22} phase of the peak PA is shown in ***Figure 3***. The phase shift required to adjust the S_{22} phase to the open condition can be θ_{L1} = 63 degrees or θ_{L2} = -297 degrees at 0.75 GHz. For 2.7 GHz, the phase shift can be θ_{H1} = -130 degrees or θ_{H2} = 230 degrees.

Theoretically, a phase pair consisting of one phase for each frequency point can meet the design requirements. Due to design limitations like bandwidth, the position of the two cut-off frequencies and the existing chip capacitors, θ_L = 63 degrees and θ_H = -130 degrees, are selected and converted into a phase pair (Φ_L, Φ_H) = ($7\pi/20$,$-13\pi/18$). To guarantee the gain and efficiency of the peak PA in the two bands, the designed phase shifter must provide the same impedance at the two operational frequencies.

To adjust the S_{22} phase response of the peak PA to the open condition, phase shifts of 63 and -130 degrees at 0.75 GHz and 2.7 GHz, respectively, must be achieved. The characteristic impedances provided in the operating bands are both 50 Ω so that the phase shifter at the output of the peak PA maintains the open condition without disturbing the optimal load condition at the output. Only the double unit structure with *N* = 2 is used to reduce the size of the phase shifter.

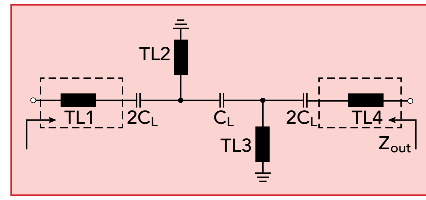

Fig. 4 **CRLH transmission line structure.**

Finally, bringing (Φ_L, Φ_H) = ($7\pi/20$, $-13\pi/18$), Z_t = 50 Ω and *N*=2 into Equations 18 through 21 yields: L_R = 4.19 nH, C_R = 1.68 pF, L_L = 10.2 nH and C_L = 4.09 pF. The right-handed line parameters are converted into a right-handed transmission line (RH-TL), as described previously and the left-handed line parameters are converted into distributed parameters due to the low self-resonant frequency of the lumped inductance. The structure of the CRLH transmission line is shown in ***Figure 4***.

FABRICATION AND MEASUREMENT

ADS software has been used for circuit simulation. The carrier PA is a Cree CGH40010F and the peak PA is a Cree CGH40025F. The DPA is implemented on Rogers 4350B (ε_r = 3.66, *h* = 0.762 mm). Gate biases are -2.8 V for the carrier PA and -6 V for the peak PA, corresponding to Class AB and Class C modes. The

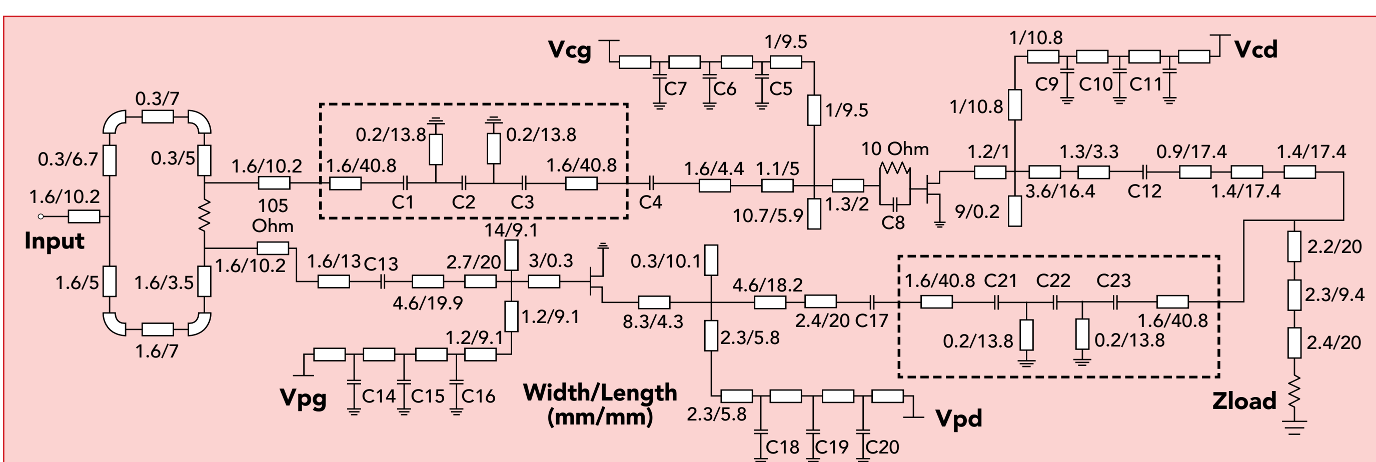

Fig. 5 **DPA circuit schematic.**

drain voltage biases of the carrier and peak PAs are slightly adjusted and set at 22 V and 32 V, respectively. The complete circuit schematic is shown in ***Figure 5***. A photo of the prototype DPA is shown in ***Figure 6***.

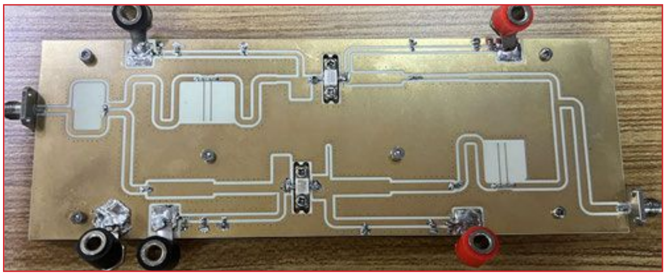

▲ **Fig. 6** **Photo of the prototype DPA.**

Measured S-parameters are shown in ***Figure 7***. In the 0.7 to 0.8 GHz band, $|S_{21}|$ is between 16.5 dB and 18 dB. Correspondingly, $|S_{11}|$ is less than -15.3 dB. In the 2.6 to 2.8 GHz band, $|S_{21}|$ is between 11.7 dB and 13 dB, while $|S_{11}|$ is less than -6.5 dB.

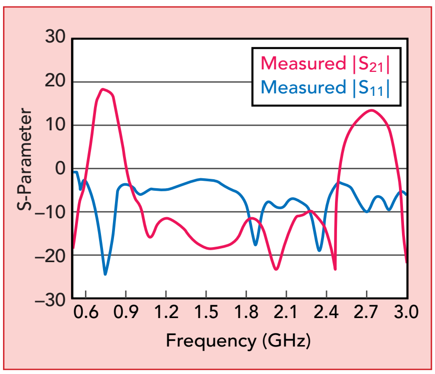

▲ **Fig. 7** **Measured S-parameters.**

Large signal measurements were made using a CW input. Simulated and measured results are plotted in ***Figure 8***. The DPA delivers 43.4 to 44.8 dBm saturated output power with a saturated drain efficiency of 55.9 to 63.8 percent in the 2.6 to 2.8 GHz band, while the gain is between 8.4 and 9.8 dB. The drain efficiency at 6 dB OBO is 46.5 to 48.3 percent and at 11 dB OBO, it is 41.5 to 47.6 percent. In the 0.7 to 0.8 GHz band, the DPA delivers a saturated output power of 44.3 to 45.9 dBm with a saturated drain efficiency of 59.3 to 68.4 percent, while the gain is between 9.2 and 10.9 dB. The drain efficiency is 41.5 to 55.9 percent at 6 dB OBO and 50.3 to 50.5 percent at 11 dB OBO.

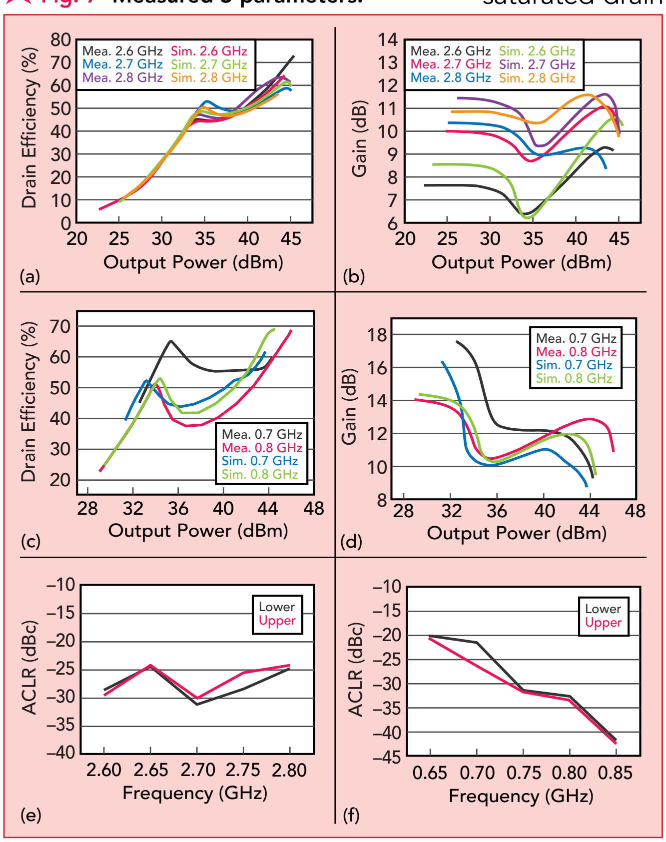

▲ **Fig. 8** **(a) Simulated and measured drain efficiency from 2.6 to 2.8 GHz. (b) Gain from 2.6 to 2.8 GHz. (c) Drain efficiency from 0.7 to 0.8 GHz. (d) Gain from 0.7 to 0.8 GHz. (e) ACLR from 2.6 to 2.8 GHz. (f) ACLR from 0.65 to 0.85 GHz.**

Figures 8e and 8f show the adjacent channel leakage ratio (ACLR) of the DPA driven by a 10 MHz LTE signal with a PAPR of 6.6 dB. It is lower than -25 dBc in the 2.6 to 2.8 GHz band and lower than -20 dBc in the 0.7 to 0.8 GHz band. With digital predistortion (DPD), the ACLR is lower than -46.9 dBc and -48.8 dBc at 2.7 GHz and 0.75 GHz, respectively. These results are shown in ***Figure 9***.

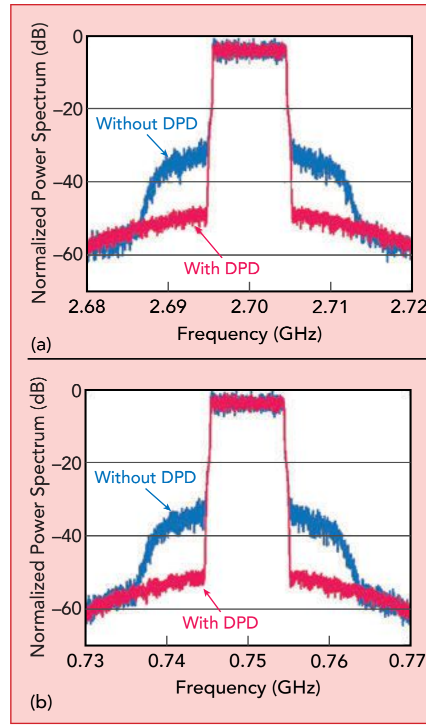

▲ **Fig. 9** **(a) Output spectrum of the prototype DPA with a 10 MHz LTE signal at 2.7 GHz. (b) Output spectrum of the prototype DPA with a 10 MHz LTE signal 0.75 GHz.**

The measured results are consistent with the simulation. The main differences are that the measured results have a higher back-off efficiency at 0.7 GHz and a reduced overall circuit gain, which is attributed to loss in the microstrip.

Table 1 compares this work with other work. Note that this work has more widely extended frequency bands (f_2/f_1 = 3.6) than the others. Higher back-off has been achieved under the premise of the two-way structure. This dual-band PA considers drain efficiency and OBO, which balances the two bands well.

CONCLUSION

A back-off enhanced dual-band DPA has been demonstrated. Adding a dual-band phase shifter to the auxiliary PA output circuit keeps the output phase response near the open circuit condition, improving the back-off range. Compared with other reported work, a dual-band DPA prototype with a large frequency ratio achieves a good compromise between efficiency and OBO. This design may be helpful in 5G communication applications with high PAPR signals. ■

TABLE 1

DPA PERFORMANCE COMPARISON

Reference	Freq. (GHz)	Type	OBO (dB)	P_{SAT} (dBm)	DE_{SAT} (%)	DE_{BO} (%)	Freq. ratio
5	1.4/3.5	Dual-band (2-way)	9	42.5/42.1	70/68	55/55.1	2.5
6	1.8/2.3	Dual-band (2-way)	9	42.8/42.1	64/62	48/42.5	1.3
14	2.0 to 2.2 3.3 to 3.6	Dual-band (3-way)	9	48/47.5	72/63	46/41	1.64
15	1.6 to 1.9	Dual-band (2-way)	10	46	78.3	46.3	-
16	1.5/2.0	Dual-band (3-way)	9.4	35.4/34.4	82.8/70	66.6/48.4	1.3
17	2.6/3.5	Dual-band (3-way)	5	43	55 to 56	49 to 50	1.35
T.W	0.7 to 0.8 2.6 to 2.8	Dual-band (2-way)	11	45.9/44.8	68/63	50.5/47.6	3.6

ACKNOWLEDGMENT

This work is supported by the Zhejiang Provincial Public Technology Research Project (Grant LGG21F010006) and the Zhejiang Provincial Science and Technology Plan Project (2024C01076).

References

1. I. Kim, J. Moon, S. Jee and B. Kim, "Optimized Design of a Highly Efficient Three-Stage Doherty PA Using Gate Adaptation," *IEEE Transactions on Microwave Theory and Techniques*, Vol. 58, No. 10, October 2010, pp. 2562–2574.
2. P. Saad, R. Hou, R. Hellberg and B. Berglund, "A 1.8-3.8-GHz Power Amplifier with 40 Percent Efficiency at 8-dB Power Back-Off," *IEEE Transactions on Microwave Theory and Techniques*, Vol. 66, No. 11, November 2018, pp. 4870–4882.
3. Z. Zhang, Z. Cheng, H. Li, H. Ke and Y. J. Guo, "A Broadband Doherty Power Amplifier with Hybrid Class-EFJ Mode," *IEEE Transactions on Circuits and Systems I: Regular Papers*, Vol. 67, No. 12, December 2020, pp. 4270–4280.
4. F. H. Raab, P. Asbeck, S. Cripps, P. B. Kenington, Z. B. Popovic, N. Pothecary, J. F. Sevic and N. O. Sokal, "Power Amplifiers and Transmitters for RF and Microwave," *IEEE Transactions on Microwave Theory and Techniques*, Vol. 50, No. 3, March 2002, pp. 814–826.
5. H. Liu, C. Zhai and K. M. Cheng, "Novel Dual-Band Equal-Cell Doherty Amplifier Design with Extended Power Back-Off Range," *IEEE Transactions on Microwave Theory and Techniques*, Vol. 68, No. 3, March 2020, pp. 1012–1021.
6. R. Kalyan, K. Rawat and S. K. Koul, "A Digitally Assisted Dual-Input Dual-Band Doherty Power Amplifier with Enhanced Efficiency and Linearity," *IEEE Transactions on Circuits and Systems II: Express Briefs*, Vol. 66, No. 2, February 2019, pp. 297–301.
7. R. Keshavarz, A. Mohammadi and A. Abdipour, "Linearity Improvement of a Dual-Band Doherty Power Amplifier Using E-CRLH Transmission Line," *AEU-International Journal of Electronics and Communications*, Vol. 131, March 2021.
8. J. Kim, J. Cha, I. Kim and B. Kim, "Optimum Operation of Asymmetrical-Cells-Based Linear Doherty Power Amplifiers-Uneven Power Drive and Power Matching," *IEEE Transactions on Microwave Theory and Techniques*, Vol. 53, No. 5, May 2005, pp. 1802–1809.
9. J. Kim, B. Fehri, S. Boumaiza and J. Wood, "Power Efficiency and Linearity Enhancement Using Optimized Asymmetrical Doherty Power Amplifiers," *IEEE Transactions on Microwave Theory and Techniques*, Vol. 59, No. 2, February 2011, pp. 425–434.
10. Y. Cao and K. Chen, "Hybrid Asymmetrical Load Modulated Balanced Amplifier with Wide Bandwidth and Three-Way-Doherty Efficiency Enhancement," *IEEE Microwave and Wireless Components Letters*, Vol. 31, No. 6, June 2021, pp. 721–724.
11. D. Y.-T. Wu and S. Boumaiza, "A Modified Doherty Configuration for Broadband Amplification Using Symmetrical Devices," *IEEE Transactions on Microwave Theory and Techniques*, Vol. 60, No. 10, October 2012, pp. 3201–3213.
12. B. Kim, J. Kim, I. Kim and J. Cha, "The Doherty Power Amplifier," *IEEE Microwave Magazine*, Vol. 7, No. 5, October 2006, pp. 42–50.
13. S. Zhou and A. K. Jha, "Characteristics Modeling of GaN Class-AB Dual-Band PA Under Different Temperature and Humidity Conditions," *IEEE Access*, Vol. 9, August 2021, pp. 121632–121644.
14. M. Liu, X. Fang, H. Huang and S. Boumaiza, "Dual-Band 3-Way Doherty Power Amplifier With Extended Back-Off Power and Bandwidth," *IEEE Transactions on Circuits and Systems II: Express Briefs*, Vol. 67, No. 2, February 2020, pp. 270–274.
15. X. Y. Zhou, S. Y. Zheng, W. S. Chan, X. Fang and D. Ho, "Post Matching Doherty Power Amplifier with Extended Back-Off Range Based on Self-Generated Harmonic Injection," *IEEE Transactions on Microwave Theory and Techniques*, Vol. 66, No. 4, April 2018, pp. 1951–1963.
16. R. Alsulami, P. Roblin, J. I. Martinez-Lopez, Y. Hahn, C. Liang, Z. Popovic and V. Chen, "A Novel 3-Way Dual-Band Doherty Power Amplifier for Enhanced Concurrent Operation," *IEEE Transactions on Microwave Theory and Techniques*, Vol. 69, No. 9, September 2021, pp. 4041–4058.
17. Y. Luo, D. Xuan, Z. Wang, W. Gao, W. Yang and S. Yuan "A Concurrent 2.6/3.5 GHz Dual-Band Doherty Power Amplifier with Matching Network Based on Composite Right/Left-Handed Unit Cell," *IEICE Electronics Express*, Vol. 19, No. 3, December 2021.